

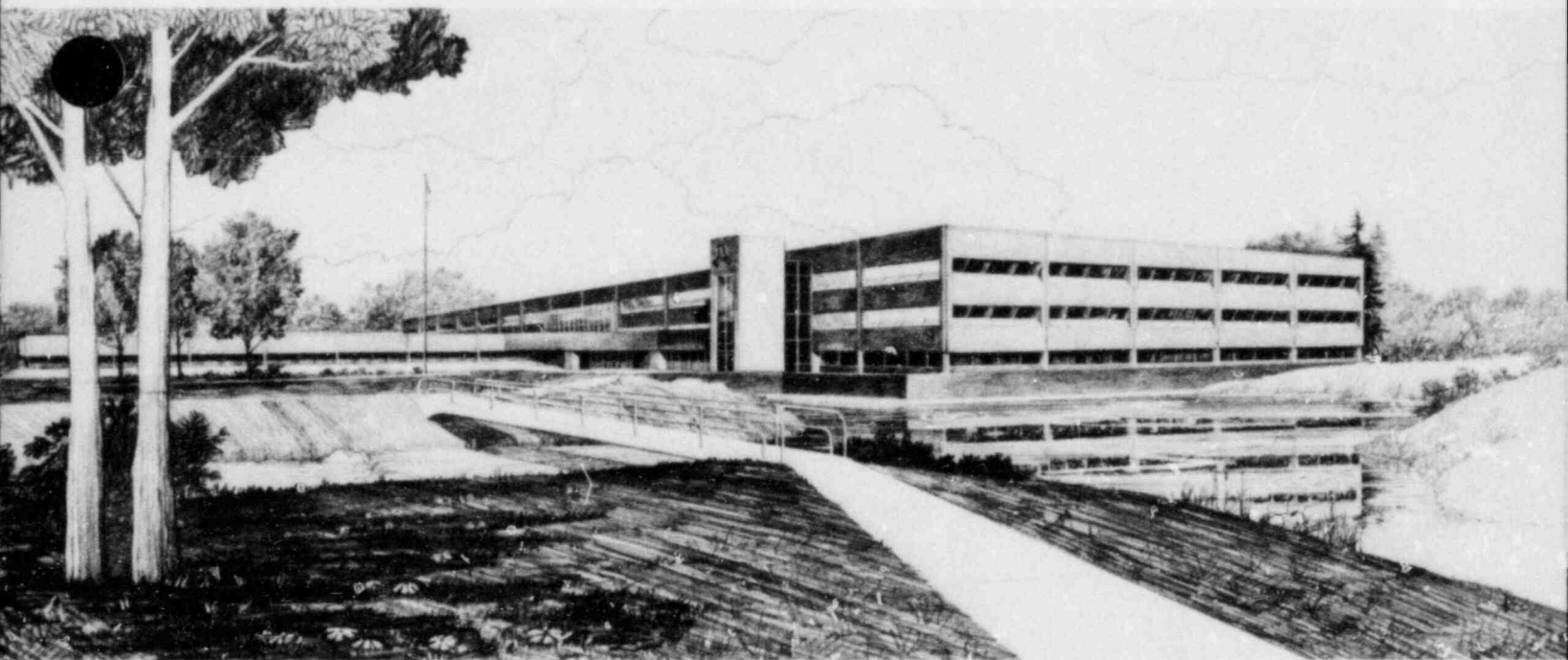
QUICK LOOK REPORT FOR SEMISCALE INTERMEDIATE
BREAK TEST S-IB-3

T. J. Boucher

M. T. Leonard

Idaho National Engineering Laboratory

Operated by the U.S. Department of Energy



This is an informal report intended for use as a preliminary or working document

8211060575 820831

PDR RES

*

PDR

Prepared for the
U.S. NUCLEAR REGULATORY COMMISSION
under DOE Contract No. DE-AC07-761D01570



INTERIM REPORT

Accession No. _____

Report No. EGG-SEMI-6013

Contract Program or Project Title:

Semiscale

Subject of this Document:

Quick Look Report for Semiscale MOD-2A Test S-IB-3

Type of Document:

Quick Look Report

Author(s):

T. J. Boucher
M. T. Leonard

Date of Document:

August 1982

Responsible NRC Individual and NRC Office or Division:

R. R. Landry, Reactor Safety Research

This document was prepared primarily for preliminary or internal use. It has not received full review and approval. Since there may be substantive changes, this document should not be considered final.

EG&G Idaho, Inc.
Idaho Falls, Idaho **83415**

Prepared for the
U.S. Nuclear Regulatory Commission
Washington, D.C.
Under DOE Contract No. **DE-AC07-76ID01570**
NRC FIN No. A6038

INTERIM REPORT

QUICK LOOK REPORT FOR
SEMISCALE INTERMEDIATE BREAK TEST S-IB-3

Approval: *Gary W. Johnsen*
G. W. Johnsen, Manager
WRRTF Experiment Planning and Analysis Branch

Approval: *Paul North*
P. North, Manager
Water Reactor Research
Test Facilities Division

ABSTRACT

Results are presented from a preliminary analysis of Semiscale Mod-2A Test S-IB-3. This test was a 21.7% communicative cold leg break loss of coolant experiment and was the last of the Intermediate Break series. The test was intended to provide reference data for comparison of Semiscale test results to results from LOBI test B-R1M. The test was also intended to provide reference data for evaluation and assessment of reactor safety code capabilities to predict integral blowdown, refill/reflood experiments for intermediate break sizes, and particularly for providing data to extend the code into the reflood regime. Particular emphasis was placed on providing extensive core fluid and heater rod measurements to facilitate this development.

FIN No. A6038
Semiscale Program

TABLE OF CONTENTS

ABSTRACT	iii
TABLE OF CONTENTS	iv
LIST OF FIGURES	v
LIST OF TABLES	viii
SUMMARY	ix
1. INTRODUCTION	1
2. SYSTEM CONFIGURATION AND TEST CONDUCT	2
2.1 System Configuration	2
2.1.1 Fluid System Configuration	3
2.1.2 Control System Configuration	11
2.1.3 Measurement System Configuration	17
2.2 Test Procedures	20
2.2.1 Pretest Day Checkouts	20
2.2.2 Test Day Warmup Operations	20
2.2.3 Initial Conditions and Sequence of Controlled Events	20
2.3 Comparison of Specified and Actual Configuration and Operations	25
2.3.1 Configuration	25
2.3.2 Initial Conditions	25
2.3.3 Controlled Parameters	27
3. TEST RESULTS	30
3.1 Description of the Transient	30
3.1.1 General System Response	30
3.1.2 Reactor Vessel and Loop Hydraulics	30
3.1.3 ECC and Core Thermal Response	47
4. COMPARISON OF PRETEST PREDICTION TO SELECTED DATA	58
5. CONCLUSIONS	76
6. REFERENCES	78
7. APPENDIX	79

LIST OF FIGURES

1.	Mod-2A system for IB test series	4
2.	Semiscale Mod-2A pressure vessel	5
3.	Axial core power profiles	6
4.	Upper head, upper plenum schematic drawing showing upper head internals modifications	7
5.	Cross-section of the Semiscale Mod-2A steam generator	9
6.	Break simulator for Test S-IB-3	10
7.	Normalized core power decay curve for Test S-IB-3	14
8.	Normalized pump speeds from beginning of coastdown for broken and intact loop pumps	15
9.	LPIS injection rate	16
10.	Core and downcomer measurements	18
11.	Heater rod and core fluid thermocouple locations	19
12.	Measured core power	28
13.	Actual and specified core power	29
14.	Core bottom liquid level	31
15.	Highest measured heater rod temperature (184 cm in rod B3)	32
16.	Upper plenum pressure	35
17.	Hot leg, cold leg, and saturation temperatures for Test S-IB-3	36
18.	Liquid level in Broken loop pump suction upflow leg	37
19.	Liquid level in Intact loop pump suction upflow leg	39
20.	Guide tube momentum flux and flow direction	40
21.	Comparison of primary system pressure to Broken loop steam generator secondary pressure	42
22.	Broken loop hot leg volumetric flow	43
23.	Liquid level in Intact loop steam generator upflow side tubes	44

24. Liquid levels in vessel and downcomer showing manometric behavior for Test S-IB-3	45
25. Differential pressure in Intact loop pump suction downflow leg (indicative of liquid level)	46
26. Accumulator volumetric flow	48
27. Liquid level in upper head (top of bypass line 230 cm above top of support plate)	49
28. Volumetric flow in the downcomer	51
29. Average core heater rod temperature	52
30. Fluid density in high power region of core (183 cm from core bottom)	54
31. Comparison of core midplane temperatures in row 2	55
32. Comparison of core midplane temperatures in column D	56
33. Comparison of core axial temperatures in heater rod B3	57
34. Comparison of measured and calculated upper plenum pressures	59
35. Comparison of measured and calculated upper plenum and pressurizer pressures	60
36. Comparison of measured and calculated pressurizer surge line flow rate	62
37. RELAP5 calculated densities in the pressurizer	63
38. Comparison of measured and calculated pump suction collapsed liquid levels (downside)	64
39. Comparison of measured primary and secondary pressures	66
40. Comparison of calculated primary and secondary pressures	67
41. Comparison of measured vessel and downcomer collapsed levels	68
42. Comparison of calculated vessel and downcomer collapsed levels	69
43. Comparison of measured to calculated core heater rod peak cladding temperature	70
44. Comparison of measured to calculated Intact loop accumulator flow rate	72

45. RELAP5 calculated cold leg densities	73
46. Calculated mass flows and velocities through inlet annulus	74

LIST OF TABLES

1. General System Configuration	12
2. Miscellaneous Configuration Items	13
3. Specified Initial Conditions	21
4. Specified Sequence of Controlled Events	23
5. Specified, Measured and Calculated Initial Conditions	26
6. Chronology S-IB-3	33

SUMMARY

This report presents the results of a preliminary analysis of data from Semiscale Mod-2A Intermediate Break Test S-IB-3. This test duplicated, as closely as possible, a test (LOBI B-R1M) conducted in March of 1981 in the Loop Blowdown Investigation Facility in Ispra, Italy. The LOBI B-R1M Test was a 25% break test in the LOBI facility which, when area-to-volume scaled to the Semiscale facility, represents a 21.7% break test in the Semiscale facility. This test simulated a cold leg break loss-of-coolant accident (LOCA) in a pressurized water reactor (PWR) with inverted top hat, non-UHI upper internals. The intact loop accumulator pressure was set at 2.7 MPa as was specified for the LOBI B-R1M Test. Data from Test S-IB-3 will be used to provide reference data for comparison of Semiscale test results to LOBI test results, and to provide reference data for evaluation and assessment of reactor safety code capabilities to predict integral blowdown, refill/reflood experiments for intermediate break sizes. Data will also be used to expand the break spectrum data base to cover the 10 to 200% range.

Initial conditions for this test were equivalent to, or scaled from, the LOBI Test B-R1M operating conditions. Following rupture of the pressure boundary, continuous depressurization took place and the system was observed to void predominantly from the upper elevations downward. Fluid in the upper head drained from approximately 20 to 140 seconds. As the system voided, fluid in the pump suction formed a seal which impeded steam flow around the loops. Asymmetric operation of the steam generators may have caused the Broken loop pump suction liquid seal to clear early which in turn caused the Intact loop pump suction liquid seal clearing to be delayed. This resulted in a depression of the vessel liquid level in the period from 22 to 130 s, by which time the pump suction had been cleared out. This depression of the vessel liquid level resulted in a dryout and heatup of the heater rods in an extensive portion of the core. As the pump suction were being cleared out, coolant returned to the vessel and rewet the entire core. The heater rod temperature excursions due to seal formation started at about 50 seconds with peak temperatures in the range of 740 to 760 K.

After the pump suction seals voided, the loops remained relatively clear of liquid. The liquid in the vessel and downcomer boiled off while ECC accumulator water bypassed the downcomer to the break between 163 and 190 seconds. Because of this period of core boil off the heater rod temperatures again experienced an excursion at about 190 seconds. After 190 seconds the accumulator water began to penetrate the downcomer and refill started. As the vessel refilled, the heater rod temperatures reached a plateau at about 240 seconds. At that time the system pressure reached 1 MPa and the low pressure injection system (LPIS) began pumping cold water into the vessel. The combined accumulator and LPIS flow quenched most of the core at about 280 seconds, with the highest elevations in the core being quenched at about 350 seconds. After 350 seconds the heater rod temperatures followed close to the saturation temperature until the end of the test.

A comparison of the RELAP5/MODi pretest prediction calculation to experimental data showed good agreement in the overall response of the system to the intermediate break transient. In particular, the calculated primary coolant system depressurization and cold leg accumulator flow rate were shown to be well within the data uncertainty.

Some discrepancies between the predicted and observed core thermal-hydraulic response were found. The primary cause for these discrepancies is a disagreement between the predicted and observed pump suction liquid seal behavior. A core level depression due to liquid seal formation was not accurately predicted. The observed core boil-off and heater rod dryout following the time of pump suction blowout was predicted and agreed well with data. The final core quench was not predicted because the accumulator injected liquid was calculated to bypass the downcomer and exit the system through the break.

1. INTRODUCTION

Testing performed in the Semiscale Mod-2A is part of the water reactor safety research effort directed toward assessing and improving the analytical capability of computer codes which are used to predict the behavior of pressurized water reactors (PWR's) during postulated accident scenarios. For this purpose, the Mod-2A system was designed as a smallscale model of the primary system of a four loop PWR nuclear generating plant. The system incorporates the major components of a PWR including steam generators, vessel, pumps, pressurizer, and loop piping. The intact loop is scaled to simulate the three intact loops in a PWR, while the broken loop simulates the single loop in which a break is postulated to occur in a PWR. Geometric similarity has been maintained between a PWR and Mod-2A, most notably in the design of a 25 rod, full-length (3.66 m), electrically heated core, full-length upper-head and upper-plenum, component layout, and relative elevations of various components. Equipment in the upper-head of the Mod-2A vessel has been designed to simulate the fluid flow paths found in a PWR which has the inverted top hat upper-head internals package.^a The scaling philosophy followed in the design of the Mod-2A system (modified volume scaling) preserves most of the important first order effects thought important for LOCA transients.²

This report presents a preliminary analysis of data from Semiscale Test S-IB-3 which is the last of the three-test Intermediate Break series. It was conducted on February 23, 1982. This test was a 21.7%, communicative, cold leg break loss-of-coolant experiment. The primary objective of this test was to provide reference data for comparison of Semiscale test results to LOBI B-R1M test results. Also, another important objective was to provide reference data for evaluation and assessment of reactor safety code capabilities to predict integral blowdown, refill/reflood experiments for intermediate break sizes. Still another

a. This is a recent modification to the Semiscale Mod-2A reactor vessel upper-head. The modification is described in Reference 1.

important objective was to expand the break spectrum data base to cover the 10 to 200% range in order to determine if other phenomena are important to core cooling and to evaluate the Mod-2A system response to breaks in this range.

The experiment incorporated an (electrical) core power decay profile calculated to best represent the LOBI B-R1M test core power decay profile. The primary coolant pumps were subjected to controlled speed transients similar to the LOBI B-R1M test pump speed transients. Emergency core coolant consisted of accumulator and low pressure injection system flows. The test was initiated using a rupture disc assembly and the system effluent was directed to and contained in a partially water filled pressure suppression tank.

The following sections present a preliminary analysis of S-IB-3 test results. Section 2 contains a detailed description of the configuration of the fluid, control and measurement systems, and of the test procedures, initial conditions and sequence of controlled events. Section 3 presents selected test results and analysis. Section 4 contains a comparison of some test results with pretest prediction calculations and Section 5 presents preliminary conclusions.

2. SYSTEM CONFIGURATION AND TEST CONDUCT

2.1 System Configuration

The entire test facility consists of the fluid system (pipes, pumps, vessel, heat exchangers, etc.), the control system (power to core, pumps, valves, and instrument air and control signals), and the experimental measurement system (transducers, amplifiers, digital data system). These are described in detail in Reference 1 and will only be summarily described here.

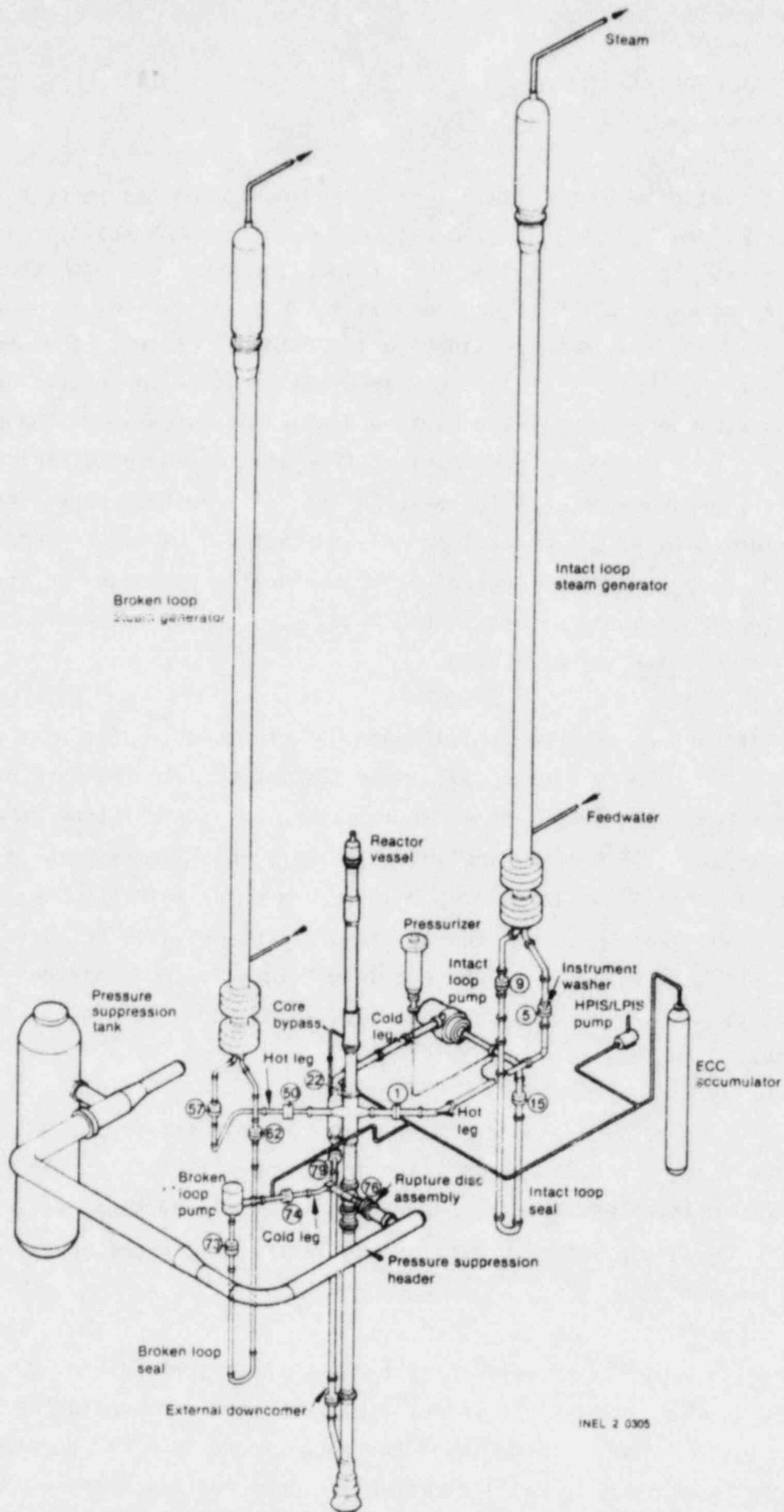
2.1.1 Fluid System Configuration

The Semiscale Mod-2A fluid system configured for the IB test series is shown in Figure 1. It is a 2500 psi, 650°F 1-3 in. IPS stainless steel type system. It consists of an Intact loop and a Broken loop, the former representing three of the four loops in a PWR. Thus, flow rates and equipment sizes are in the ratio of 3:1 for the two loops. The pressurizer is connected to the Intact loop hot leg, the pressure suppression header and tank are connected via the rupture disk break assembly to the Broken loop cold leg. Emergency core coolant from an accumulator and high or low pressure (low pressure only for S-IB-3) injection system pumps are routed to the loop cold legs (Intact loop only in these IB tests). Feedwater is supplied to the two steam generators from a heated tank and the steam routed through control valves to the atmosphere, i.e., an open loop secondary coolant system is used.

In Semiscale, the PWR vessel's annular downcomer is replaced with an external pipe to permit extensive instrumenting of both the core and downcomer regions. These are shown in Figure 2. Most of the fluid system components are full height, including the core which consists of a 5 x 5 array of electrically heated 3.66 m long rods which simulate the fuel rods in a 15 x 15 type PWR core. The number of turns per inch of the electrical heating coil is varied along the rod length to give the staircase approximation of a cosine axial heat flux shape shown in Figure 3. Total core power is 2 MW.

The upper-head upper-plenum and core flow bypass arrangement in the Semiscale reactor vessel was modified in November 1981 to better simulate a Westinghouse inverted top hat, upper-head internals package design (the older UHI design no longer exists). The modifications are noted in Figure 4.

The steam generators incorporate the standard PWR 7/8 in. OD Inconel inverted U-tubes, six in the Intact loop generator and two in the Broken loop unit. The tube lengths cover the range found in a PWR generator. The tubes are supplied with small diameter Inconel sheathed thermocouples



INEL 2 0305

Figure 1. MOD-2A system for IB test series.

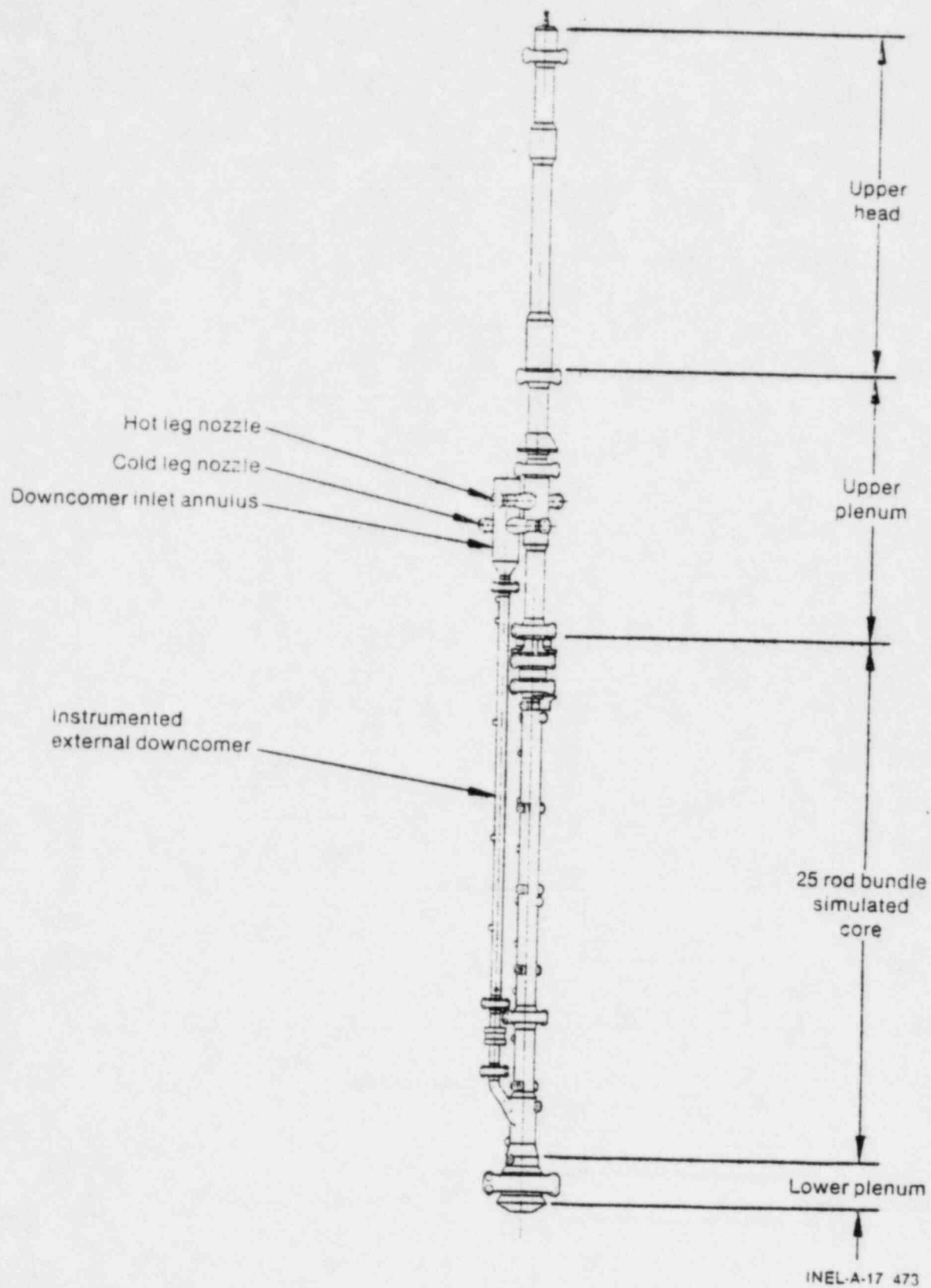


Figure 2. Semiscale Mod-2A pressure vessel.

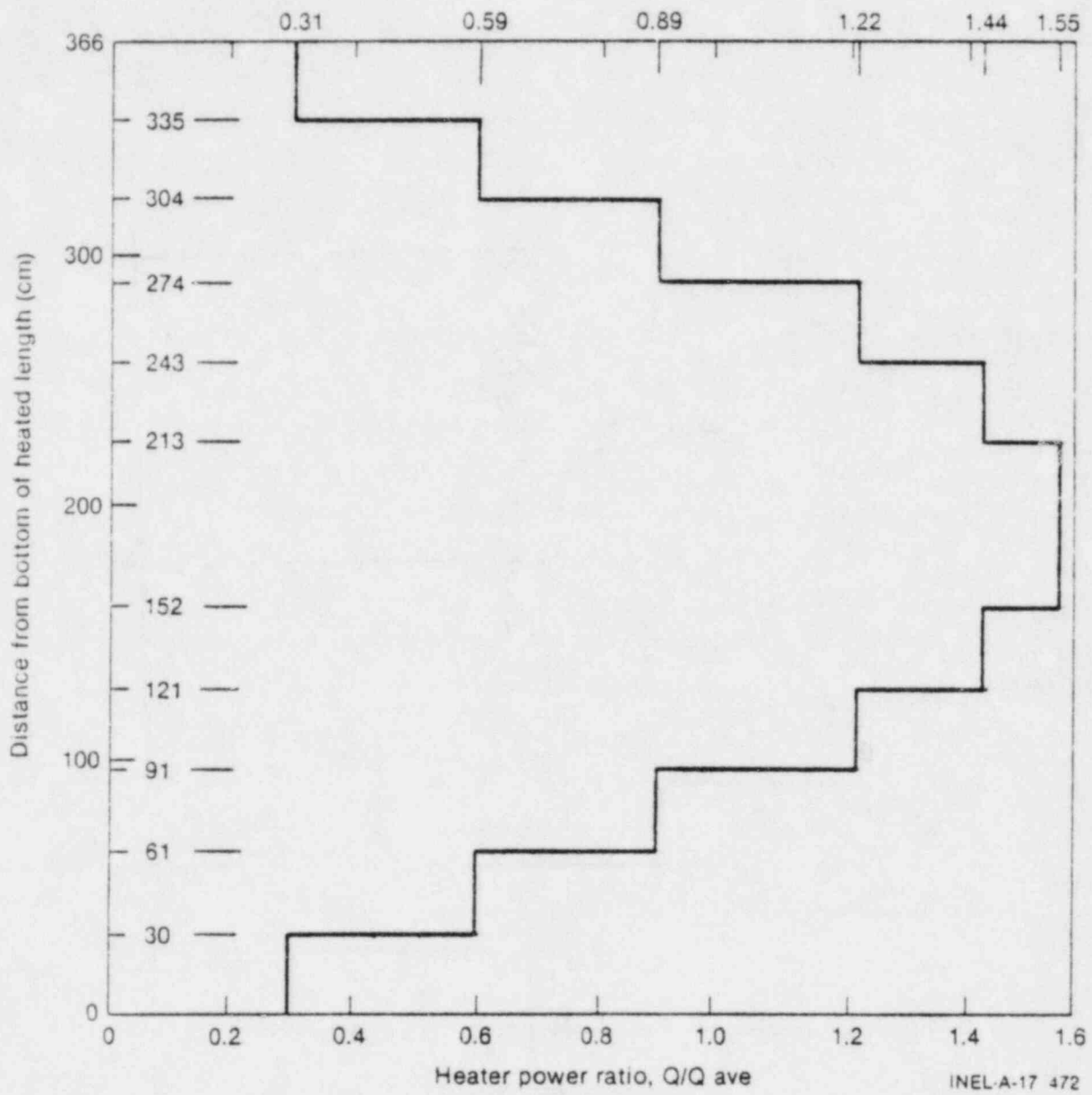


Figure 3. Axial core power profile.

* MODIFICATIONS MADE TO BETTER SIMULATE WESTINGHOUSE STD PLANT UPPER HEAD/UPPER PLENUM FLOW PATHS AND HYDRAULIC RESISTANCES.

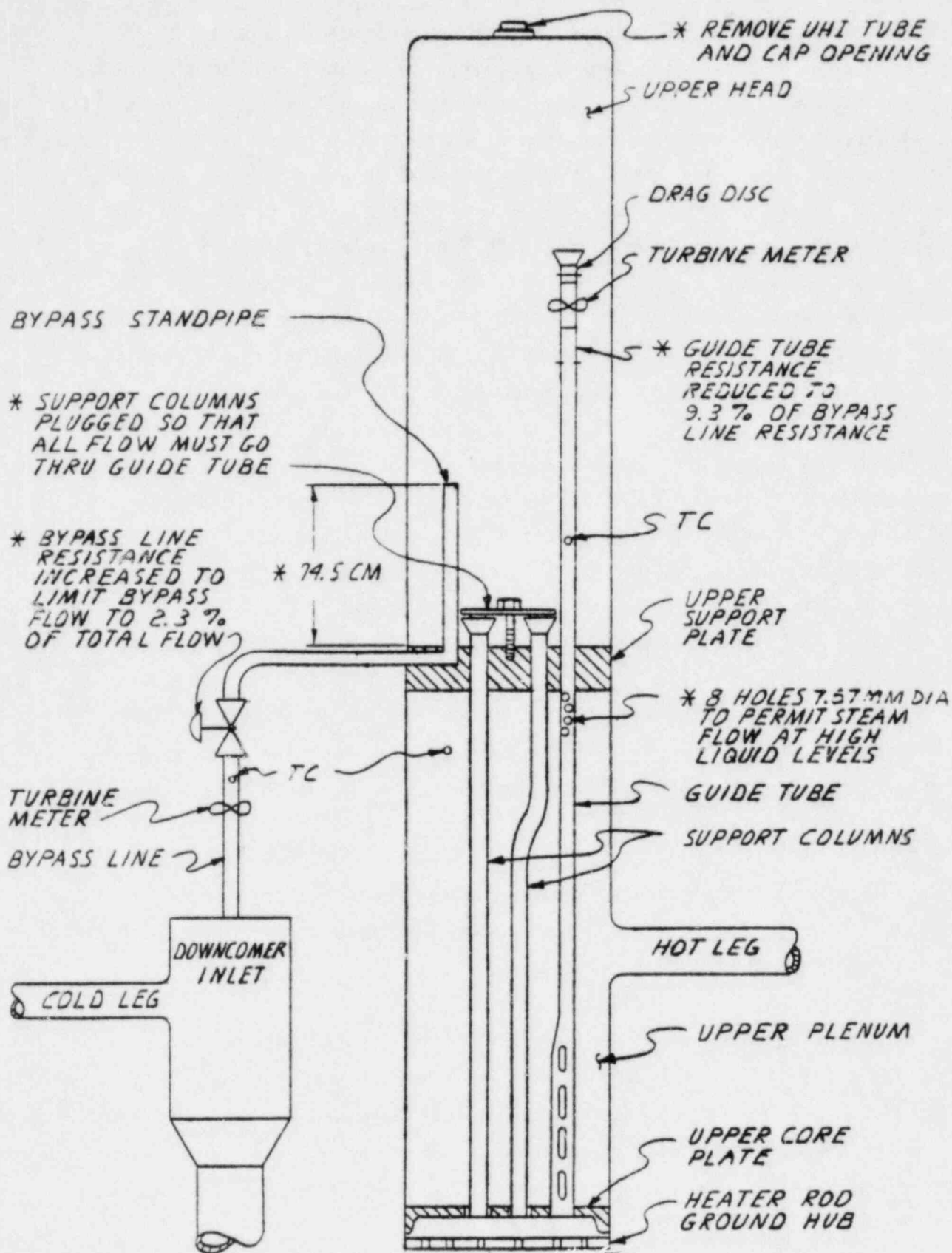


Figure 4. Upper-head upper-plenum schematic drawing showing upper head internals modifications.

brazed to the tubes which provide primary and secondary coolant temperatures and tube wall temperature at various elevations in the upflow and downflow legs. Two tubes are instrumented in each generator for a total of seventy-five thermocouples per generator. A cross section of the generators is shown in Figure 5. Note that the major portion of the secondary flow area/volume is taken up by filler pieces in order to obtain the approximately correct secondary side liquid volume and velocity.

The communicative break converging diverging nozzle assembly is shown in Figure 6. The upstream end of the T-shaped section shown is connected between the Broken loop pump and downcomer inlet. The downstream end is connected via the rupture disc assembly to the pressure suppression (containment simulation) system. As shown in the figure, the break nozzle is located at the horizontal midplane of the cold leg pipe and at a position relative to that pipe simulating a break in its wall. Thus, when the disc is ruptured, critical flow is established across the break nozzle and the system fluid upstream of the nozzle is subjected to reasonably realistic flow direction/length type changes in order to exit the system. The entrance of the nozzle is elliptical in shape. Note that the 21.7% break nozzle throat diameter reflects the PWR/Semiscale (thermal power) scale factor of $3411/2$ applied to the PWR cold leg ID. This is not, however, the ID of the Semiscale Broken loop cold leg which is somewhat larger than the scaled ID.²

The external pipe heaters used in earlier Semiscale long-term-transient test series to make up for system heat losses are not used in the short-term-transient IB test series.

Also for this test, the resistances in the Intact loop and Broken loop were decreased in an effort to improve the simulation of the LOBI loop resistances. Although the Intact loop resistance could not be decreased to the scaled value, it was decreased significantly to the limit obtainable without major system design modifications. The resistance was incorporated by taking all orifices out of the Intact loop.

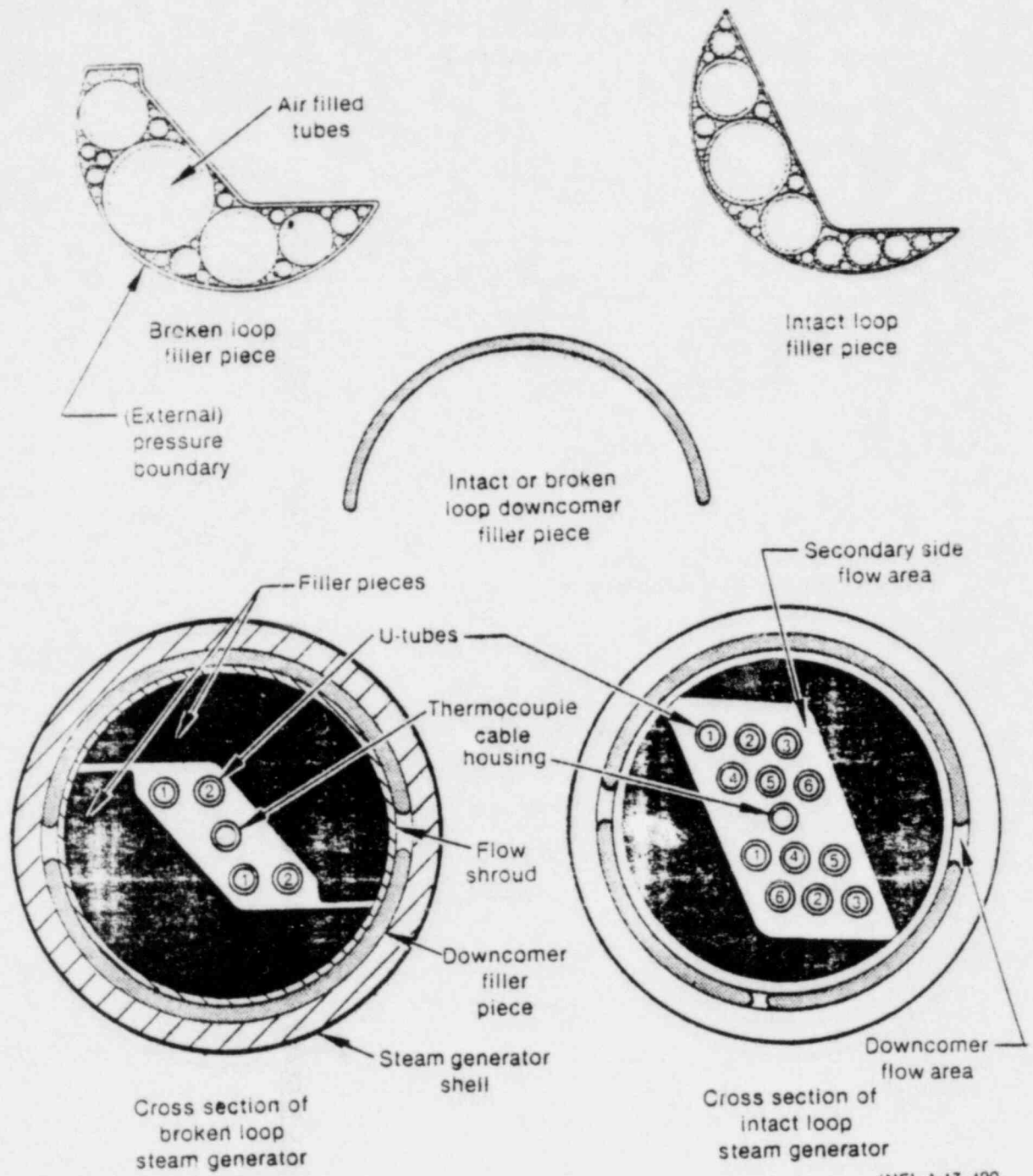
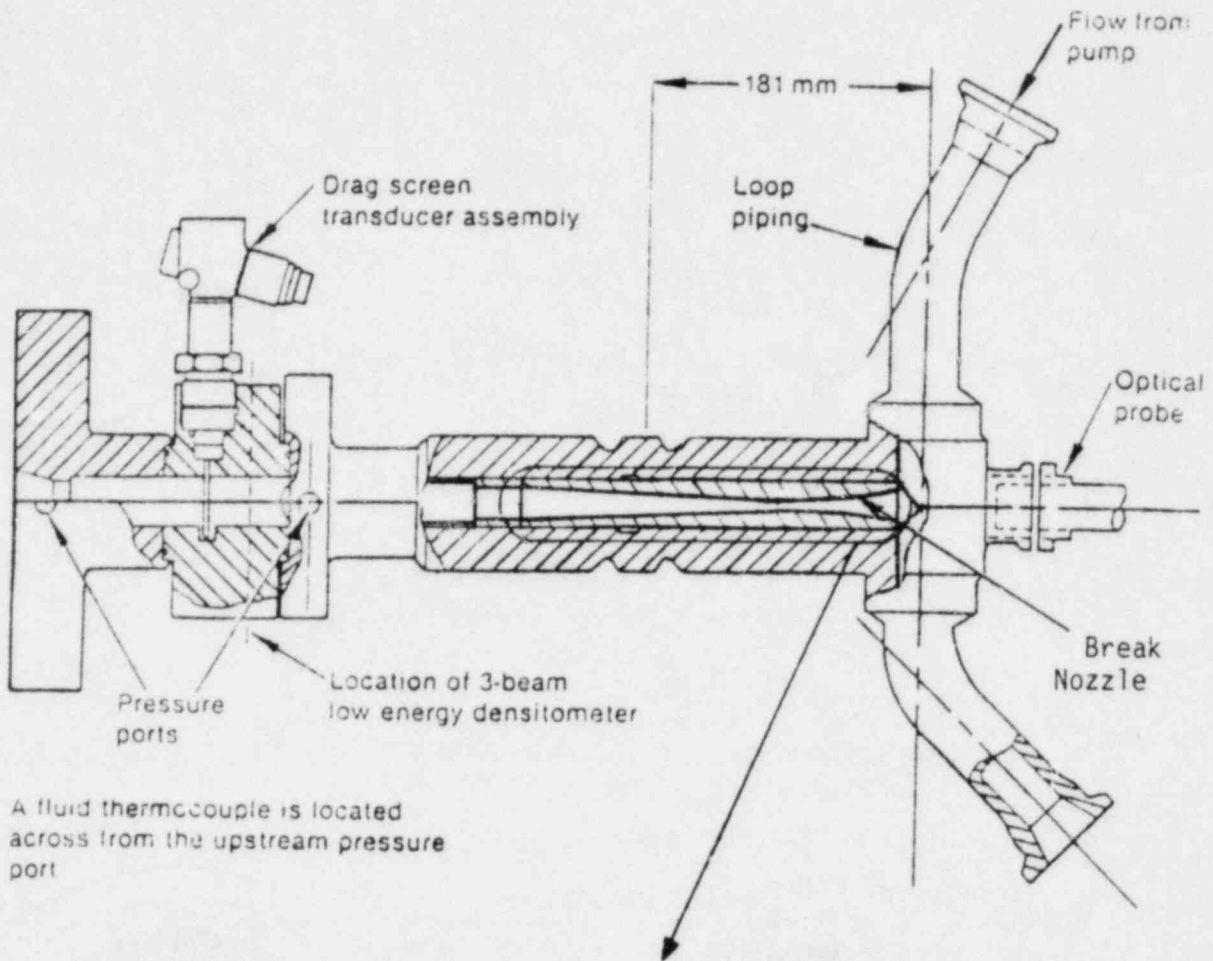


Figure 5. Cross-section of the Semiscale Mod-2A steam generators.



21.7% Break Nozzle
(All dimensions in mm)

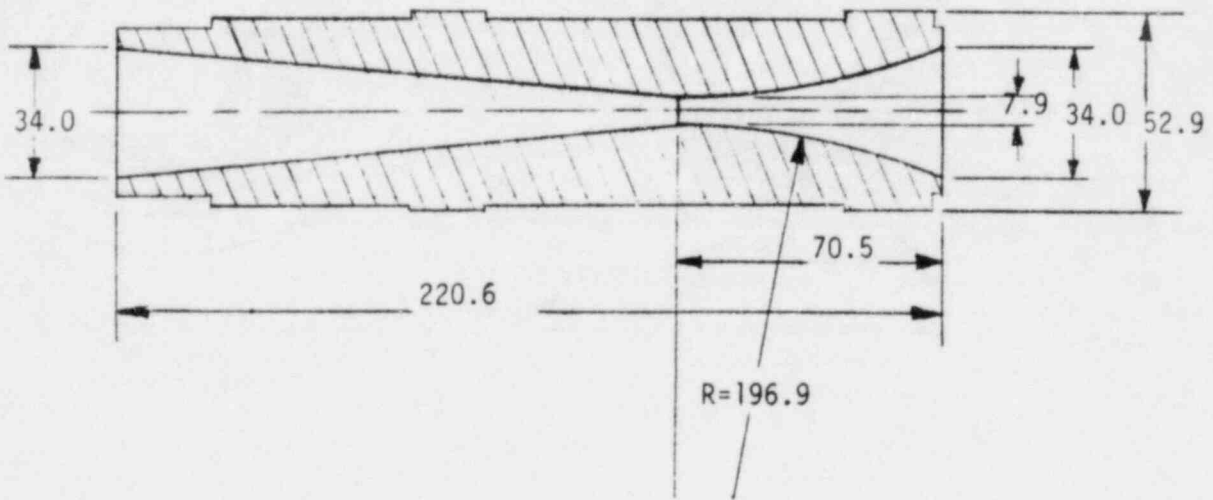


Figure 6. Break simulator for Test S-IB-3.

The resistance was decreased in the Broken loop by replacing the orifice plate at the pump discharge with one having essentially the same diameter as the cold leg ID. This resistance is reflected in the DPB*74*73 pump head measurements. Table 1 summarizes the general fluid system configuration and Table 2 lists miscellaneous configuration information of interest.

2.1.2 Control System Configuration

The functions of the control system of particular significance to these tests are the control of the core power, primary coolant pump speed, LPIS pump speed and isolation of the steam generators. The normal control functions involved in obtaining and maintaining steady-state initial conditions and then in the break initiation itself are not discussed here.

Core power is provided via seven DC power supplies, three units supplying the nine center rods and the other four units supplying the fourteen heated peripheral rods. Control signals to the power supplies come from a mini-computer, operating in an open loop mode, which has been programmed to provide a specified power decay profile. The profile, Figure 7, is based on the LOBI B-R1M test power decay profile.

Figure 8 shows the specified Intact and Broken loop pump speeds and Figure 9 the LPIS flow rate versus pressurizer pressure. The pumped injection flows are combined into a single trace since it is convenient, in Semiscale, to have a single, computer-controlled pump provide the total flow. The specified rate reflects the assumption that one of the two ECC and charging pump PwR trains fail, resulting in only 78% of the flow from two train operation. The steam generator steam valves are closed at 1.0 MPa pressurizer pressure trip, but the feed valves are closed on a ramp with the broken loop feed valve starting to close at 1 s after break initiation and being fully closed at 3.5 s after break initiation, and the intact loop feed valve starting to close at break initiation and being fully closed at 25 s after break initiation.

TABLE 1. GENERAL SYSTEM CONFIGURATION

Basic fluid system configuration	Mod 2A with unpowered external heaters
Major fluid systems used	Intact and Broken Loop Primary Coolant; Secondary Coolant; Coolant Injection; Pressure Suppression.
Reactor Vessel	Inverted top hat upper head internals.
Core	23 powered rods (A1, E5 not powered); flat radial profile; open loop control of heater rod power.
Steam Generators	Secondaries operational to establish primary coolant initial conditions, but then isolated during transient; feedwater injected at bottom of downcomers; no auxiliary feedwater used.
Primary Coolant Pumps	Open loop controlled speed reduction.
ECC	Accumulator and LPIS into Intact loop only.
LPIS	Delayed start; closed loop flow control on basis of primary system pressure.
Accumulator	Inject both water and then nitrogen
Break	
Location	Cold leg
Configuration	Communicative, rupture disc assembly connected to pressure suppression system
Size	21.7%

TABLE 2. MISCELLANEOUS CONFIGURATION ITEMS

Item	Drawing Number or other Reference ID	Status
Broken Loop Pump Discharge Resistance	410748, Rev. A	Installed orifice plate, part number -2 (orifice hole diameter = 3.25 cm)
Break flow spool bleed flow		Tubing connected from tap located between instrumented spool 76 and rupture disc assembly to suction of Broken loop pump (Spool 73). Flow restricted by use of small diameter tubing; Remotely controlled (on/off) valve in tubing line was closed before break initiation.
Accumulator CI-T-3 and diptube (ECC to Intact loop only)		Total volume of 0.067 m ³ (which includes 0.0056 m ³ in injection line) of water injection followed by 0.015 m ³ of nitrogen injection. (See Table 3.)
ECC injection line valve CI-V-4	404726, Rev.N	Adjust to achieve injection line R' of $2.0 \pm 0.2 \times 10^{10} \text{ m}^{-4}$ (specified)
Pressurizer surge line orifice		Provide orifice to achieve surge line R' of $3.2 \pm 0.3 \times 10^9 \text{ m}^{-4}$ (specified)
Downcomer/Upper Head Bypass Line Valve		Adjust to achieve 9.3% pressure drop ratio and record bypass/core flow ratio (Pressure drop ratio: upper head to upper plenum ΔP /downcomer to upper head ΔP)

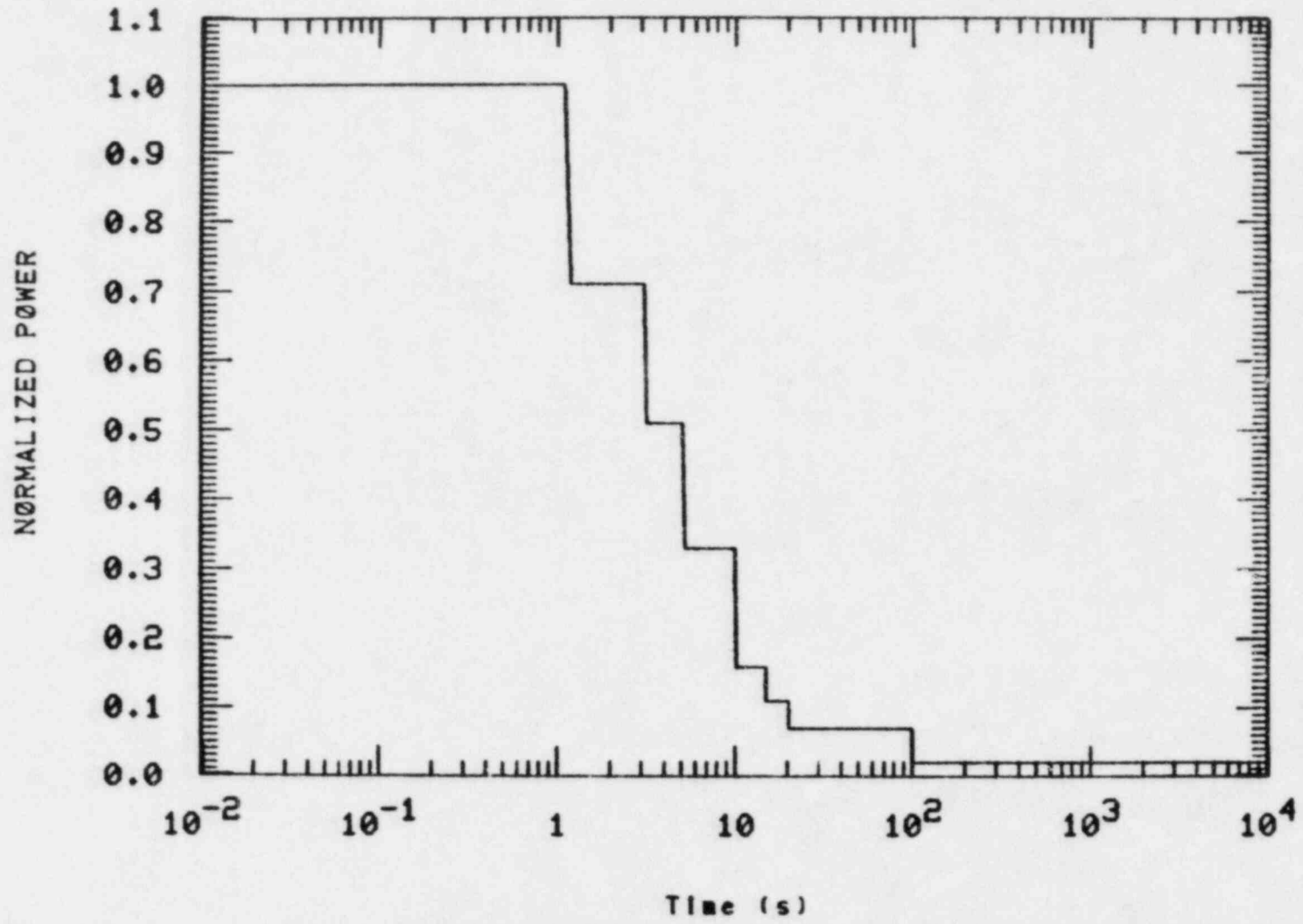


Figure 7. Normalized core power decay curve for Test S-IB-3.

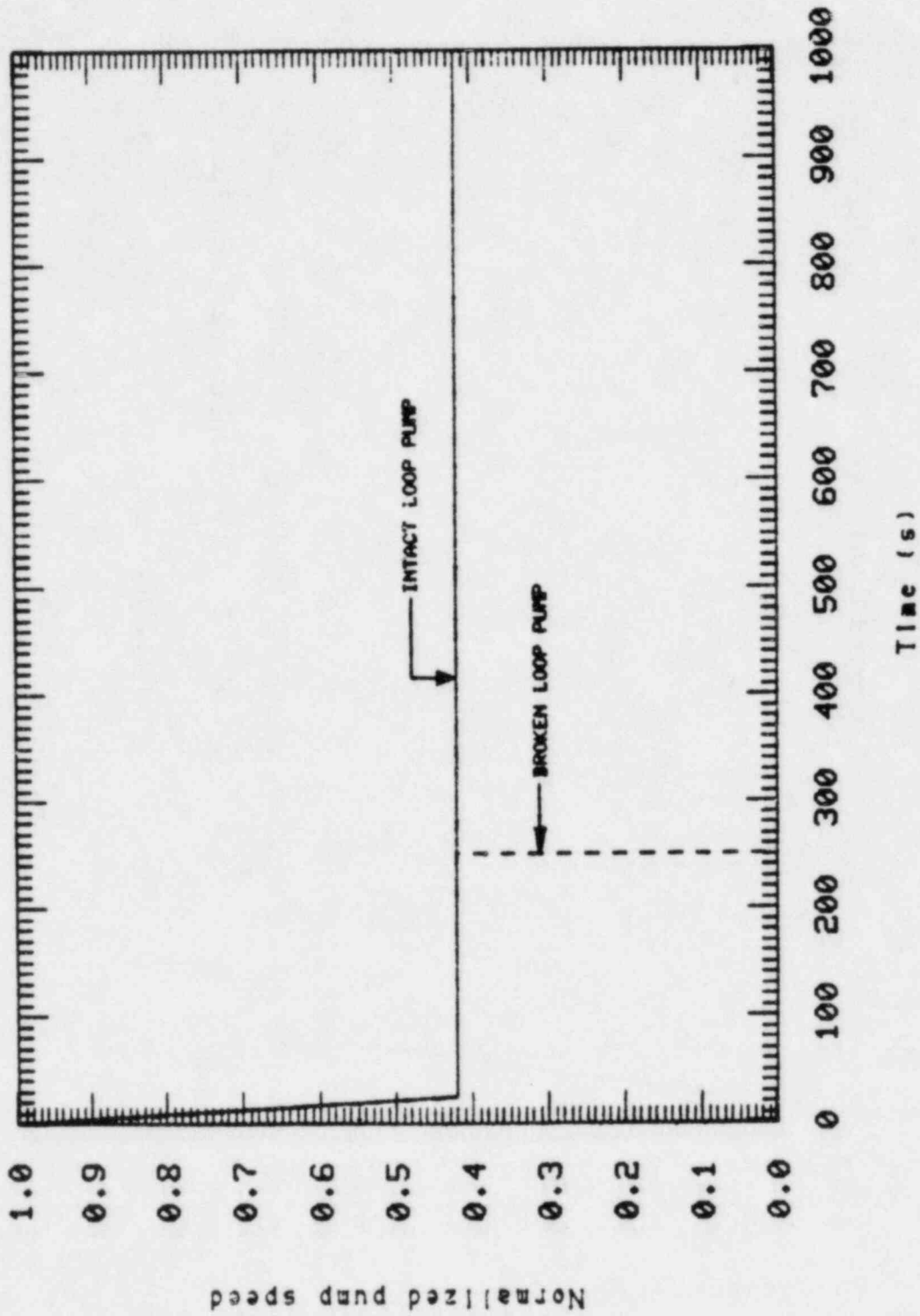


Figure 8. Normalized Pump Speeds From Beginning of Coastdown for Broken and Intact Loop Pumps.

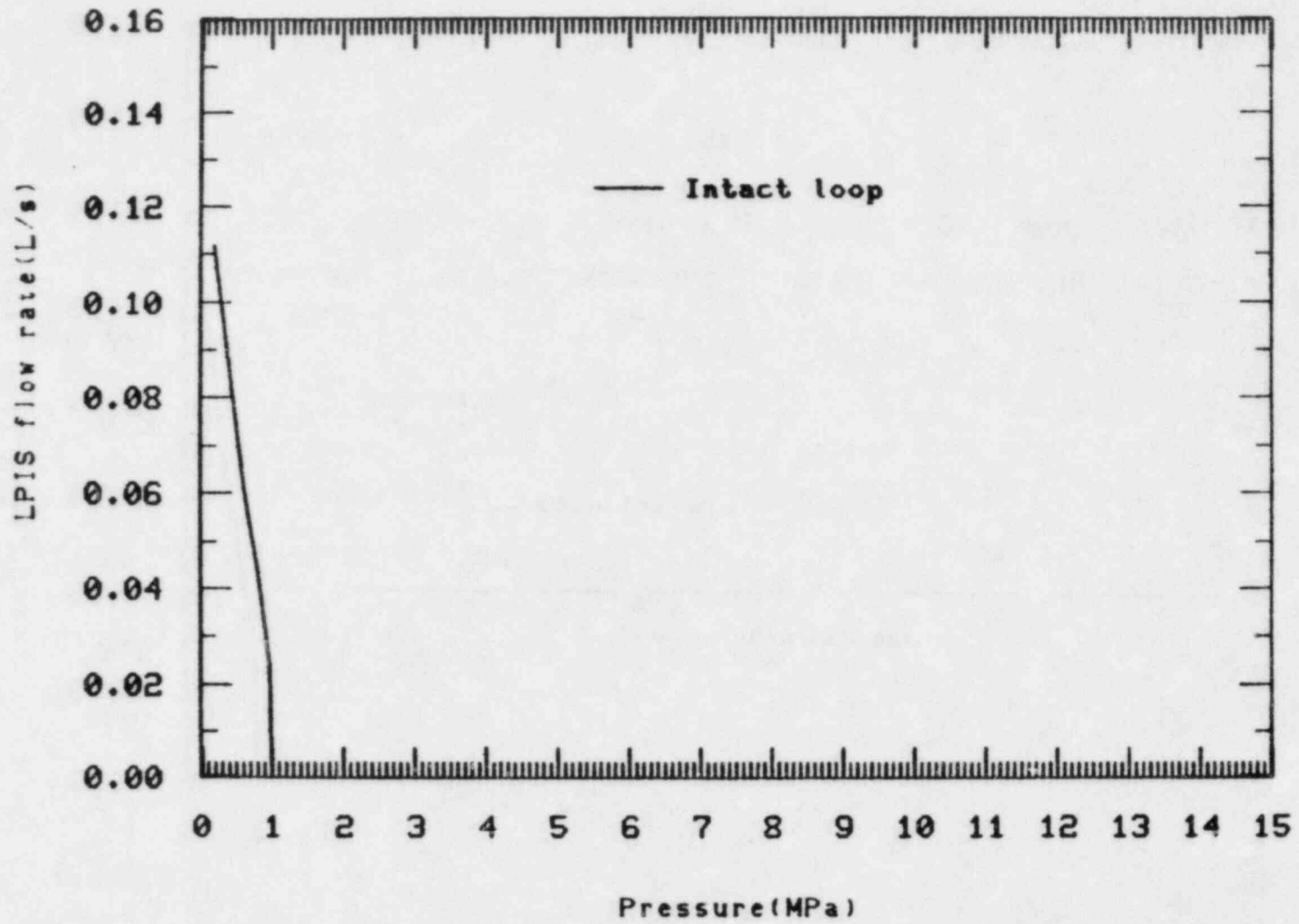


Figure 9. LPIS injection rate.

2.1.3 Measurement System Configuration

The 314 experimental measurements specified for this test are listed in the Appendix along with the initial condition values for each. These are preliminary data. Not necessarily have all obvious errors been found. The measurement identifier code is explained in detail in Reference 3. In general the code is intended to identify the measured parameter (TF - fluid temperatures) and the measurement location (I - Intact loop; 1 - spool piece No. 1). Thus, TFI*1 is as explained. Figure 1 identifies the locations of the instrumented spool pieces in the Intact and Broken loops. The system elevation reference is the cold leg centerline, above which elevations are positive. Generally, elevations in a vessel are listed in cm measured from a reference point on that vessel, e.g., the top of the steam generator tube sheet. The elevations of these vessel reference points, relative to the cold leg centerline, are listed in Reference 3.

Figure 10 shows the measurements made in the core and downcomer regions of the reactor vessel, as well as the location of the grid spacers and of the cosine staircase steps. Figure 11 shows the azimuthal orientations of the heater rod thermocouples in the core, as well as a cross section of a typical rod showing the radial location of the measuring element, and finally, the x-y locations of the in-core fluid temperature measurements. These thermocouples are attached to the core grid spacers and measure the fluid temperature about 1.2 cm above the tops of the spacers.

Voltages were digitized by the data systems at the rate of 40 times per second for those measurements on System I and 80 times per second on System II. System I/II information is included with each measurement listed in the Appendix. The instrument amplifier filter 3 db frequency was set at 3 Hz for all channels except the absolute pressures, for which the setting was 50 Hz. These channels are also identified in the Appendix list. All measured-data plots in this report reflect the results of the Semiscale data compression process. Thus, for the compression rate of three on a typical -10 to +60 s plot, each plotted point is the arithmetic average of the three succeeding values initially recorded on the data

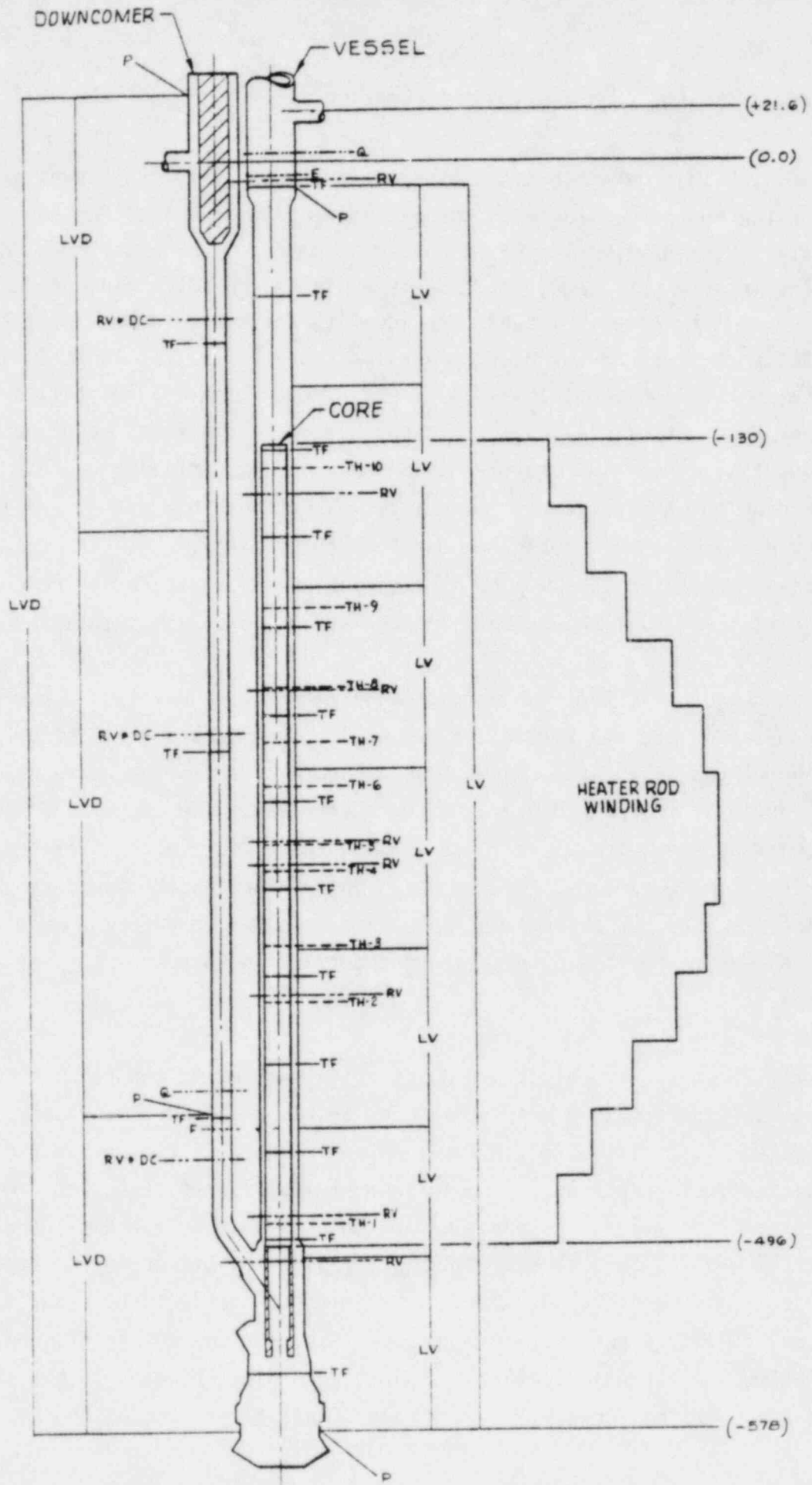


Figure 10. Core and downcomer measurements.

Densities	Levels	Grid Spacer ^{a,b} Fluid T/C's	Fluid T/C's	Flows	Pressures
RV*AB-6	LV-13M-105	TFV*D1+122	TFV*UPM-13	QV*UP+1	PV*UP-13
RV*23+13	LV-105-195	TFV*D1+162	TFV*UP-63	FV*UP-9	PV*LP-578
RV*23+113	LV-195-278	TFV*D1+323	TFV*LP-552		
RV*AB+173	LV-278-360	TFV*B3+45			
RV*23+183	LV-360-442	TFV*B3+122	TFV*DC-84	QV*DC-423	PV*DC+29
RV*23+253	LV-442-501	TFV*B3+162	TFV*DC-270	FV*DC-441	PV*DC-435
RV*23+342	LV-501-578	TFV*B3+242	TFV*DC-436		
RV*UP-11	LV-13M-578	TFV*B3+323			
		TFV*A4+79			
RV*DC-72	LVD+29-170	TFV*A4+162			
RV*DC-260	LVD-170-435	TFV*A4+242			
RV*DC-456	LVD-435-578	TFV*A4+283			
	LVD+29-578	TFV*A4+323			
		TFV*A4+361			

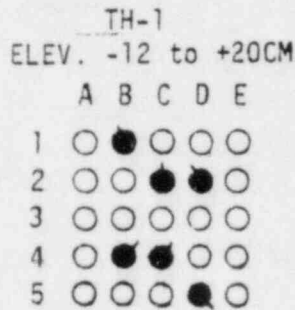
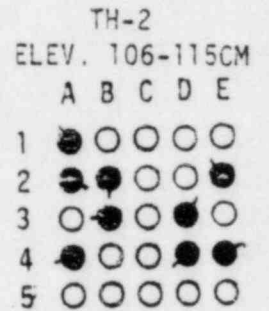
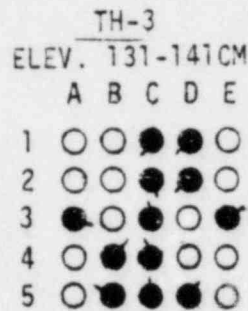
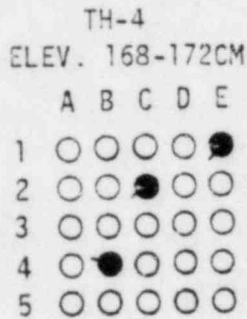
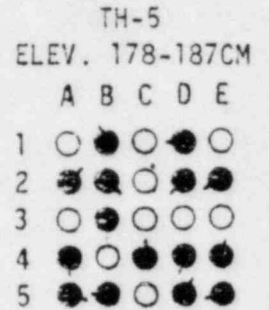
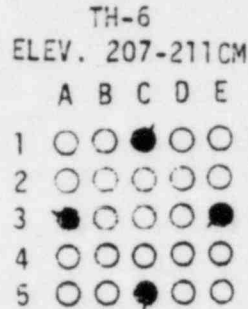
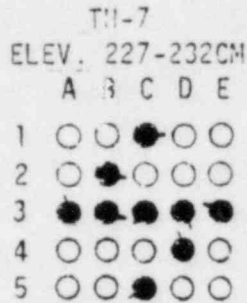
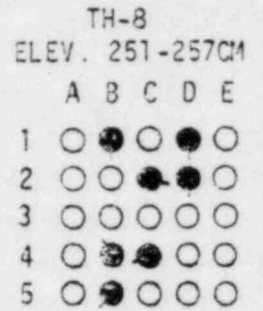
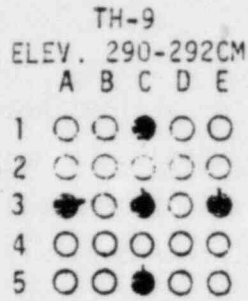
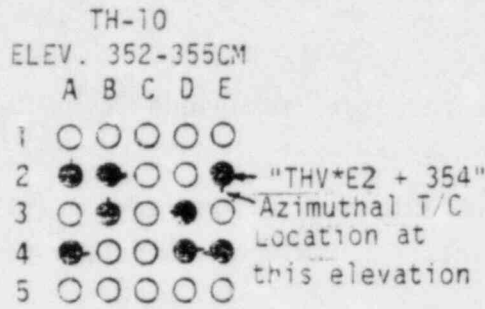
HEATER ROD T/C GROUPS^b

(TH-1 thru TH-10)

Group 1	Group 2	Group 3	Group 4	Group 5
(Elev. -12 to 20)	(Elev. 106 to 115)	(Elev. 131 to 141)	(Elev. 168 to 172)	(Elev. 178 to 187)
THV*B1+11	THV*A1+115	THV*A3+137	THV*B4+170	THV*A2+182
THV*B4-12	THV*A2+112	THV*B4+140	THV*C2+168	THV*A4+185
THV*C2+16	THV*A4+115	THV*B5+133	THV*E1+172	THV*A5+185
THV*C4+20	THV*B2+107	THV*C1+140		THV*B1+183
THV*D2+16	THV*B3+114	THV*C2+137		THV*B2+180
THV*D5+13	THV*D3+109	THV*C3+140		THV*B3+184
	THV*D4+106	THV*C4+142		THV*B5+180
	THV*E2+109	THV*C5+133		THV*C4+187
	THV*E4+112	THV*D1+131		THV*D1+178
		THV*D2+138		THV*D2+185
		THV*D5+139		THV*D4+179
		THV*E3+141		THV*D5+184
				THV*E2+181
				THV*E4+183
				THV*E5+181
Group 6	Group 7	Group 8	Group 9	Group 10
(Elev. 207 to 211)	(Elev. 227 to 232)	(Elev. 251 to 257)	(Elev. 290 to 292)	(Elev. 352 to 355)
THV*A3+208	THV*A3+228	THV*B1+253	THV*A3+291	THV*A2+353
THV*C1+211	THV*B2+227	THV*B4+256	THV*C1+292	THV*A4+355
THV*C5+207	THV*B3+229	THV*B5+252	THV*C3+292	THV*B2+353
THV*E3+211	THV*C1+232	THV*C2+254	THV*C5+290	THV*B3+354
	THV*C3+231	THV*C4+257	THV*E3+292	THV*D3+354
	THV*C5+228	THV*D1+251		THV*D4+352
	THV*D3+227	THV*D2+254		THV*E2+354
	THV*D4+228			THV*E4+354
	THV*E3+231			

a. All thermal-hydraulic measurements in the region of the core have elevations referenced to the bottom of the heated length (496 cm below cold leg centerline).

b. TF's shown in core are grid spacer locations; fluid T/C's are approximately one-half inch above or below the grid spacers.



TFV LOCATIONS

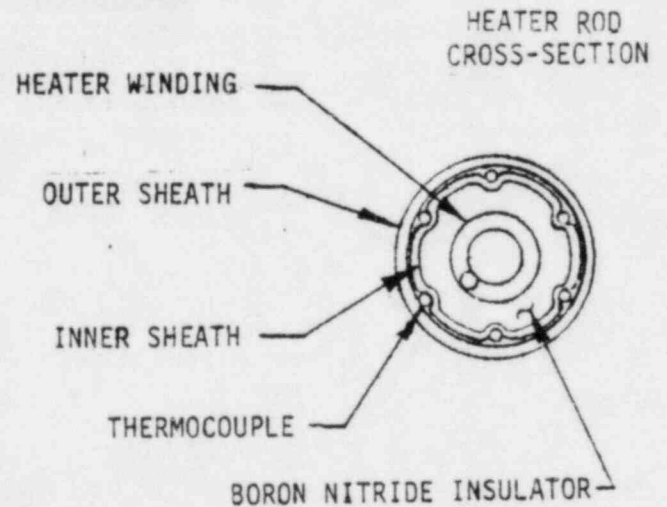
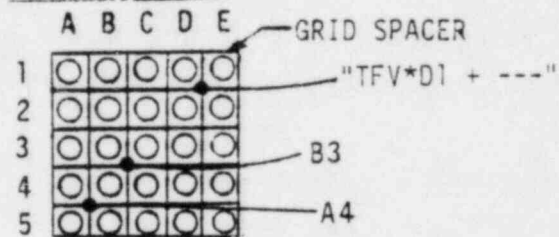


Figure 11. Heater rod and core fluid thermocouple locations.

system during the test. The present data reduction technique forms this average value prior to conversion to engineering units, and some conversion relations are non-linear. Software modifications in progress will reverse this averaging/conversion processing of data for tests in later series.

2.2 Test Procedures

2.2.1 Pretest Day Checkouts

Reference 1 lists the various measurement checks, controlled parameter checks, injection line resistance checks, etc. which were specified and accomplished in the two days before test day. These included such checks as liquid level "drain condition" differential pressures, densitometer empty/full ratios, turbine and drag screen flow checks, pressure checks, etc.

2.2.2 Test Day Warmup Operations

On test day, the fluid system is warmed to initial fluid temperatures and pressures over a few hour period and during this warmup, various additional measurement checks are performed. These include flow/no-flow comparisons, power pulse (to identify a sensitivity of any measurement to time varying core electrical power), leak rates, etc. These checks are done to establish and verify the operational readiness of the facility and measurement and control systems to perform the specified test.

2.2.3 Initial Conditions and Sequence of Controlled Events

The specified initial conditions are given in Table 3, abstracted from Reference 1, and the specified sequence of controlled events is given in Table 4.

TABLE 3. SPECIFIED INITIAL CONDITIONS^e

1. Primary Coolant System

Intact/Broken loop flow rate ratio (QI*1, QB*50)	3:1 ^a
Pressurizer pressure	15.5 ± 0.2 MPa
Core temperature rise	33 ± 2 K ^b
Cold leg fluid temperature (average of both loops at downcomer inlet)	563 ± 2 K
Total core electrical power	1.44 ± 0.05 MW
Core flow rate	7-8 kg/s ^c
Pressurizer liquid mass	8.2 ± 0.1 kg

2. Secondary Coolant System

Steam generator steam dome pressure (average)	5.4 ± 0.2 MPa
Steam generator feedwater temperature (average)	483 ± 2 K
Steam generator steam and feed flows and secondary levels	See Note d

3. Coolant Injection System

Intact loop accumulator	
Accumulator pressure	2.7 ± 0.1 MPa
Water volume	0.061 ± 0.001 m ³ , f
Nitrogen volume	0.015 ± 0.001 m ³
Water temperature	305 ± 10 K

4. Pressure Suppression System

Suppression tank pressure	0.24 ± 0.01 MPa
Suppression tank liquid level	0.0 ± 0.02 m downcomer submergence

a. Intact loop pump speed could be lower than past normal settings because of the lower flow rate in the loop and the reduced loop resistance. The Broken loop pump speed could be lower than past normal settings because of the reduced resistance at its discharge and the lower required flow rate in the loop, but this effect may be offset by the need for extra flow through the pump involved with the bleed flow from spool piece 76 to 73 (also see Table 2).

b. Core temperature rise may be temporarily determined by Intact loop hot leg/cold leg temperature difference while arrangements are being made to obtain actual core inlet/outlet measurements.

c. Approximate value; flow should be adjusted to achieve required core ΔT .

TABLE 3. (continued)

d. Maximum stable secondary liquid levels should be used. Steam and feed flow rates should be adjusted to obtain required primary side temperature and ΔT .

e. Initial conditions should be maintained for approximately ten (10) minutes (feedwater availability permitting) to establish and verify their steadiness and reproducibility. At least three (3) sets of time-average data should be obtained during this time.

f. This is the volume of water in the accumulator tank only and does not include the 0.0056 m^3 in the injection line. (See Table 2.)

TABLE 4. SPECIFIED SEQUENCE OF CONTROLLED EVENTS

Preblowdown

Final initial condition data set has been taken and steadiness of initial conditions (Table 3) has been verified.

- | | | |
|----|---------------|---|
| 1. | T-60 seconds | Start sequencer |
| 2. | T-30 seconds | Start countdown |
| 3. | T-28 seconds | Start continuous experimental data acquisition |
| 4. | T-15 seconds | Verify operational data system |
| 5. | T-2.5 seconds | <ul style="list-style-type: none"> A. Valve out the primary coolant ion exchanger if not done previously B. Close isolation valve in the circulation line from spool piece 76 to 73. C. Turn off makeup pump system D. Turn off pressurizer heaters |
| 6. | T-0.2 s | Pressurize rupture disk assembly to start blowdown transient |

Blowdown

- | | | |
|----|-----------------|--|
| 1. | T = 0.0 seconds | <ul style="list-style-type: none"> A. Core power computer begins controlling electrical power to heater rods. (See Figure 7.) B. Primary coolant pump speeds begin controlled transients. (See Figure 8.) C. Initiate intact loop steam generator feed valve closure. |
|----|-----------------|--|

Postblowdown

- | | | |
|----|------------------|---|
| 1. | T + 0.01 seconds | Isolate rupture disk pressurization system |
| 2. | T + 1 second | <ul style="list-style-type: none"> A. Valve off N₂ supply to ECC accumulator and enable accumulator liquid flow to start (when accumulator pressure exceeds system pressure). |

TABLE 4. (continued)

	B. Initiate broken loop steam generator feed valve closure.
3. Pressurizer pressure reaches 12.6 MPa	Enable LPIS
4. $t = 3.5$ seconds	Broken loop steam generator feed valve closed.
5. $t = 25$ seconds	Intact loop steam generator feed valve closed.
6. Pressurizer pressure reaches 1 MPa	LPIS pump starts injection into the intact loop (only) with flow rate corresponding to pressurizer pressure at that time per Figure 9. Close intact and broken loop steam valves.
	Trip broken loop pump power.
7. Terminate test	Trip core power; trip LPIS pump power; trip Intact loop pump power; secure system.

2.3 Comparison of Specified and Actual Configuration and Operations

None of the differences enumerated below, either taken singly or in concert, were considered to be sufficient to prevent general achievement of the test objectives. However, it is considered useful to note these differences in order to provide a better understanding of the test results.

2.3.1 Configuration

The configuration was as specified in Tables 1 and 2 except as follows. The pressurizer surge line R' (resistance) was $1.4 \times 10^9 \text{ m}^{-4}$ compared to the specified $3.2 \times 10^9 \text{ m}^{-4}$. Minor differences were found in the core bypass/upper head internals pressure drop and flow rate.

2.3.2 Initial Conditions

Table 5 is a comparison of specified, measured and calculated (RELAP5) initial conditions. Although the average of the measured cold leg temperatures falls within the specified range, both of the individual values were outside that range, the Intact cold leg temperature being 559 K and the Broken loop being 566 K. This is also reflected in the different steam generator pressures, and the fact that the broken loop steam generator steam valve was nearly closed at initial conditions. Also, the amount of makeup water added to the pressurizer to makeup for a primary coolant system leak was larger than necessary, resulting in a larger mass of water (10.1 kg) in the pressurizer at blowdown than the specified 8.2 kg of water.

The accumulator pressure at initial conditions was low (2.6 MPa versus 2.7 MPa specified). The actual accumulator water volume was lower than specified (.066 versus .067 m^3) as determined by liquid level.

TABLE 5. SPECIFIED, MEASURED AND CALCULATED INITIAL CONDITIONS

	<u>Specified</u>	<u>Measured</u>	<u>RELAP5 Calculated</u>
<u>1. Primary Coolant System</u>			
Intact/Broken loop flow rate	3:1	2.9:1	3:1
Pressurizer pressure, MPa	15.5 + 0.2	15.53	15.5
Upper plenum pressure (MPa)	15.5 ± 0.2	15.58	15.5
Cold leg temperature (K)			
Intact loop	563 + 2	559.4	565
Broken loop	563 ± 2	566.4	564
Hot leg temperature (K)			
Intact loop	596 + 2	596.1	596
Broken loop	596 ± 2	596.9	596
Core temperature rise, K			
Intact loop	33	36.7	31
Broken loop	33	30.5	32
Total core electrical power, MW	1.44 ± 0.05	1.45	1.44
Core inlet flow rate, (kg/s)	7-8	8.02	7.48
Core Bypass Flow (% of Total)	2.5	3.7	2.62
Pressurizer liquid mass, kg	8.2 ± 0.1	10.1	8.2
<u>2. Secondary Coolant System</u>			
Steam Generator Secondaries Pressure:			
Intact loop (MPa)	5.4 + 0.2	6.48	6.4
Broken loop (MPa)	5.4 ± 0.2	7.53	6.6
Feedwater Temperature:			
Intact loop (K)	483 + 2	492.5	483
Broken Loop (K)	483 ± 2	484.7	483
Steam Temperature:			
Intact loop (K)	542 + 2	553.5	553
Broken Loop (K)	542 ± 2	564.4	555
<u>3. Coolant Injection System</u>			
Intact loop accumulator			
Pressure, MPa	2.7 + 0.1	2.6	2.7
Water volume, (m ³) (including injection line)	0.067 ± 0.001	0.066	0.067
Nitrogen volume, (m ³)	0.015 ± 0.001	0.015	0.015
Water temperature, (K)	305 ± 10	298	305
<u>4. Pressure Suppression System</u>			
Suppression tank			
Pressure (MPa)	0.024 + 0.01	0.25	--
Water level (m)	0.0 ± 0.02	--	--

2.3.3 Controlled Parameters

The LPIS flow rate was as specified.

The actual core power is shown in Figure 12 and is shown with the specified power profile in Figure 13. The decrease in actual power that was to have started at 1.1 s started at 1.6 s and lasted until 2.2 s (should have been over at 1.2 s). The actual power increased from 4.3 s to 4.8 s and decreased back to the specified value between 4.8 s and 5.4 s. Other than this short term deviation the actual power followed the specified behavior thereafter with a .5 s delay on the start of power decreases and 0.5 s delay on reaching new power levels.

The Intact loop pump speed went to 37% of the initial speed instead of the specified 42%, and the Broken loop pump speed went to 52% of the initial speed instead of the specified 42%. The Intact loop steam generator feed valve closed at 30 s instead of the specified 25 s, and the Broken loop steam generator feed valve closed at 2.5 s instead of the specified 3.5 s. The steam generator steam valves were closed as specified.

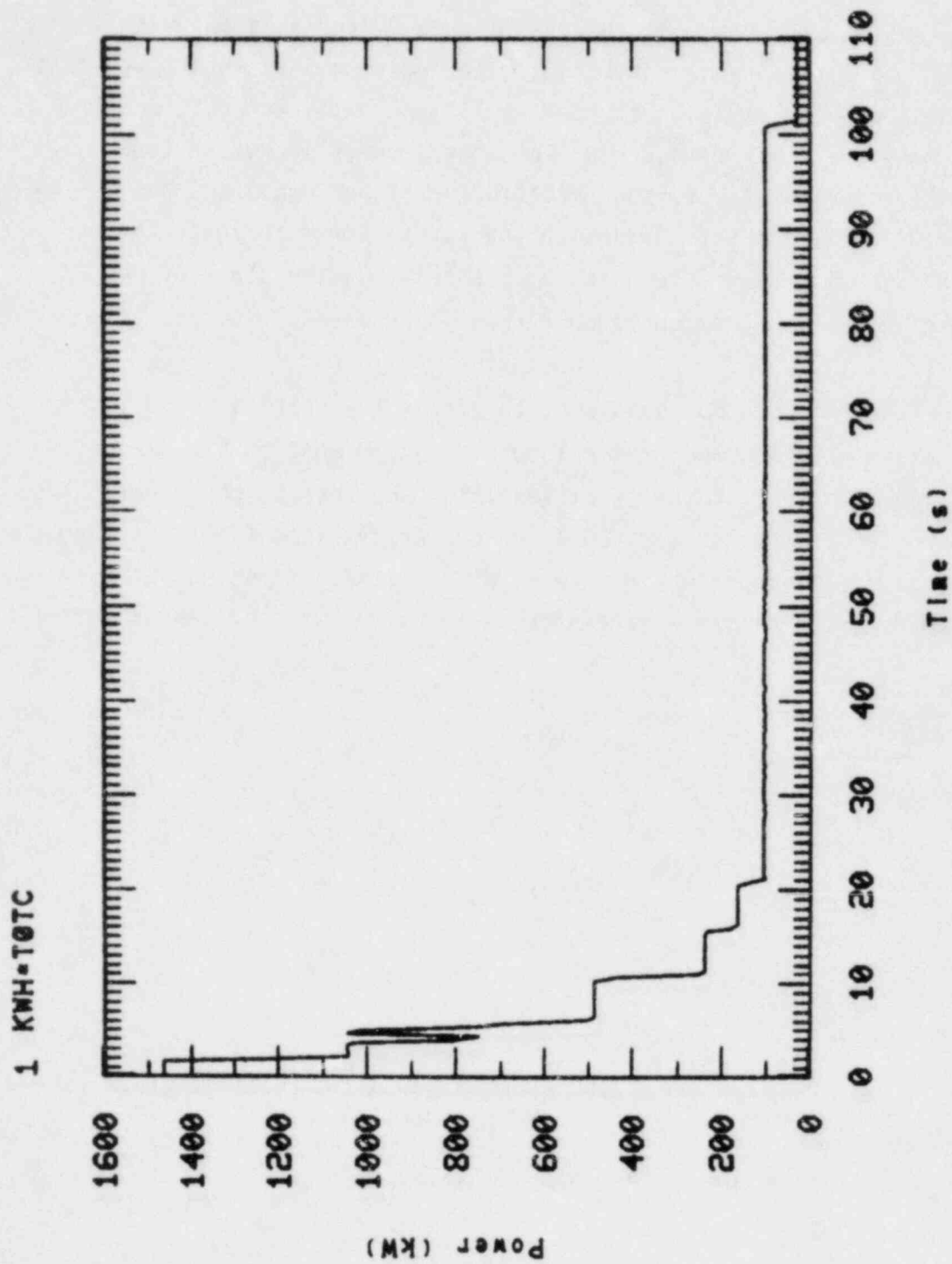


Figure 12. Measured core power.

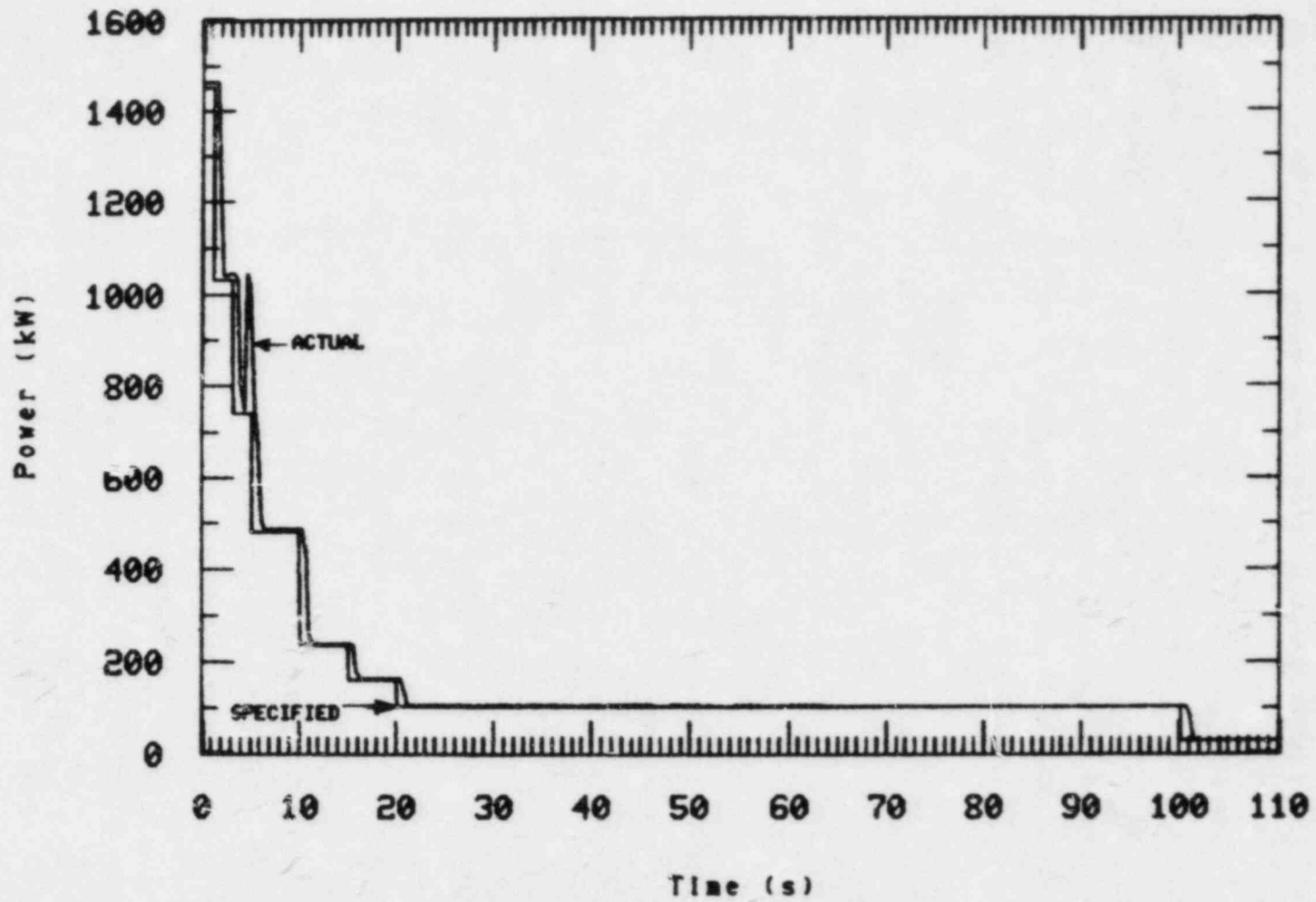


Figure 13. Actual and specified core power.

3. TEST RESULTS

3.1 Description of the Transient

3.1.1 General System Response

Data were obtained to approximately 530 seconds after system rupture was initiated. Of this time, the first 240 seconds was consumed in blowdown; the formation of liquid seals in the Intact and Broken loop pump suction started at about 10 seconds; the Broken loop pump suction liquid seal cleared between 27 and 34 seconds; the Intact loop pump suction liquid seal cleared between 89 and 160 seconds; refilling of the lower plenum was completed at about 92 seconds (Figure 14); and reflood started at about 190 seconds. Two temperature excursions were observed. The first excursion occurred at about 50 seconds and was caused by a depressed core liquid level, due to the Intact loop pump suction liquid seal. The second excursion occurred at about 190 seconds and was caused by boil off of liquid in the core. The highest parts of the core were quenched at about 350 seconds. The highest measured heater temperature occurred during the first temperature excursion in heater rod B3, at the core midplane, 184 cm (Figure 15), at 102 seconds and was 764 K. Table 6 lists events of interest, most of which occurred during the blowdown.

3.1.2 Reactor Vessel and Loop Hydraulics

Figure 16 shows the upper plenum pressure. The fluid had reached saturation and started to flash by 2 seconds in the upper plenum, by 3 seconds in the Intact loop hot leg, and by 5 seconds in the Broken loop hot leg. The flashing in the upper plenum shows up as a slight plateau in the depressurization at 2 s in Figure 16. The flashing of the Intact and Broken loop hot legs is shown by the slight repressurization at 5 s in Figure 16. Figure 17 compares the hot leg, cold leg, and saturation temperatures and shows that nearly all of the system became saturated by 15 to 20 s. This shows up as a knee in the pressure curve in Figure 16 at about 15 seconds. The depressurization rate increases slightly at 34 s once the Broken loop pump suction had substantially cleared out (Figure 18)

1 VLBET-442-501

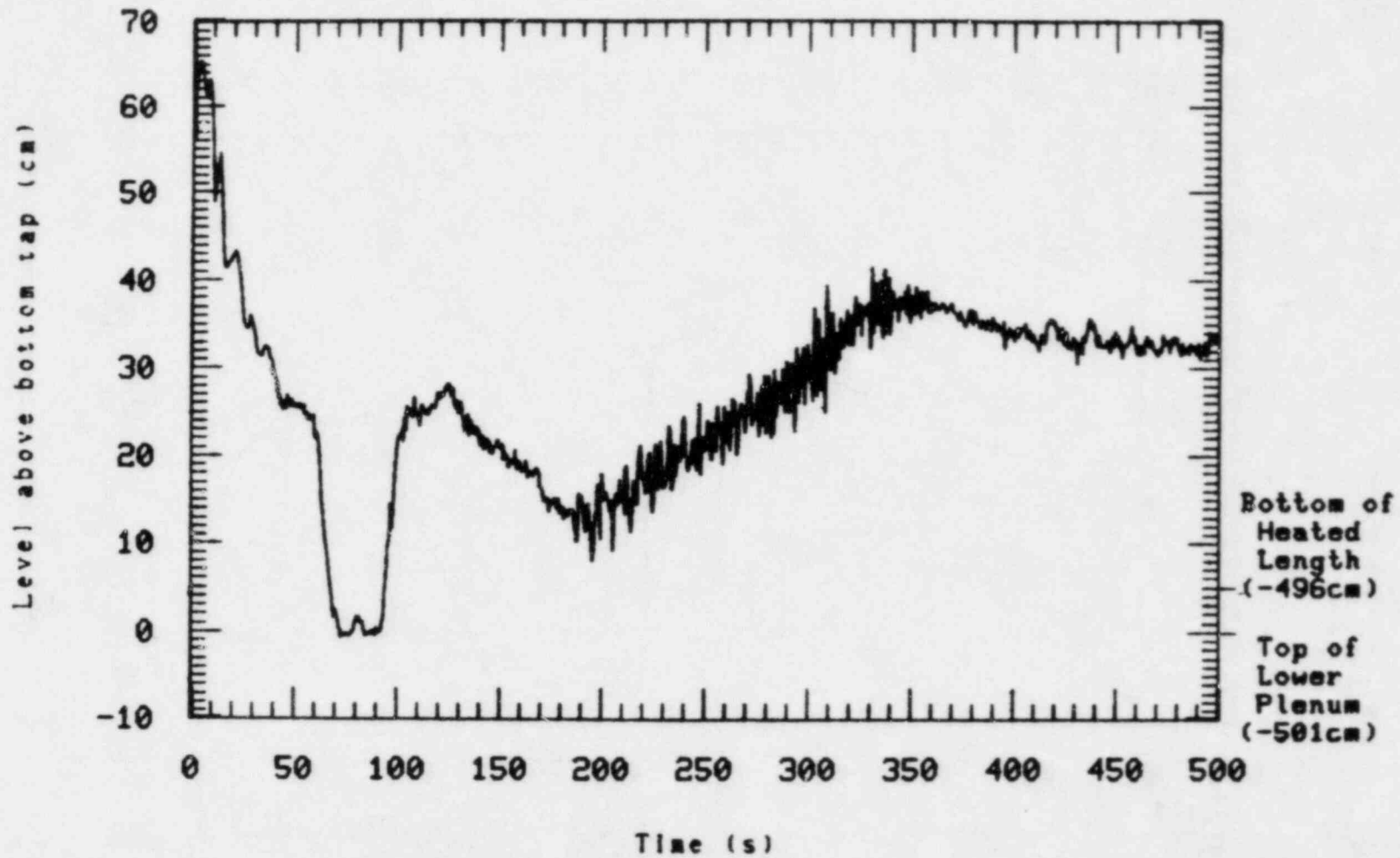


Figure 14. Core bottom liquid level.

1 THV-B3-184

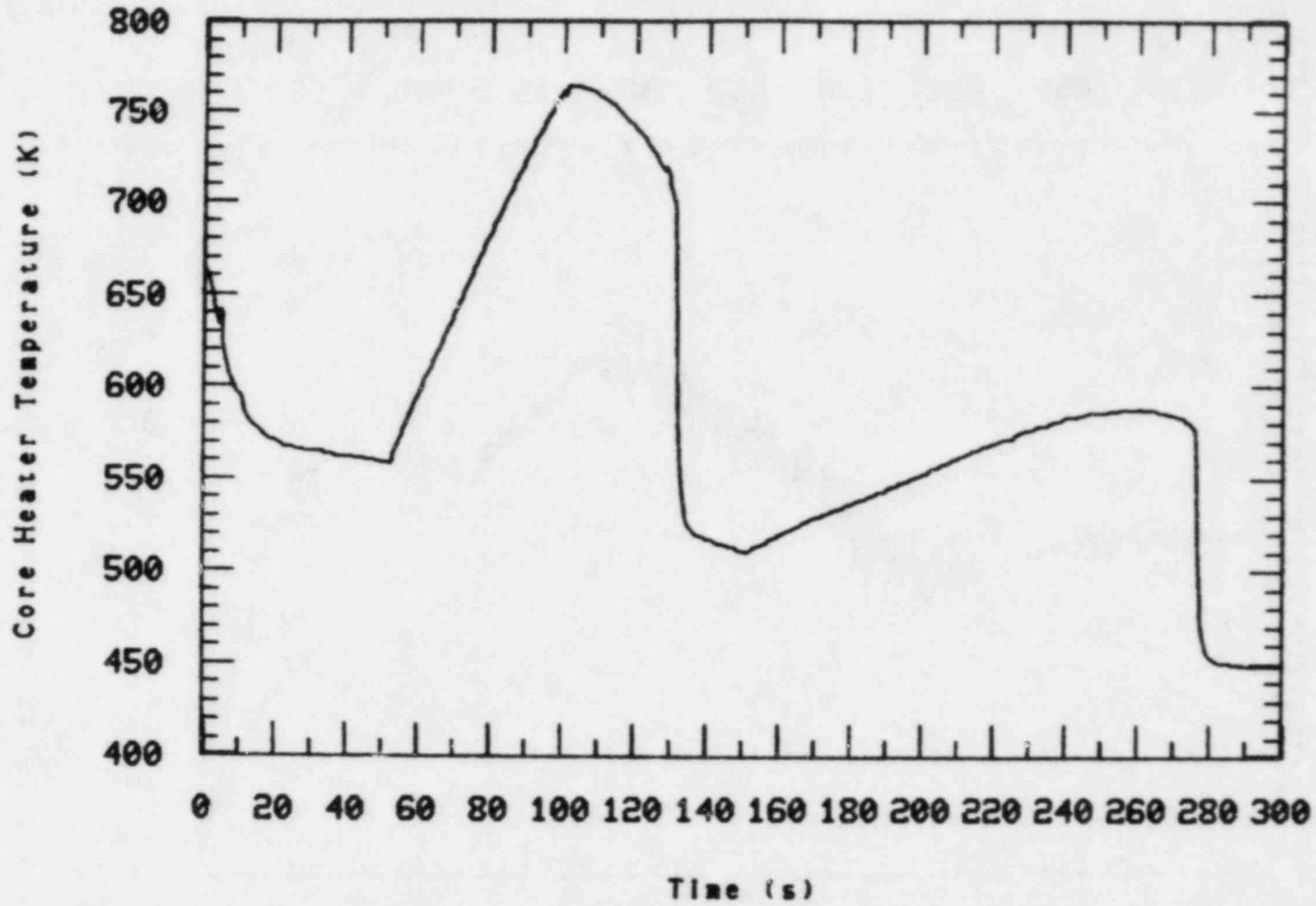


Figure 15. Highest measured heater rod temperature (184 cm in rod B3).

TABLE 6. CHRONOLOGY S-IB-3

Event	Time, Seconds
Rupture initiated; core power, pump speed transients started	0
Broken loop cold leg flow reverses between vessel and break	<1
Upper plenum fluid saturates	1.5
Fluid in Intact loop hot leg saturates	2.2
Broken loop steam generator feed valve closed	2.5
Fluid in Broken loop hot leg saturates	4.5
Pressurizer empties	7
Guide tube flow reverses	14
Core bypass line flow reverses	14
Fluid in Broken loop cold leg (downcomer to break) saturates	16
Fluid in Intact loop cold leg saturates	17
Intact loop pump head fully degraded	17
Broken loop pump head fully degraded	22
Flow reverses in Broken loop hot leg	22
Broken loop steam generator secondary becomes energy source	22
Broken loop pump suction liquid seal starts to clear	27
Flow in guide tube stagnates	27
Intact loop steam generator feed valve closed	30
Intact loop pump reaches steady (.37) of initial speed	30
Broken loop pump reaches steady (.52) of initial speed	30
Flow stagnates in downcomer	41
First temperature excursion starts	50
Top of guide tube uncovers	52
Steam starts flowing down guide tube	57

TABLE 6. (continued)

Event	Time, Seconds
Top of bypass line uncovers	80
Intact loop pump suction liquid seal starts to clear	89
Lower plenum refilled	92
Core power drops to (0.02) of initial power	100
First temperature excursion reaches peak	102
Intact loop steam generator secondary becomes energy source	105
Upper head liquid level falls below 173 cm	119
First temperature excursion quenched	130
Upper head empty	140
Flow stagnates in guide tube	156
Accumulator liquid flow starts	163
Flow reverses in downcomer	163
Steam flow starts up guide tube	170
Accumulator liquid bypass ends; Refill starts Second temperature excursion starts	190
Blowdown is over; Broken loop pump tripped, LPIS flow starts, Intact and Broken loop steam valves closed; Second temperature excursion reaches a plateau	240
Most of core quenched	280
Upper elevations of core quenched	350
Data acquisition system shut down	531

1 PV=UP-13

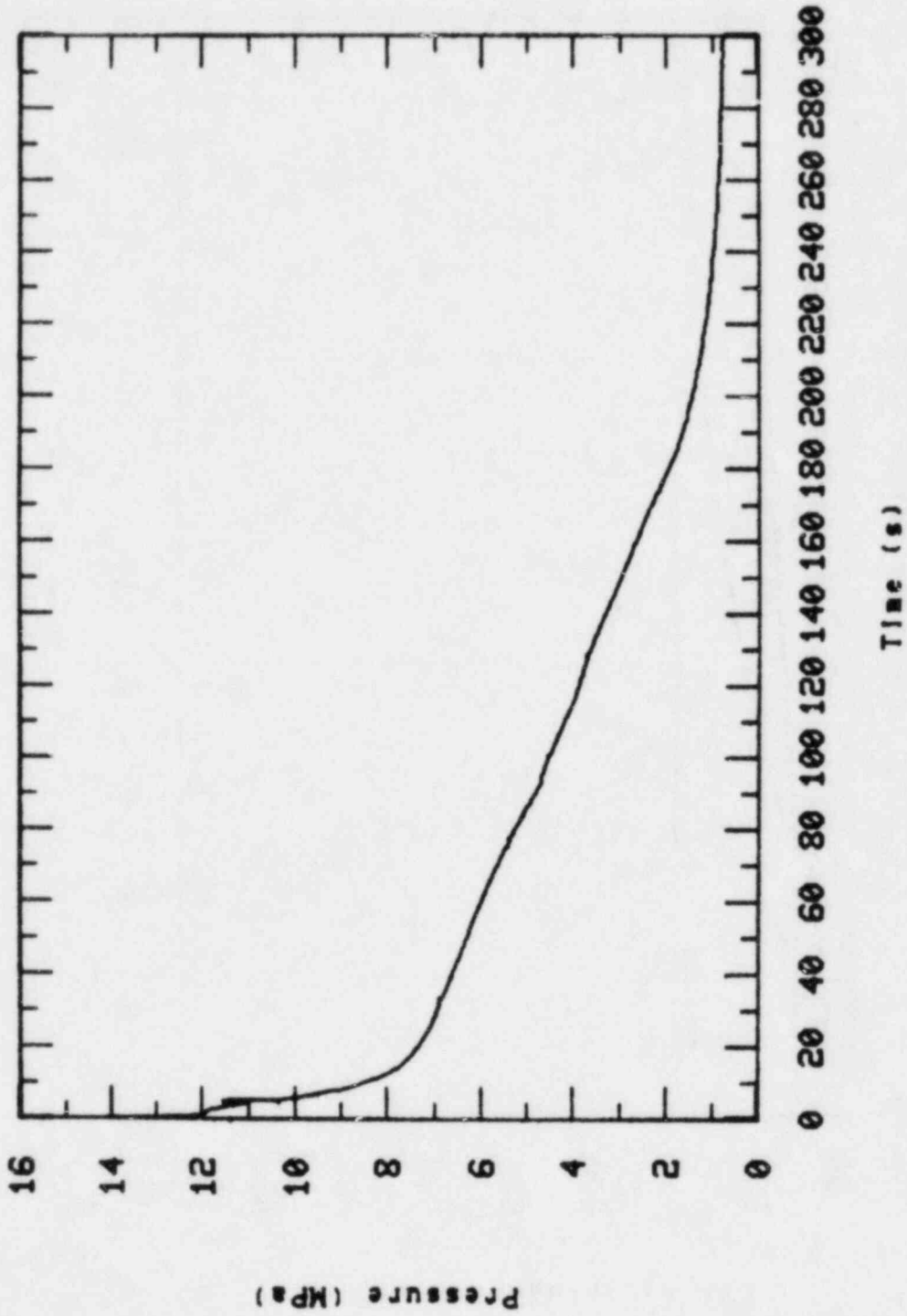


Figure 16. Upper plenum pressure.

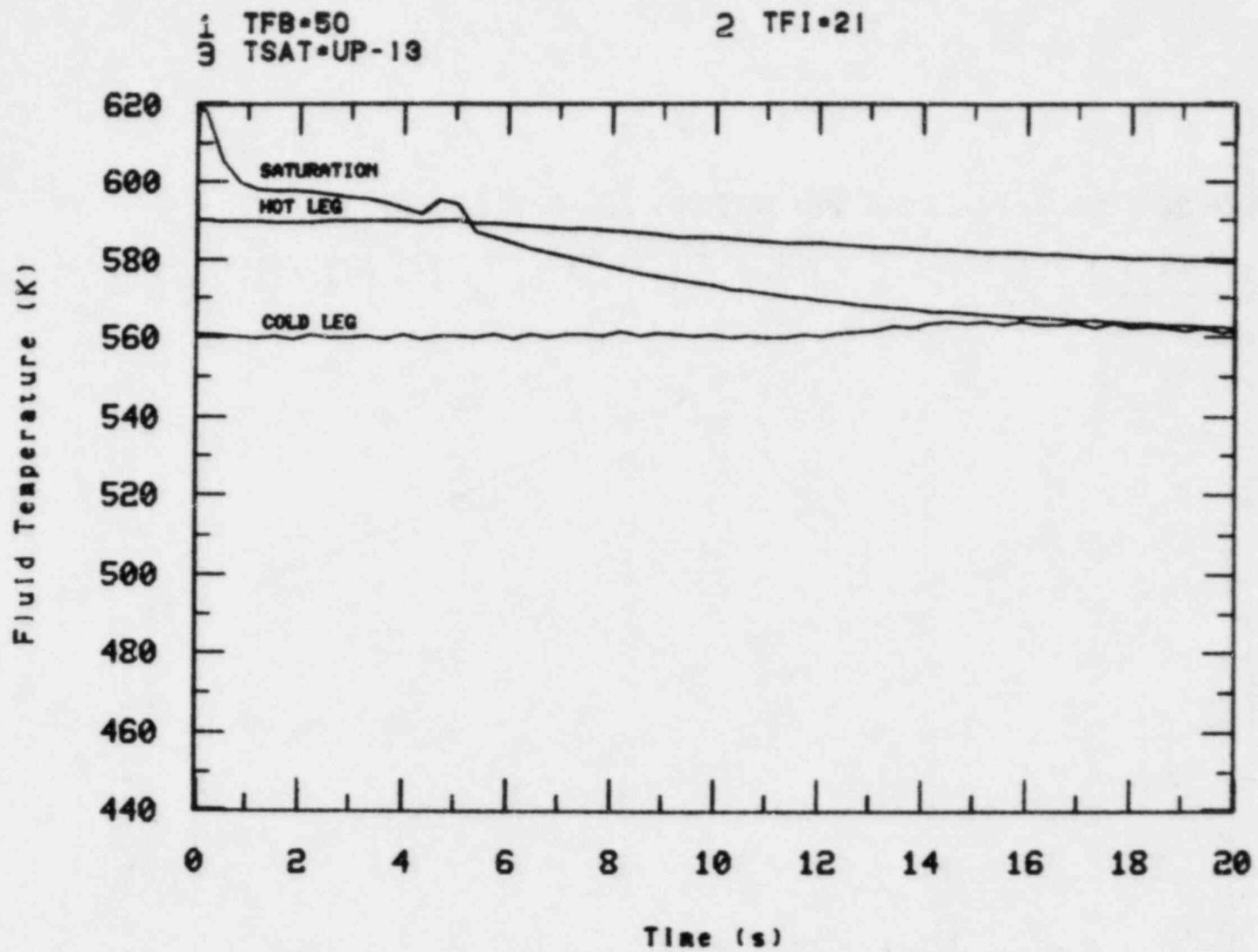


Figure 17. Hot leg, cold leg, and saturation temperatures for Test S-IB-3.

1 LEVEL-BET-05-73

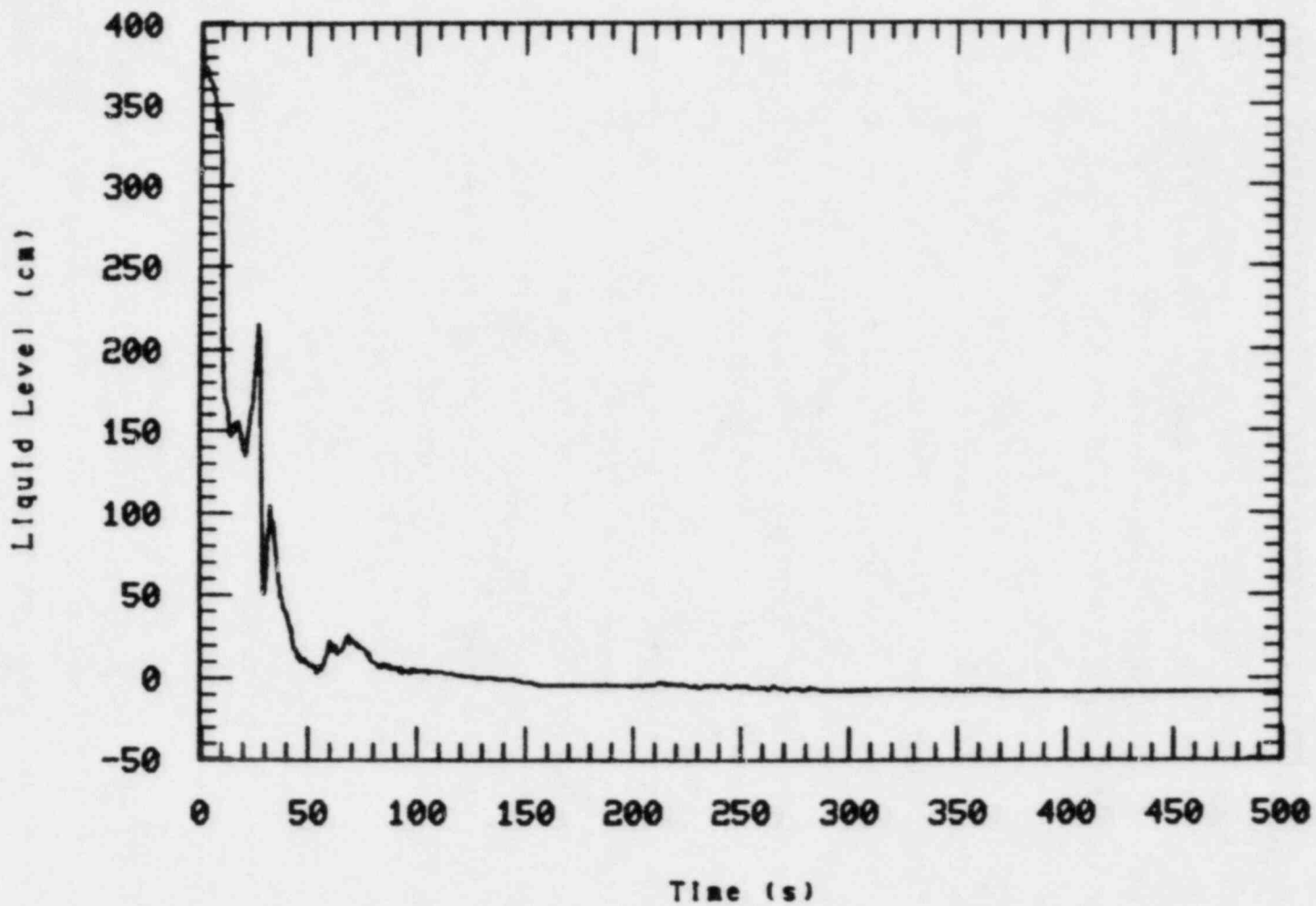


Figure 18. Liquid level in broken loop pump suction upflow leg.

and higher quality fluid reached the break. The depressurization rate also increased slightly at about 130 s once the Intact loop pump suction had substantially cleared out (Figure 19) and afforded the steam in the vessel a lower resistance path to the break.

System behavior during the first 130 s of the transient was characterized by continuous voiding from the upper elevations downward. The phenomena of interest include gravity drain, liquid holdup in the steam generator tubes and pump suction upflow legs due to steam flow, and the formation of liquid seals in the pump suction piping.

Immediately after rupture, the pressurizer began injecting its fluid into the Intact loop hot leg and continued until empty at about 7 s. Within the first second after rupture, the flow in the Broken loop cold leg between the vessel and the break reversed direction. The upper plenum fluid became saturated at 1.5 s. Steam, formed in the upper plenum, flowed into the hot legs to the top of the steam generator tubes where it replaced the water that had drained from the higher elevations.

Liquid had completely drained from the downflow side of the steam generator tubes by 10 to 15 s. The fluid in the pump suction legs then formed seals that impeded vapor flow around the loops. This restriction of vapor flow around the loops caused vapor in the vessel to flow up the guide tube into the upper head, reversing the flow in the guide tube at about 14 s (Figure 20). Thus the upper head pressure increased and the flow in the bypass line reversed at about 14 s and started down the bypass line to the downcomer inlet annulus (see Figure 4).

Due to the asymmetric operation of the steam generators prior to blowdown, the Broken loop steam generator steam valve was essentially closed prior to and at blowdown. Since the steam valves were specified to be left open at their steady state operating position until the system pressure reached 1 MPa (blowdown over), at which time they were to be closed, the Broken loop steam generator was essentially isolated throughout the blowdown while the Intact loop steam generator was not. This effective isolation of the Broken loop steam generator caused the secondary pressure

1 LEVEL-0ET-14.18

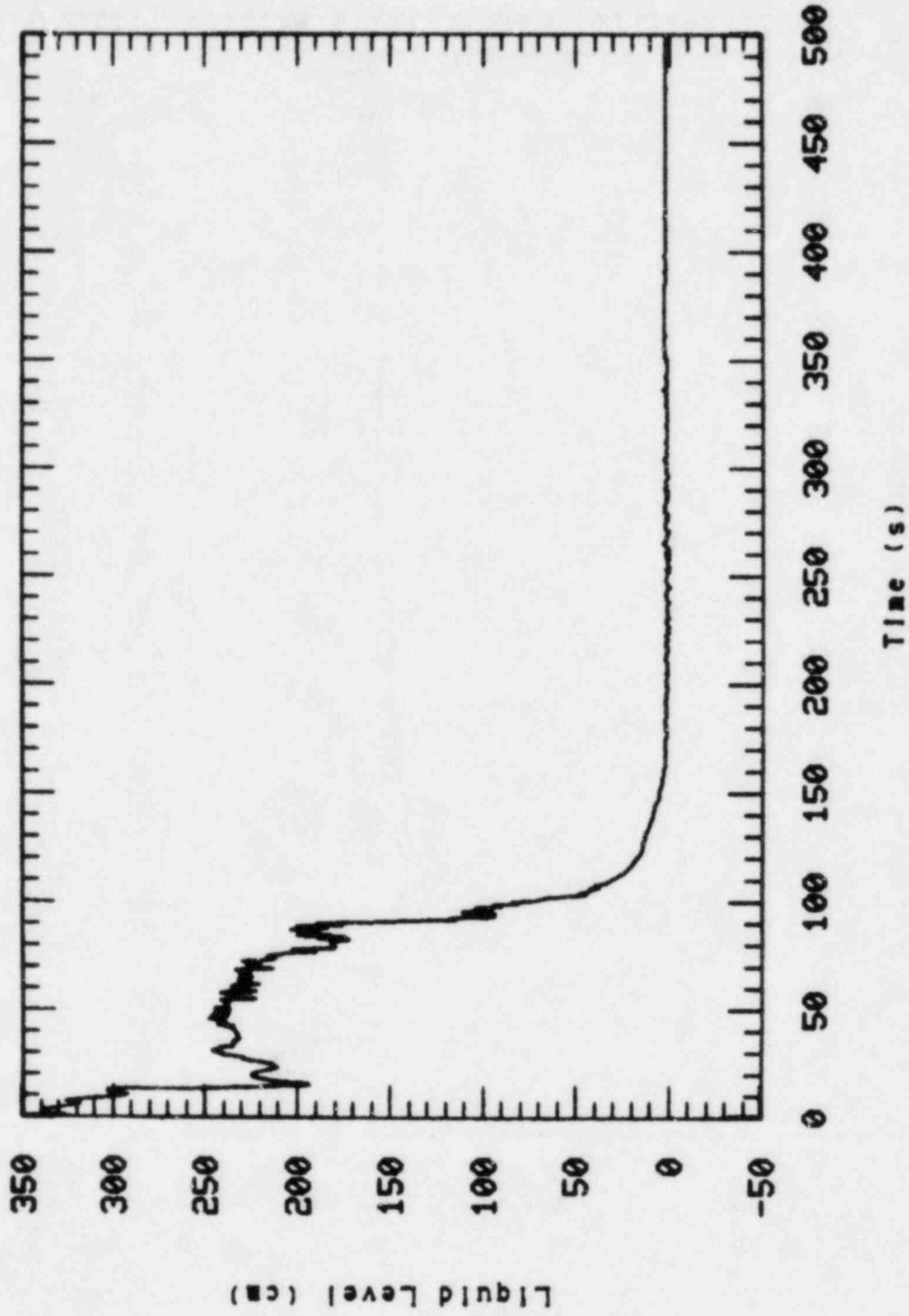


Figure 19. Liquid level in intact loop pump suction upflow leg.

1 FV-GT-330

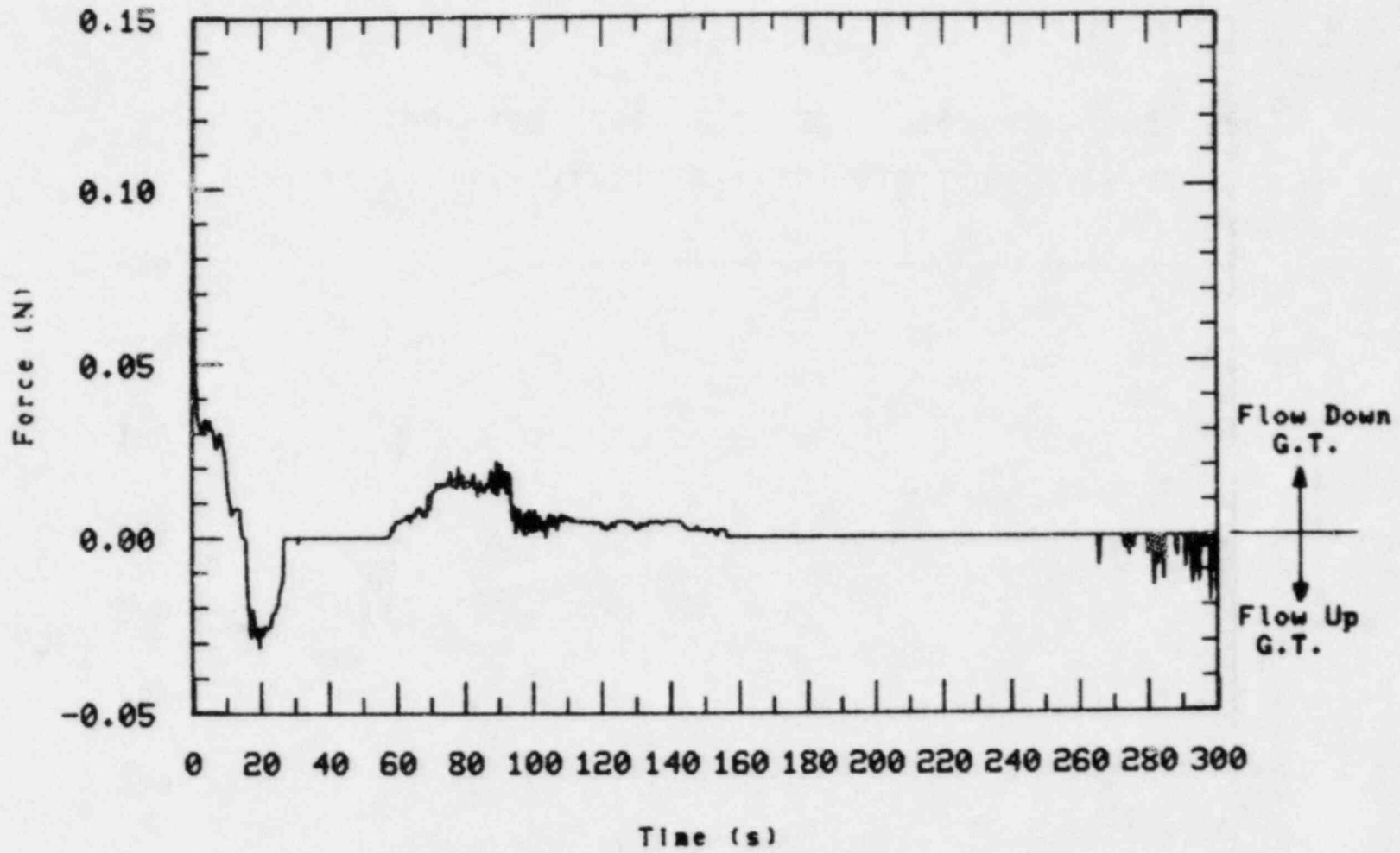


Figure 20. Guide tube momentum flux and flow direction.

in the Broken loop steam generator to remain very near to the initial secondary pressure and thus the Broken loop steam generator became a heat source earlier (between 15 and 25 s; Figure 21) than it should have. Once the Broken loop steam generator became a heat source the vapor in the tubes of the generator was no longer condensed. Consequently the liquid seal in the pump suction was not replenished by condensate. It is believed that this probably caused the Broken loop pump suction liquid seal to start to clear prematurely (between 27 and 34 s; Figure 18). Posttest calculations will investigate this further.

Prior to the pump suction starting to clear, the flow in the Broken loop was being restricted and actually stagnated at about 22 s. This restricted flow caused liquid which was being held up in the upflow leg of the steam generator tubes to fall back down the tubes and forced the flow in the Broken loop hot leg to reverse at about 22 s (Figure 22). The reversed flow continued until the Broken loop pump suction liquid seal started to clear, reducing the flow restriction, and allowing the vapor generated in the vessel to flow through the Broken loop hot leg. Steam flow in the upflow side of the Intact loop steam generator tubes held up some liquid in the tubes until 150 s (Figure 23). As the tubes in the Intact and Broken loop steam generators voided, poor heat transfer between the secondary and voided primary tubes decoupled the two systems. While the pump suction contained liquid, steam generation in the core region caused the vessel liquid level to depress and forced liquid into the downcomer (Figure 24).

The clearing of the Intact loop pump suction was delayed due to the early clearing of the Broken loop pump suction. The downflow side of the Intact loop pump suction was cleared of fluid from 22 to 72 s (Figure 25). The upflow side of the Intact loop pump suction was cleared of fluid from 89 to 160 s (Figure 19). As liquid was being swept up and out of the upflow side of the intact loop pump suction, the pressure differential between the vessel and cold leg diminished and the vessel partially refilled, rewetting the rods that had started to heat up. However, there was enough water held up in the upflow side of the steam generators and pump suction to prevent rapid equalization of pressures around the

1 PV•UP-13

2 PBS•1117

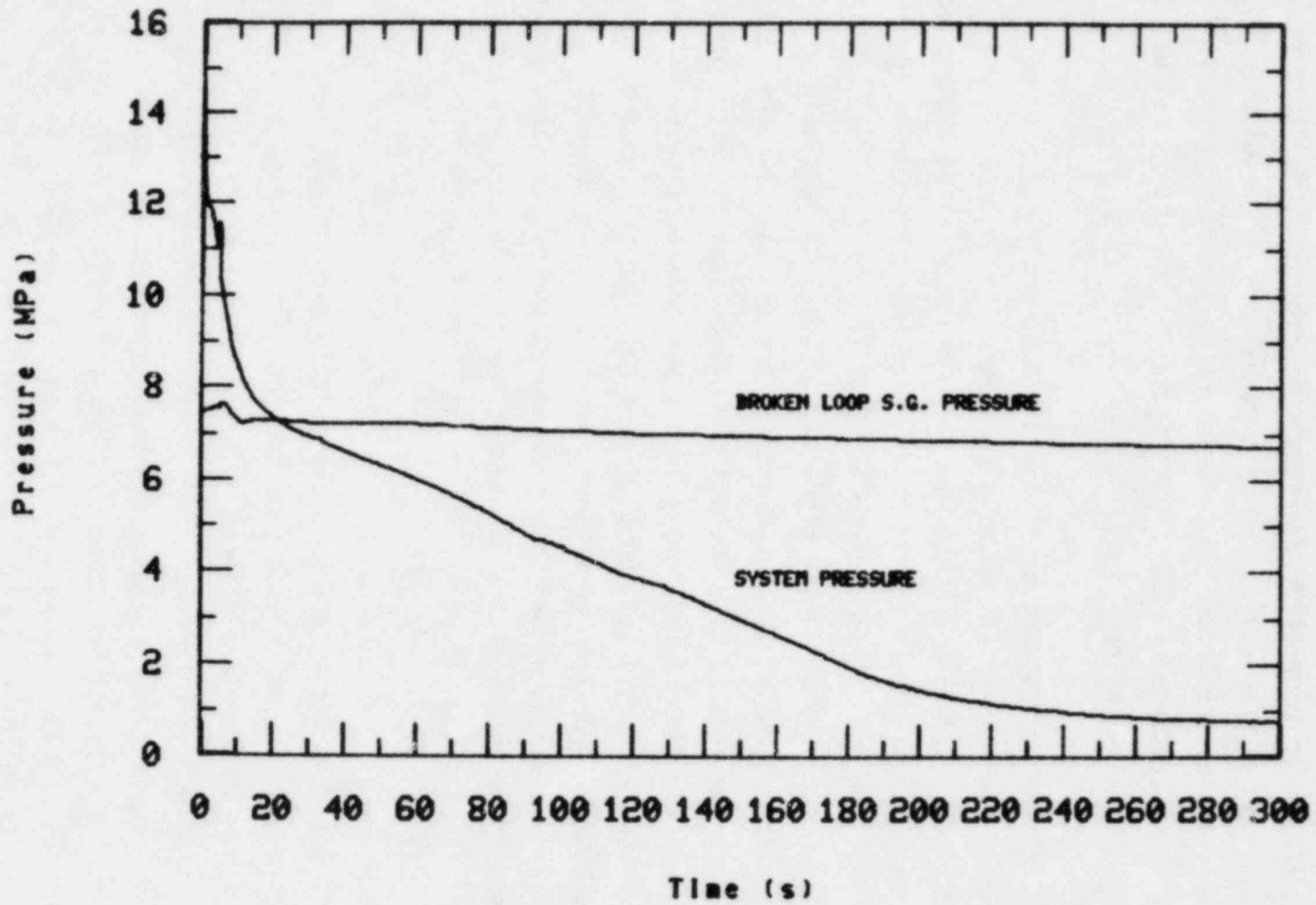


Figure 21. Comparison of primary system pressure to broken loop steam generator secondary pressure.

1 QB-57

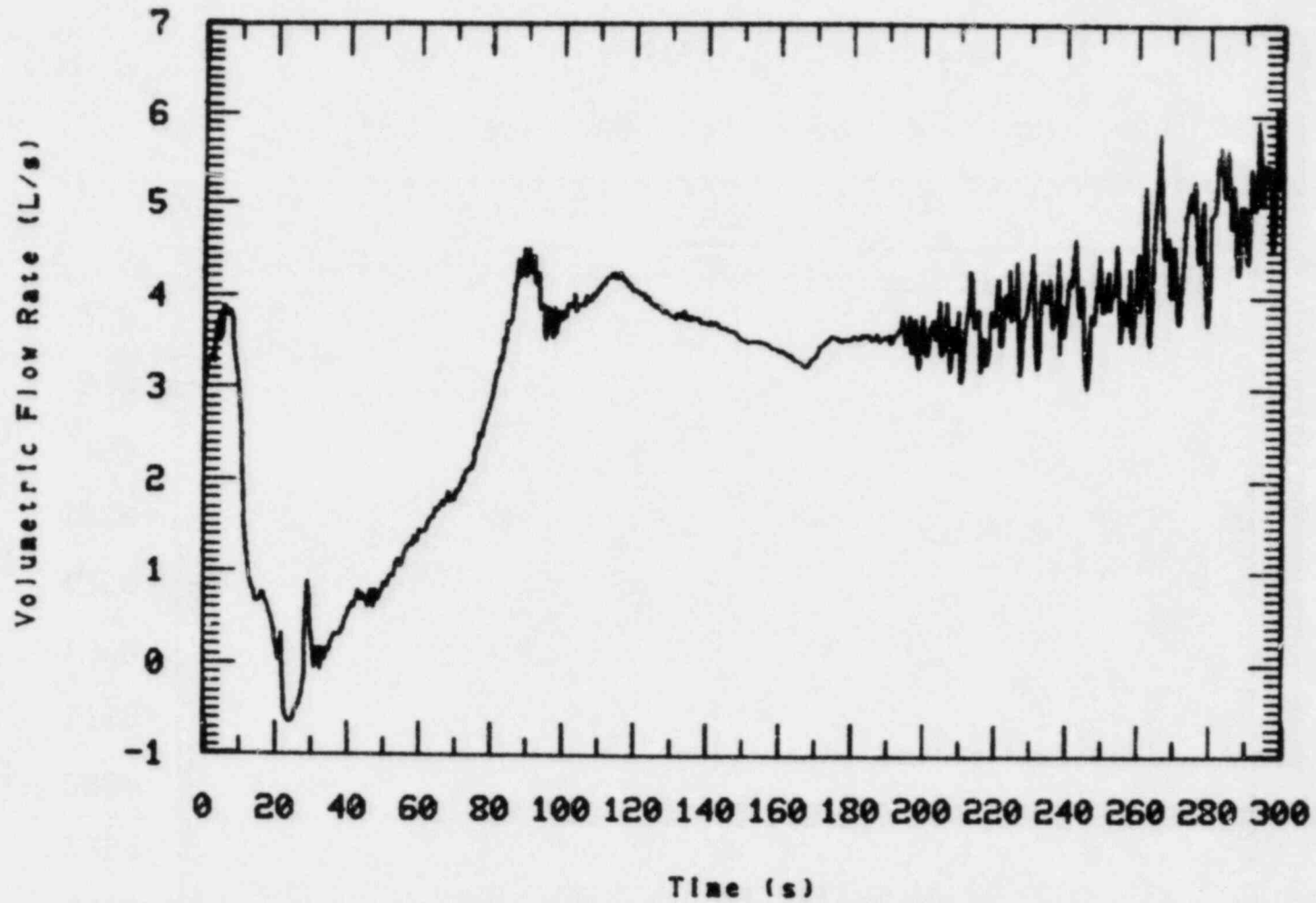


Figure 22. Broken loop hot leg volumetric flow.

1 ISGPL-BET+970-55

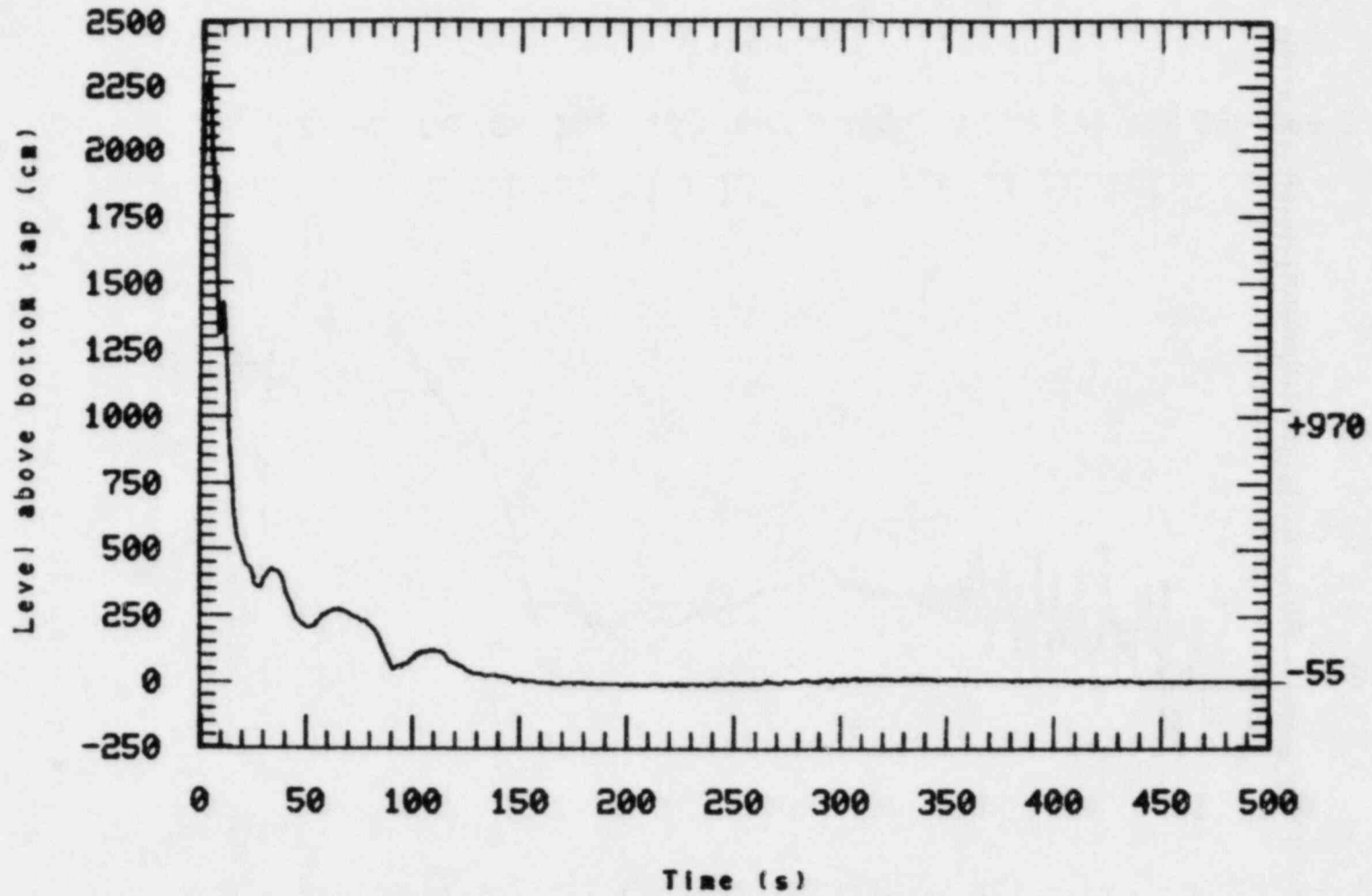


Figure 23. Liquid level in intact loop steam generator upflow side tubes.

1 VLBET-13M-578

2 VDLBET+29-578

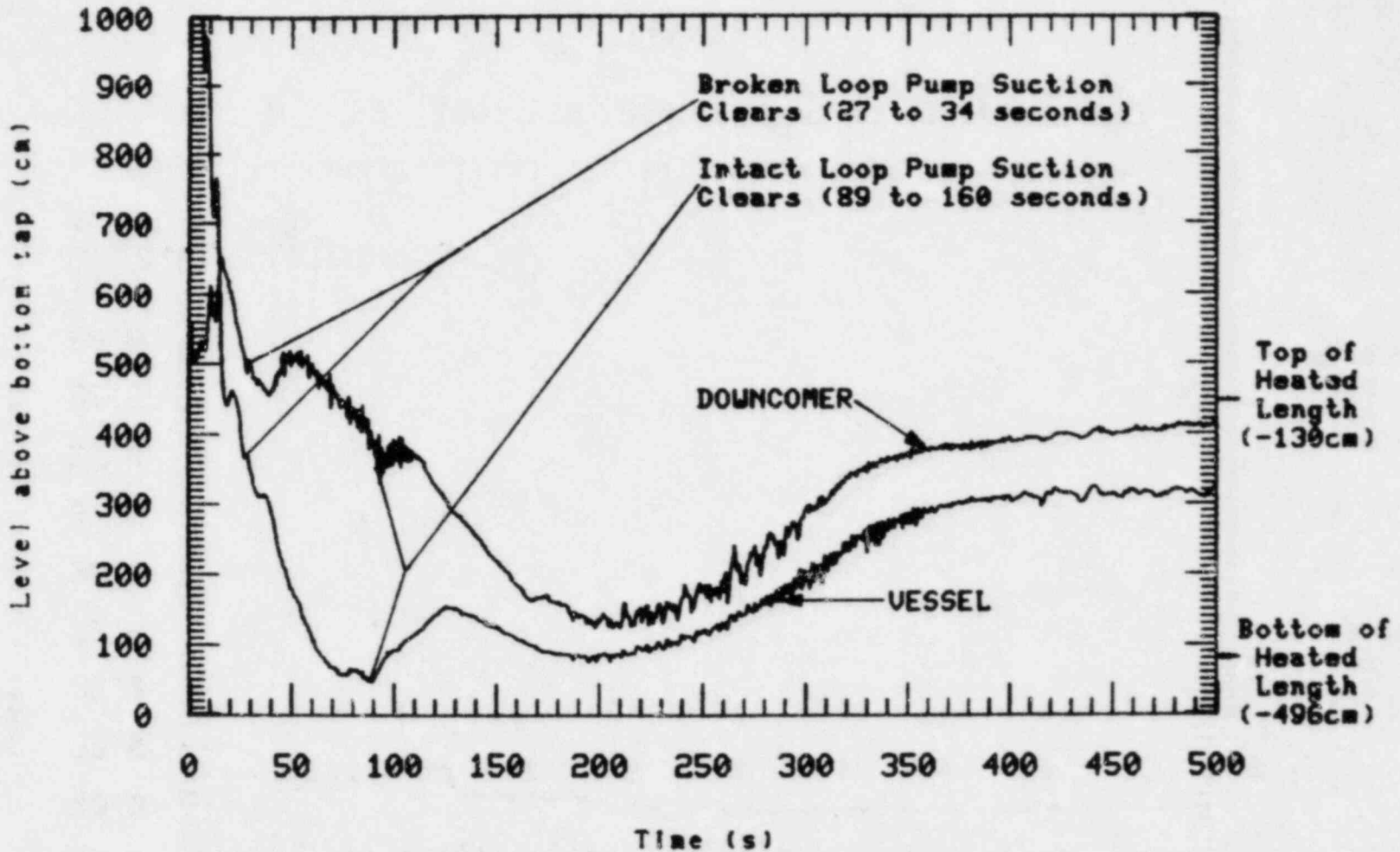


Figure 24. Liquid levels in vessel and downcomer showing manometric behavior for Test S-IB-3.

1 DPI=9.14

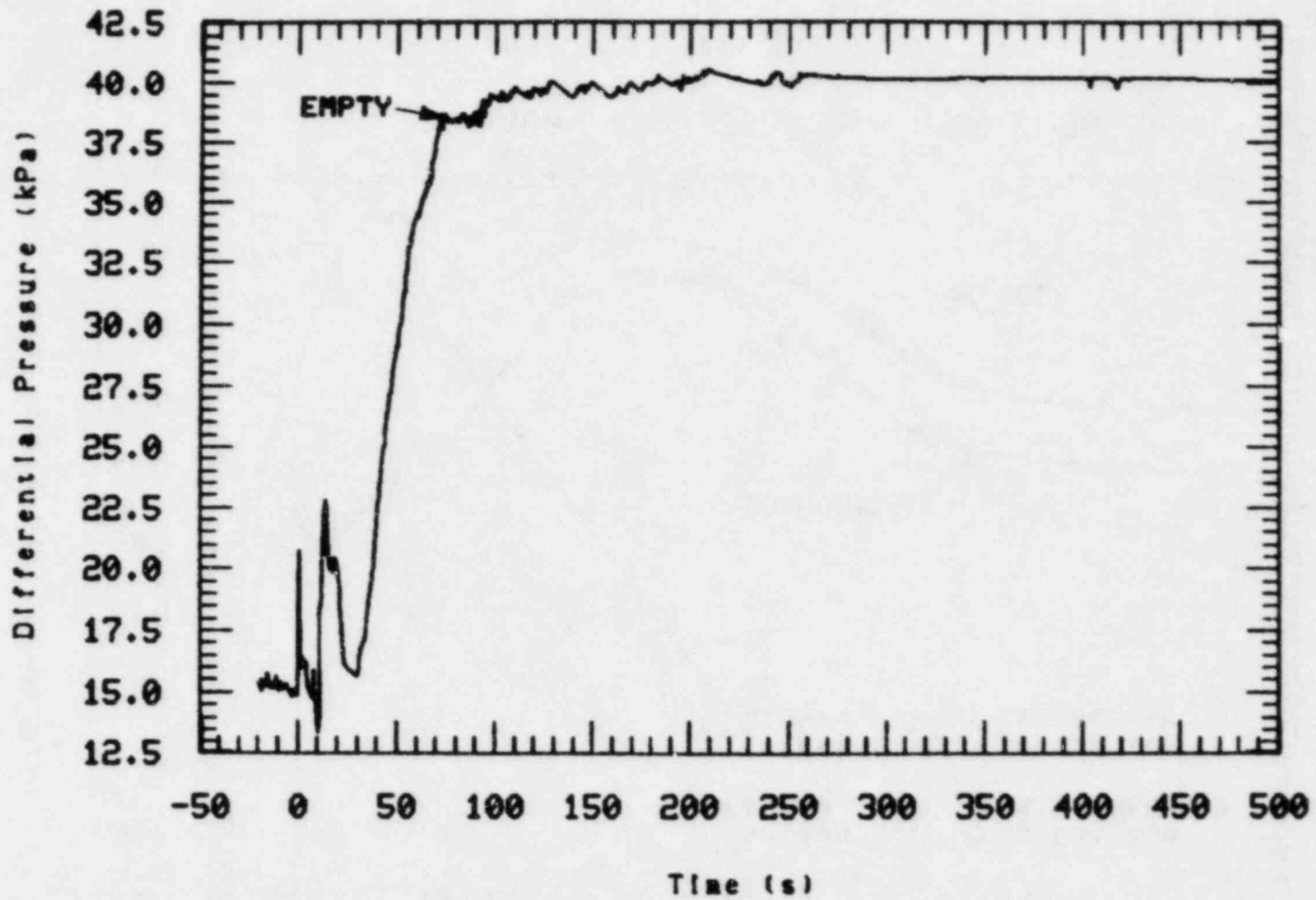


Figure 25. Differential pressure in Intact loop pump suction downflow leg (indicative of liquid level).

system. This slowed the refill of the vessel. By 125 to 130 s, the steam generators and pump suction were cleared out enough to allow good steam flow around the loops and the system pressure equalized.

The system depressurized continuously because of flow out the break until the accumulator came on at 163 s and began injecting 298 K water into the intact loop cold leg (Figure 26). The cold water injected by the accumulator caused condensation of steam in the cold leg. This lowered the pressure locally and caused the liquid level to rise in the downcomer and decrease in the vessel between 168 and 172 s, as shown in Figure 24.

As discussed earlier, the upper head received fluid through the bypass line (between downcomer inlet annulus and upper head) and discharged fluid through the guide tube into the upper plenum until the loop flows were restricted by the formation of liquid seals in the loop pump suction. At that time the flows in the guide tube and bypass line reversed and the upper head received steam through the guide tube and discharged liquid through the bypass line into the downcomer inlet annulus. This continued until the Broken loop pump suction started to clear (at about 27 s). Flow then started through the Broken loop, decreasing the flow in the guide tube to very near stagnation. This continued until 57 s, (about 5 s after the top of the guide tube uncovered), when steam started flowing down the guide tube. Steam flowed down the guide tube until the flow in the guide tube stagnated between 156 and 170 s. From about 170 s until the end of the test steam flowed up the guide tube from the vessel to the upper head. The flow in the bypass line continued to be reversed from about 14 s until the end of the test with transition from liquid to vapor flow at about 80 s when the top of the bypass line uncovered (see Figure 27). The upper head was completely drained of fluid by about 140 s (Figure 27).

3.1.3 ECC and Core Thermal Response

As noted earlier, accumulator liquid started flowing into the intact loop cold leg at 163 seconds (Figure 26). However because of the condensation of steam at the injection point, a region of lower pressure was formed at the injection point, causing steam to flow up the external,

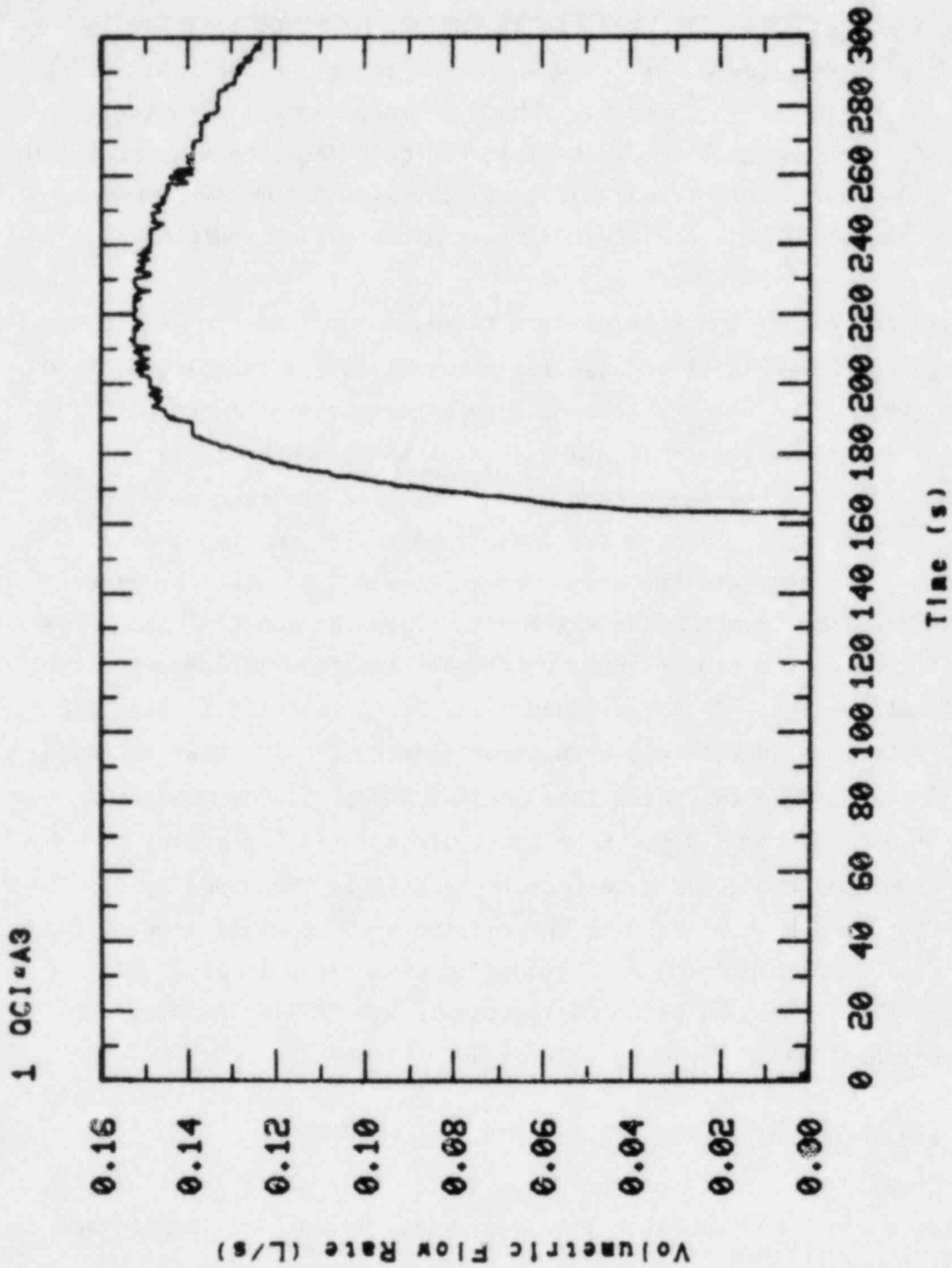


Figure 26. Accumulator volumetric flow.

1 VLBET+421+160

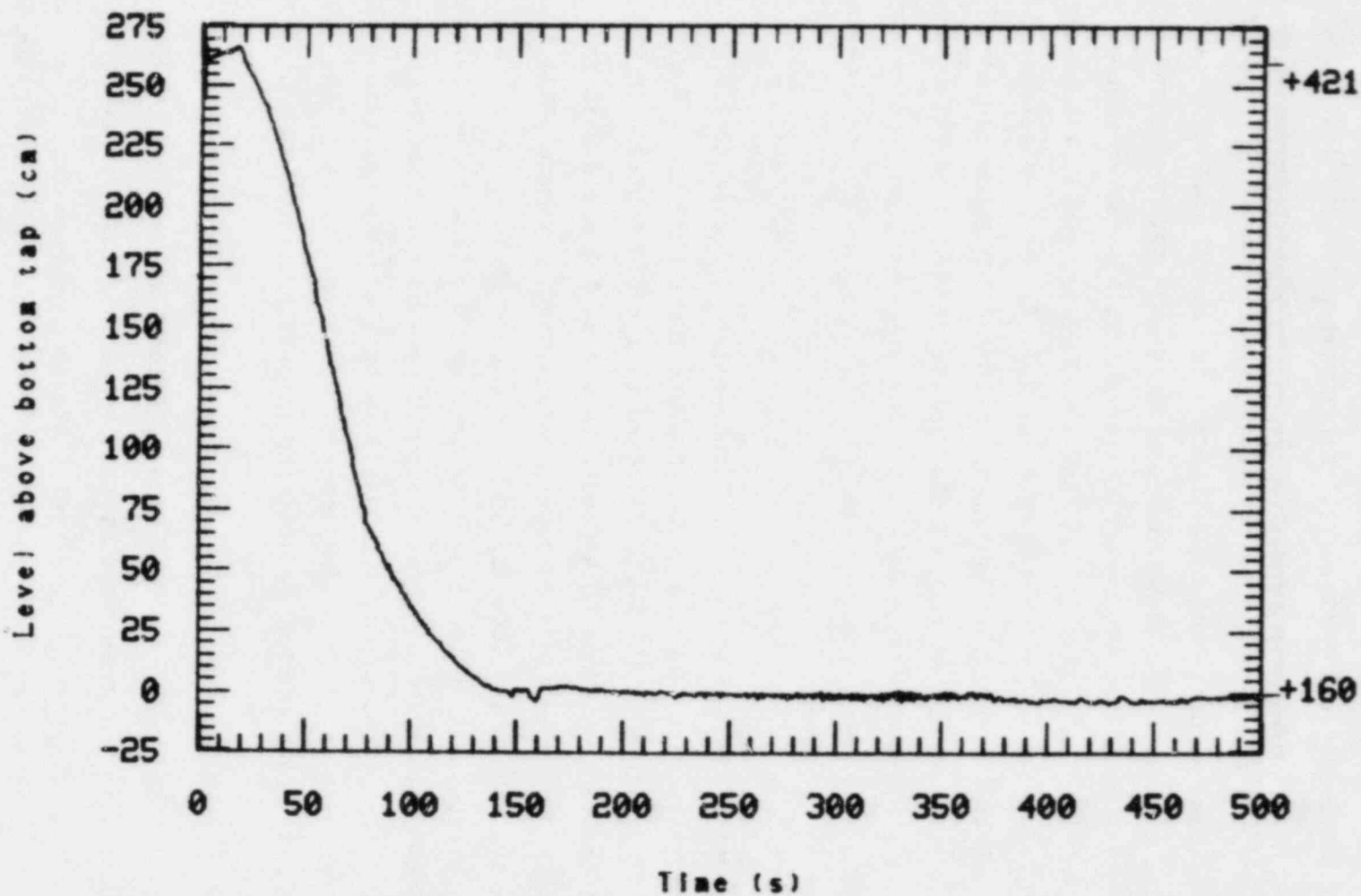


Figure 27. Liquid level in upper head (top of bypass line 230 cm above top of support plate).

single pipe downcomer (Figure 28). Also, due to the pressure differential between the vessel and the break, the steam flow up the downcomer was of sufficient magnitude to force the ECC liquid around the downcomer inlet annulus and to the break, bypassing the core between 163 and 190 s. With the blowdown nearly over, the large driving force for flow up the downcomer diminished and the ECC was able to penetrate the downcomer (and core as discussed below). Although the bypass period is characteristically long in Semiscale, accumulator ECC liquid flow continued well beyond the end of blowdown. This was due to the larger scaled accumulator water volume, scaled to the LOBI Test B-R1M volume, and the lower accumulator pressure setpoint, taken from the LOBI B-R1M Test, of 2.7 MPa. At termination of the test about 54% of the initial 0.066 cubic meter liquid volume had been injected, while about 23% of the injected volume had bypassed the downcomer to the break. This accumulator water, the formation of pump suction liquid seals, and the core power are the major factors affecting the core thermal response during blowdown.

Simply described, a composite core temperature trace (Figure 29) for this test consists of a decrease in temperature corresponding to the saturation temperature in the core, followed by a rapid increase in temperature starting at about 50 seconds, to a peak temperature in the range of 740 K, and then followed by another, slower, decrease until the core is rewet at about 133 seconds, when a rapid decrease occurs. This is followed by a reduction in the cooling rate until the temperature levels out and starts to increase again at about 190 seconds. The temperature then peaks, in the range of 630 K, and starts to gradually decrease until the rod is rewet again at about 280 seconds. From this point on the temperature drops close to and follows the saturation temperature until the end of the test.

From immediately after rupture until 2 seconds there was a rapid rise in void fraction in the upper half of the core. This void formation was caused by boiling due to the release of stored energy from the heater rods and to decay heat transferred to the fluid. When the stored energy in the rods was reduced, some of the voids collapsed in the period from 2 to

1 QV=DC-423

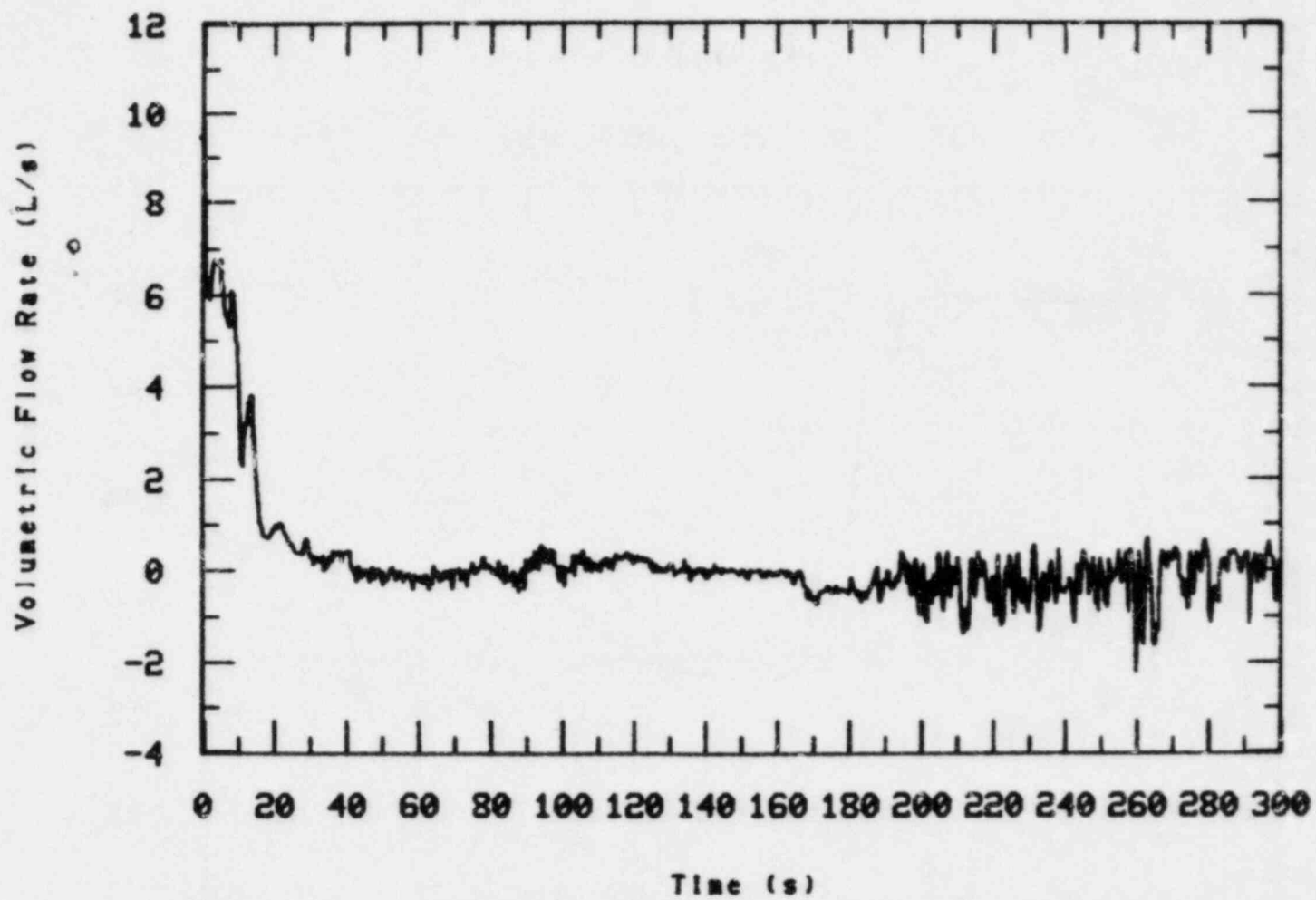


Figure 28. Volumetric flow in the downcomer.

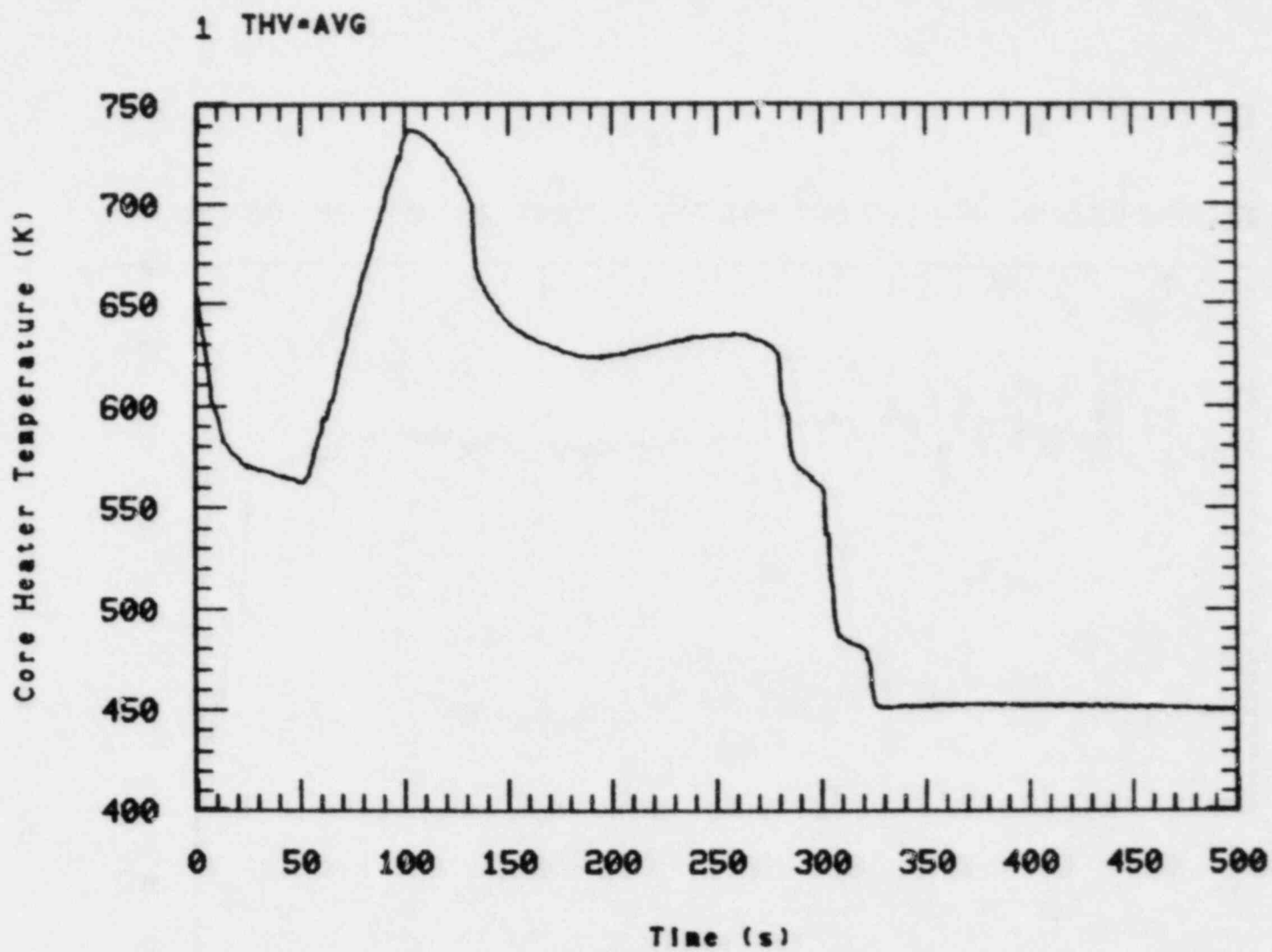


Figure 29. Average core heater rod temperature.

3 seconds in the high power region of the core as shown in Figure 30. Decay power continued to cause boiling and voiding in the core region.

After liquid formed seals in the pump suction, the steam generated in the core was restricted from flowing freely around the loops to the break. Lack of a sufficient relief path for the steam resulted in the depression of the liquid level in the vessel and pump suction upflow legs. Although the Broken loop pump suction blew out early the steam relief path continued to be restricted enough to continue the depression of liquid level in the core region and thus raise the downcomer liquid level. The lowered vessel level allowed the void fraction in the entire core to get high enough to cause dryout on all of the heater rods. The partial clearing of the Intact loop seal at 89 seconds allowed the system pressures to equilibrate enough to let some downcomer fluid flow into the core region (Figure 14) and rewet the dried out areas. A decrease in core power at 100 seconds (in accordance with the LOBI-prescribed profile) aided in this core cooling.

The lower plenum and lowest fourth of the core partly refilled by about 130 seconds and then gradually boiled down over the next 60 seconds. This caused the reduction in the cooling rate and the slow temperature increase which started at about 190 seconds. At 190 seconds the accumulator injected water started to penetrate the downcomer and the vessel started to refill. As the vessel refilled the temperatures in the core slowly stopped increasing due to the cooling provided by the accumulator water. By 240 seconds most of the core temperatures had reached a plateau and the system pressure had reached 1 MPa so that the Low Pressure Injection System had started to inject cold water into the Intact loop at the specified rate. The combined ECC injection from the accumulator and the LPIS system reached the core quickly and quenched most of the core by about 280 seconds, while the upper elevations of the core were quenched by about 350 seconds. From 350 seconds until the end of the test the cladding temperatures were kept near saturation. Figures 31-33 show typical temperature variations along two traverses of the core midplane (radial variations) and axial temperature variations in a central rod.

1 RV-23-183

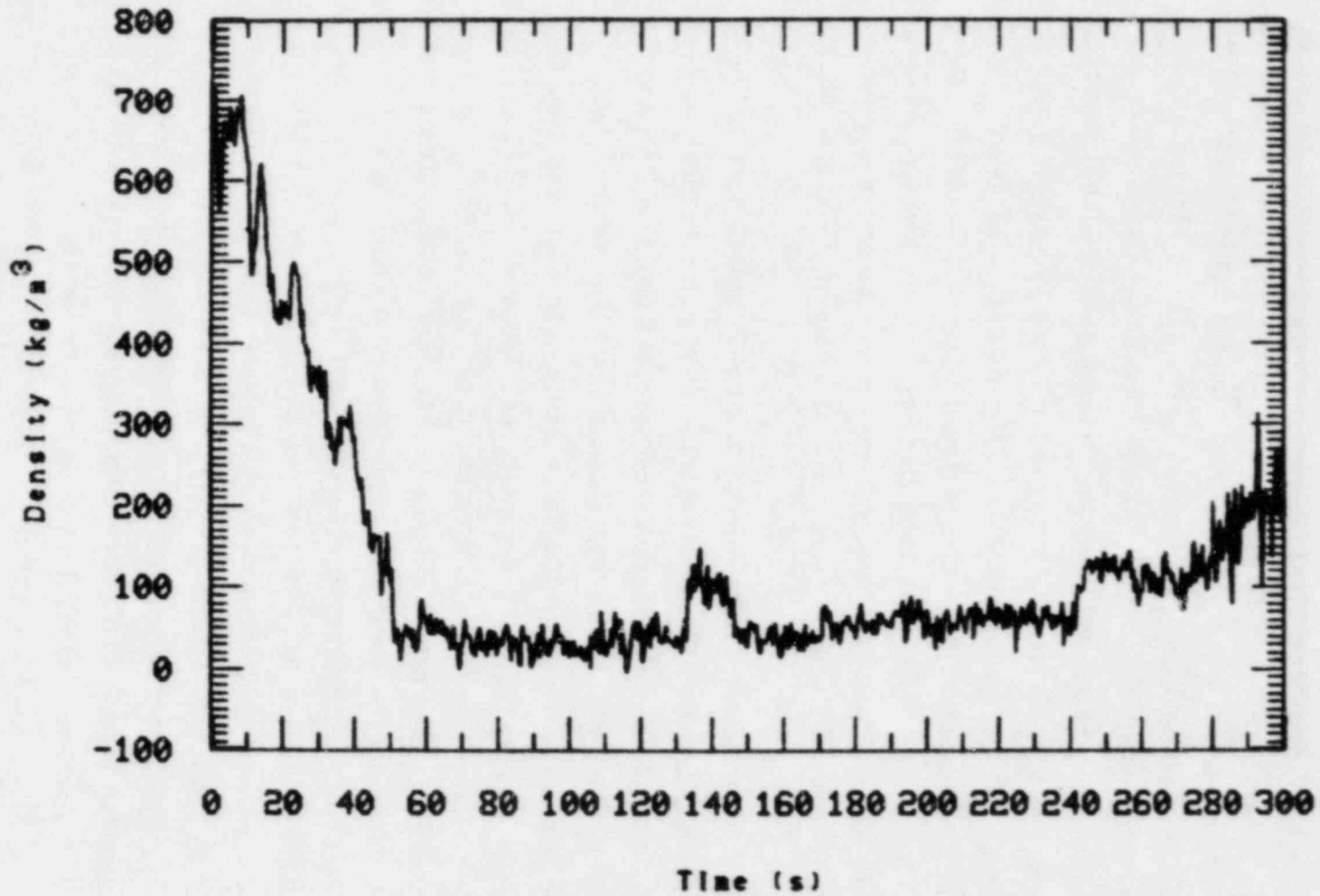


Figure 30. Fluid density in high power region of core (183 cm from core bottom).

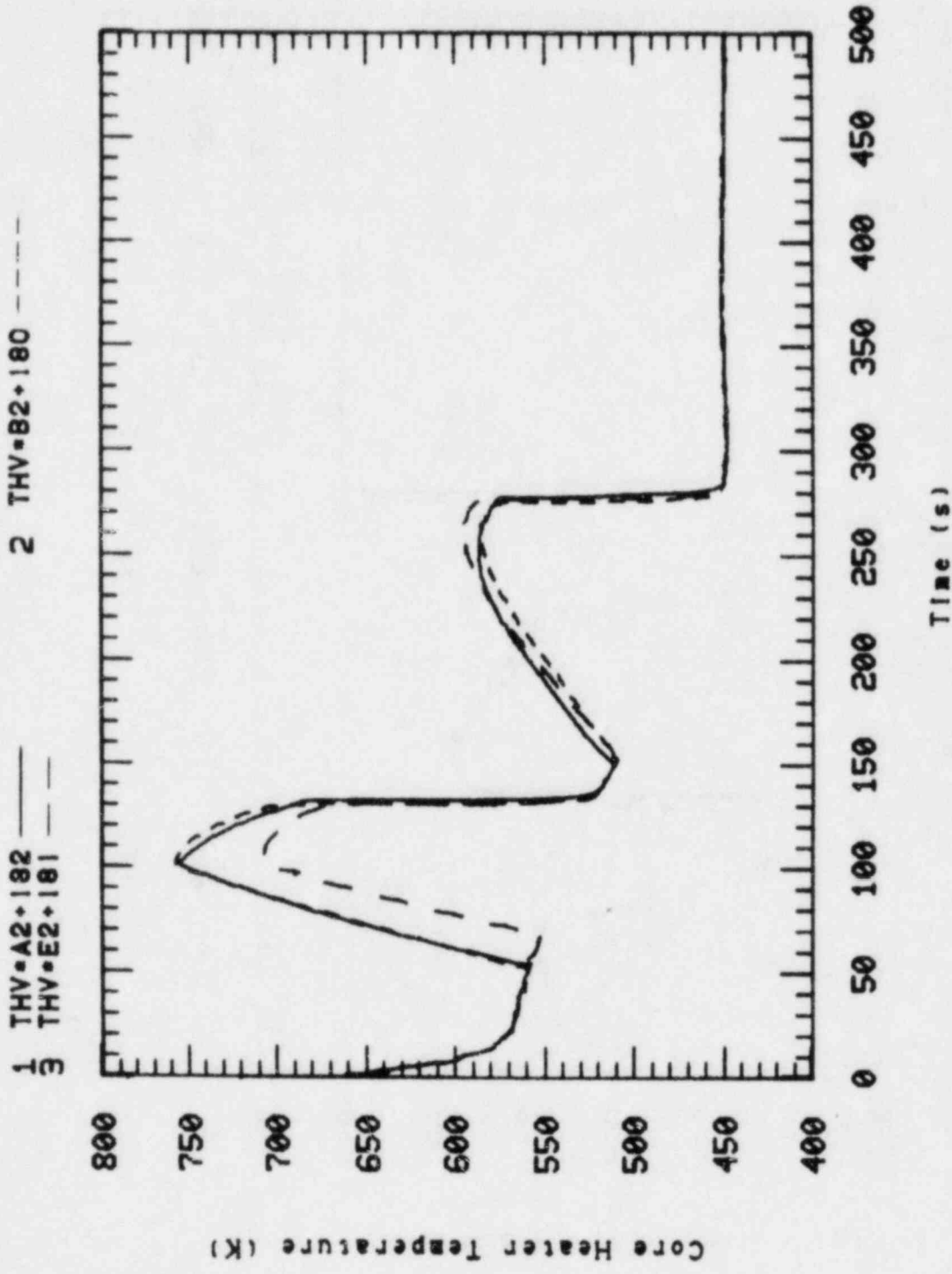


Figure 31. Comparison of core midplane temperatures in row 2.

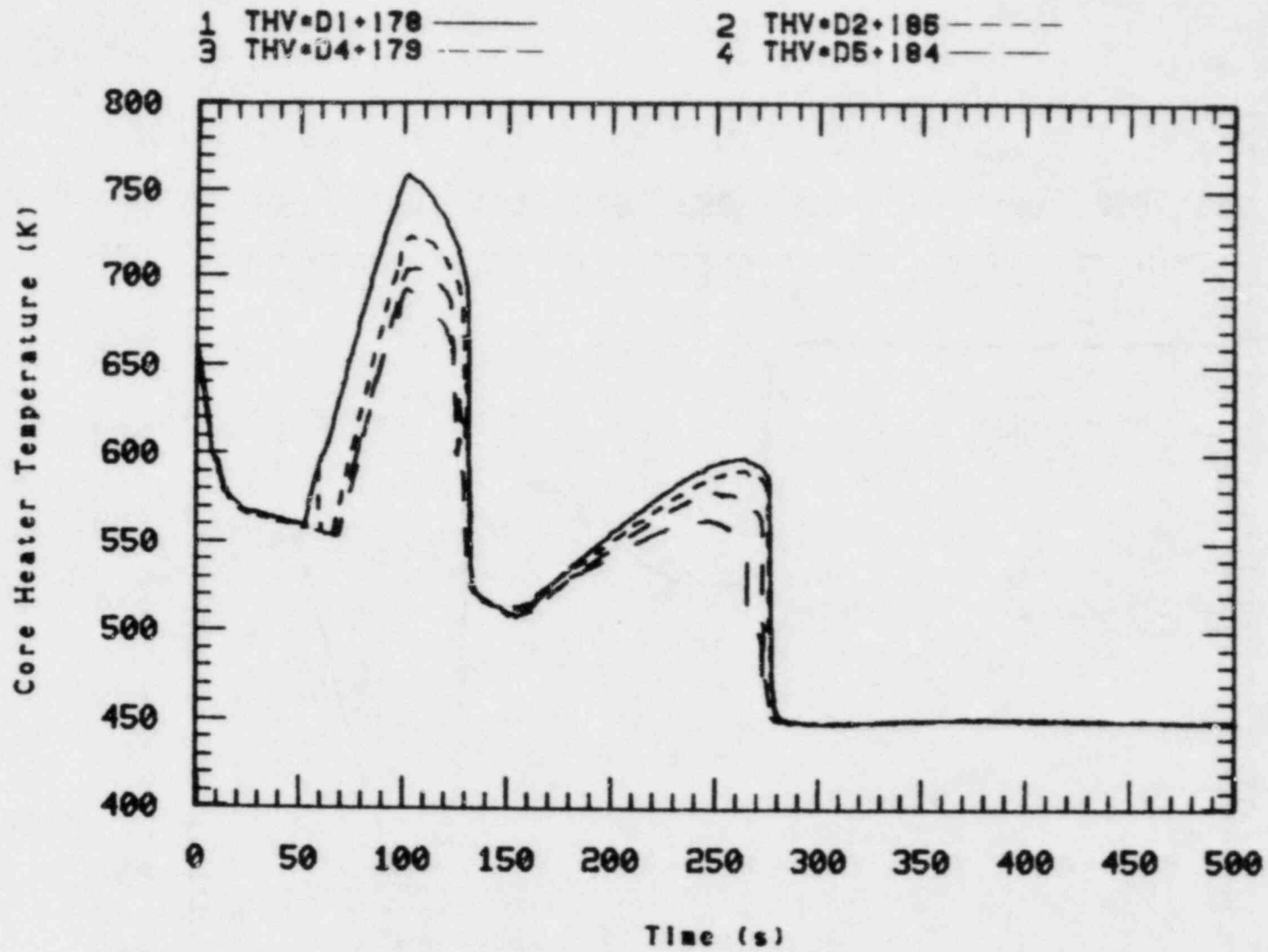


Figure 32. Comparison of core midplane temperatures in column D.

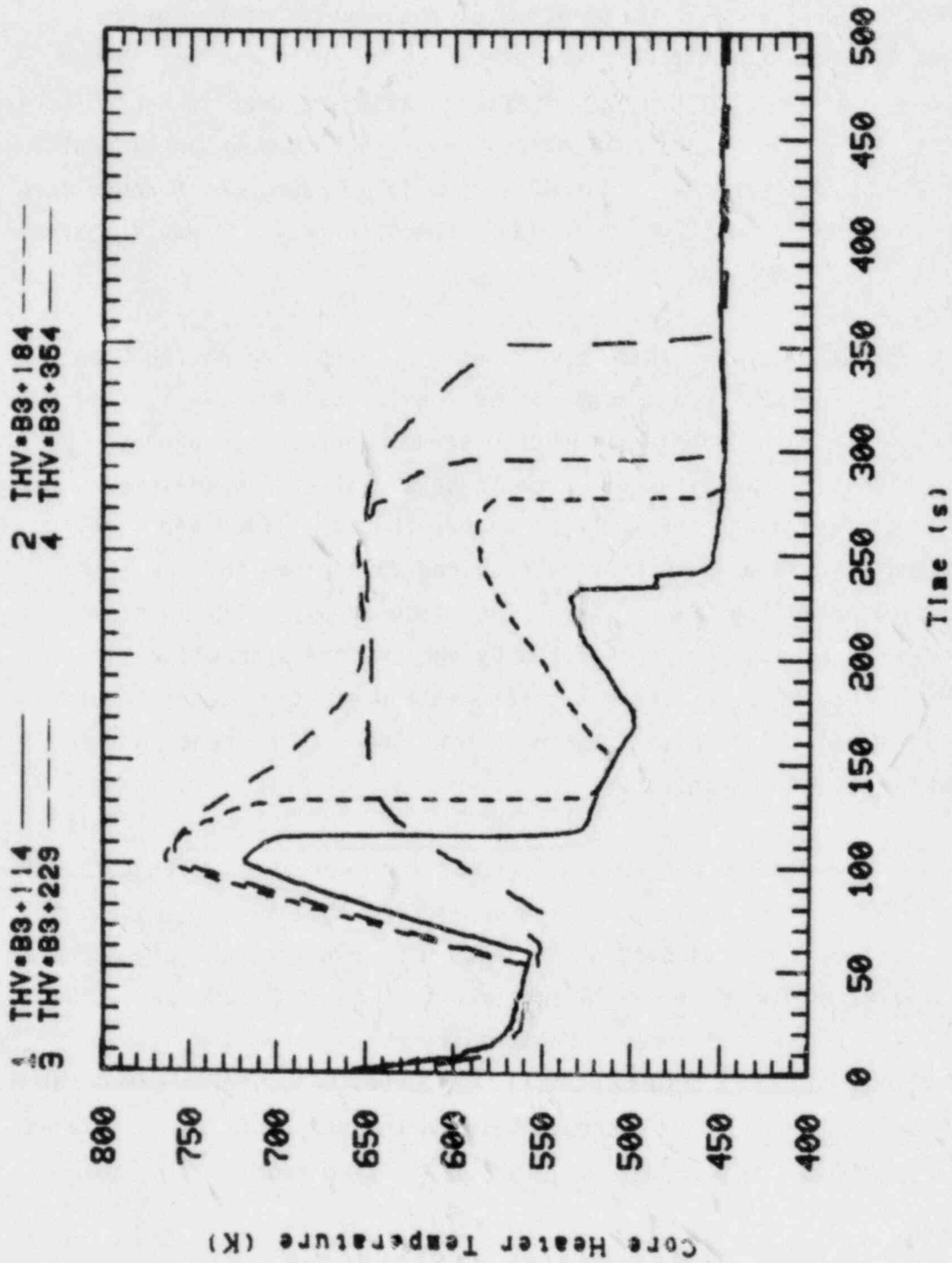


Figure 33. Comparison of core axial temperatures in heater rod B3.

4. COMPARISON OF PRETEST PREDICTION TO SELECTED DATA

A pretest prediction calculation was performed for this experiment and documented in Reference 5. The calculation was performed with the RELAP5/MOD1 computer code. Comparisons of the results of the pretest calculation to measured test data are presented in this section. Since reflood modeling capabilities are not specifically included in RELAP5/MOD1, the pretest calculation was performed only over the blowdown portion of the transient (0-300 s). Posttest calculations will be performed through core reflood with RELAP5/MOD1.5^a which includes specific reflood heat transfer models.

The calculated steady state conditions (prior to opening the break) are compared to the measured and specified conditions in Table 5. The RELAP5 steady state calculation predicted steam generator secondary conditions significantly different from those specified and measured. The code accurately predicted the trend of higher than specified secondary pressures and steam temperatures were required to achieve the specified primary coolant cold leg temperature. The measured asymmetry in steam generator operation was not represented by the pretest prediction calculation. The effect of the misrepresentation of steam generator secondary heat rejection split between the two loops is evident in the calculated transient response.

The overall calculated transient response compares well with data. In particular, the calculated and measured upper plenum pressures (Figure 34) virtually overlay. The calculated subcooled blowdown pressure signature of the pressurizer and upper plenum is compared to data in Figure 35. The calculated lag of the pressurizer pressure (resulting from the high hydraulic resistance of the surge line) is shown to be slightly exaggerated in comparison to data. The difference between the measured and calculated pressurizer pressures is due to a smoother transition from liquid to vapor

a. An interim version of RELAP5/MOD1.5 was released on April 15, 1982.

PRETEST PREDICTION COMPARISON TO SELECTED DATA
TEST S-1B-3

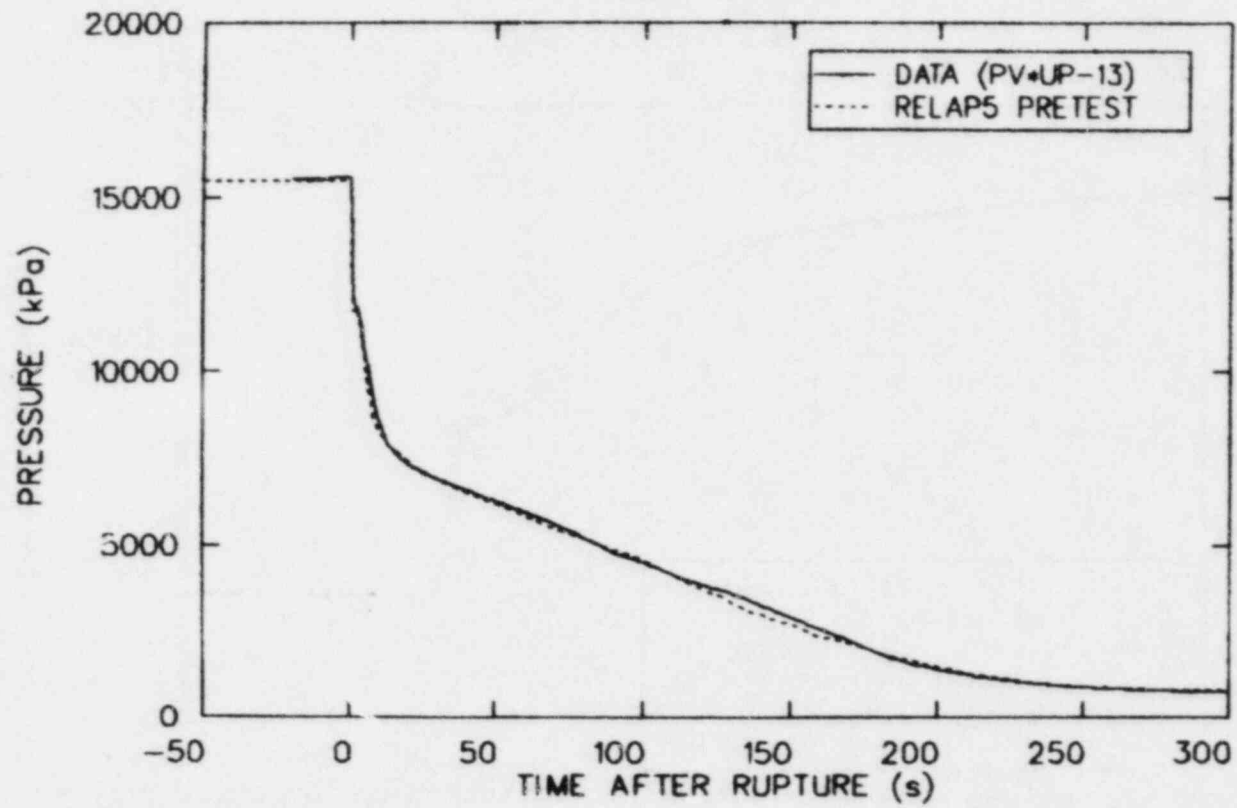


Figure 34. Comparison of measured and calculated upper plenum pressures.

PRETEST PREDICTION COMPARISON TO SELECTED DATA
TEST S-1B-3

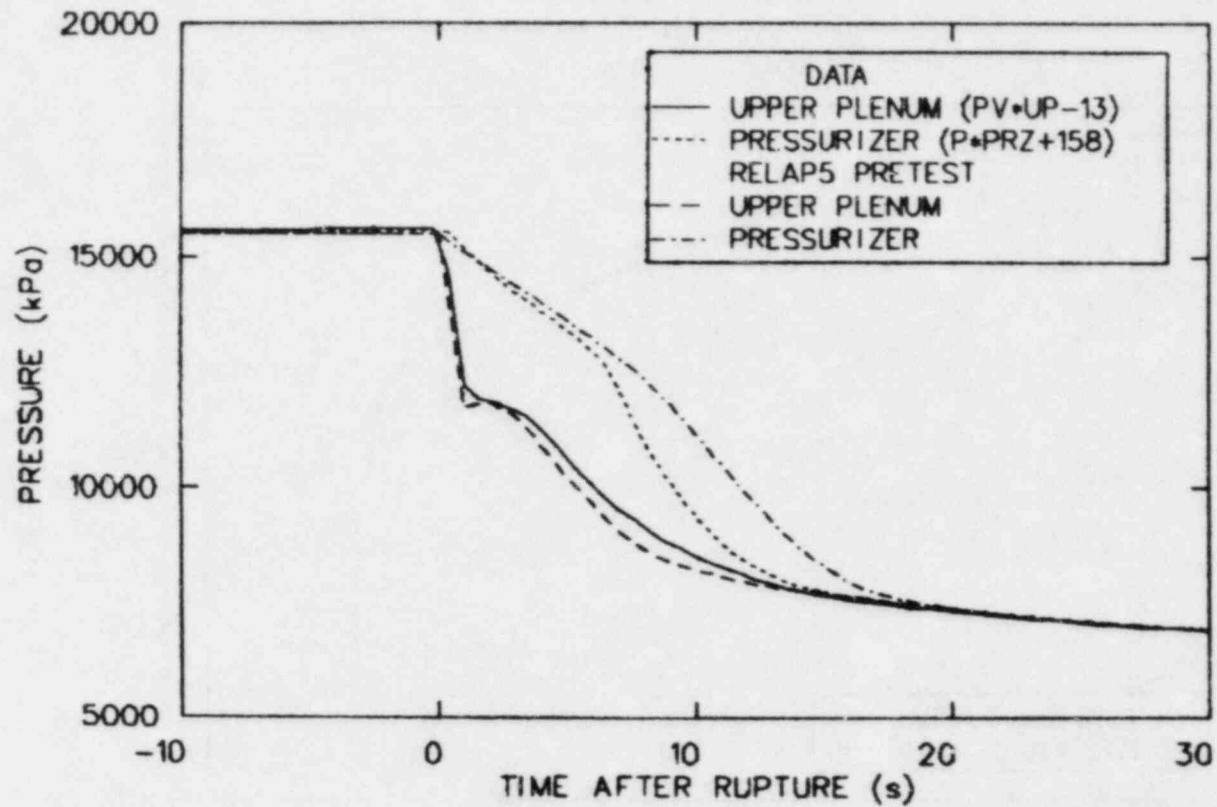


Figure 35. Comparison of measured and calculated upper plenum and pressurizer pressures.

flow out the pressurizer in the calculation than observed. The measured pressurizer volumetric flow in Figure 36 is shown to rise sharply at 7 s, characteristic of an abrupt transition from liquid to two-phase flow. In contrast, the calculated flow rate changes gradually over the draining period. The observed abrupt change from liquid to two-phase flow accounts for the change in slope of the measured pressurizer pressure signature in Figure 35. The magnitude of the change in slope was not predicted by RELAP5 since the calculated volumetric flow rate did not change very rapidly.

The disagreement in the calculated and observed pressurizer flow rate is a result of the RELAP5 prediction not adequately preserving a sharp interface between liquid and vapor within the pressurizer as it is drained. Figure 37 shows the calculated average densities for the control volumes in the pressurizer and top of the surge line below the liquid free surface. If the pressurizer were calculated to drain with a monotonically decreasing level the control volume densities would decrease monotonically and in succession. As shown in Figure 37, the control volume densities decrease, however, they do not show a continuous axial density gradient (as required to preserve the liquid free-surface) over the draining period. This calculated smearing of the liquid/vapor interface resulted in a more extended pressurizer depressurization than observed.

As discussed in Section 3.1, pump suction liquid seal behavior significantly affected the core thermal-hydraulic response early in the transient. The effects of pump suction liquid seal formation were not well predicted by RELAP5. The calculated collapsed liquid levels in the downflow side of the pump suction legs are compared to test data in Figure 38. Although the order in which the loop pump suction blowout is calculated correctly (broken loop first), the observed rapid depression and blowout of the broken loop liquid seal was not calculated.

The disagreement between the calculated and observed behavior in the pump suction legs is presently believed to be a result of the difference between the specified and experimental operation of the broken loop steam generator (see Section 2.3.2). Since the broken loop steam control valve

PRETEST PREDICTION COMPARISON TO SELECTED DATA
TEST S-1B-3

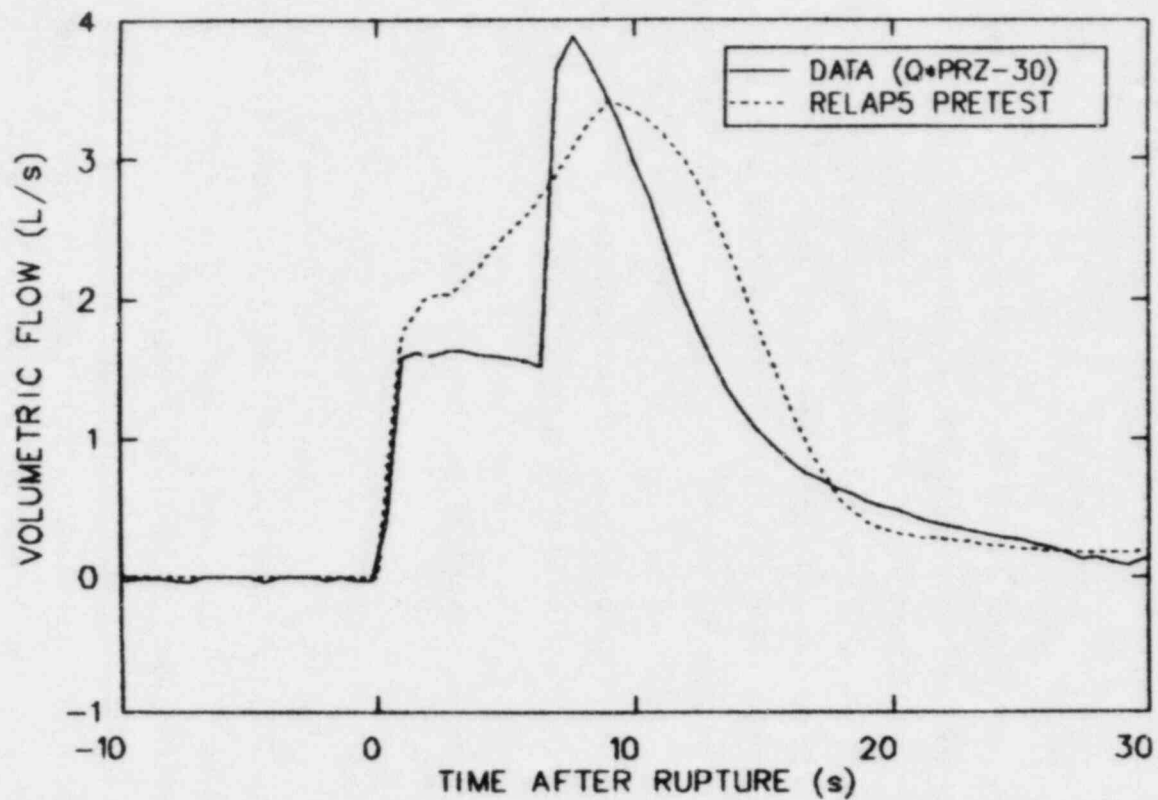


Figure 36. Comparison of measured and calculated pressurizer surge line flow rate.

PRETEST PREDICTION COMPARISON TO SELECTED DATA
TEST S-1B-3

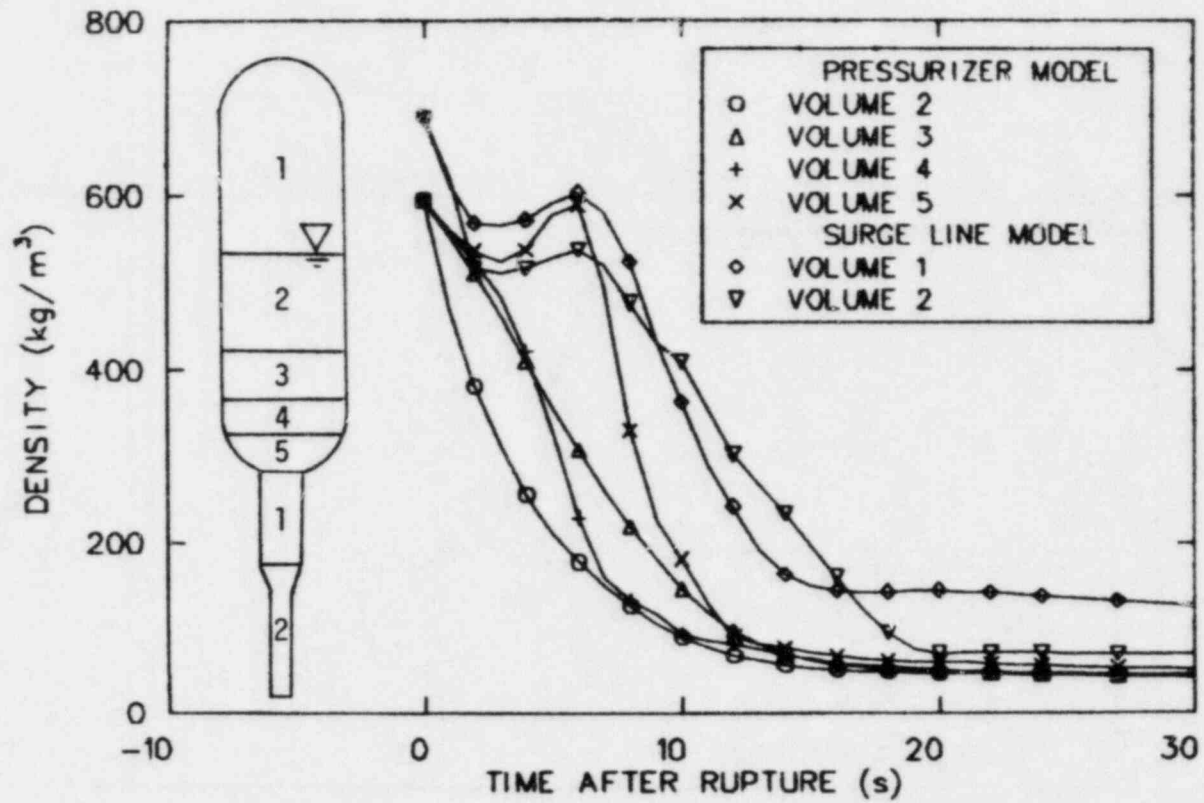


Figure 37. RELAP5 calculated densities in the pressurizer.

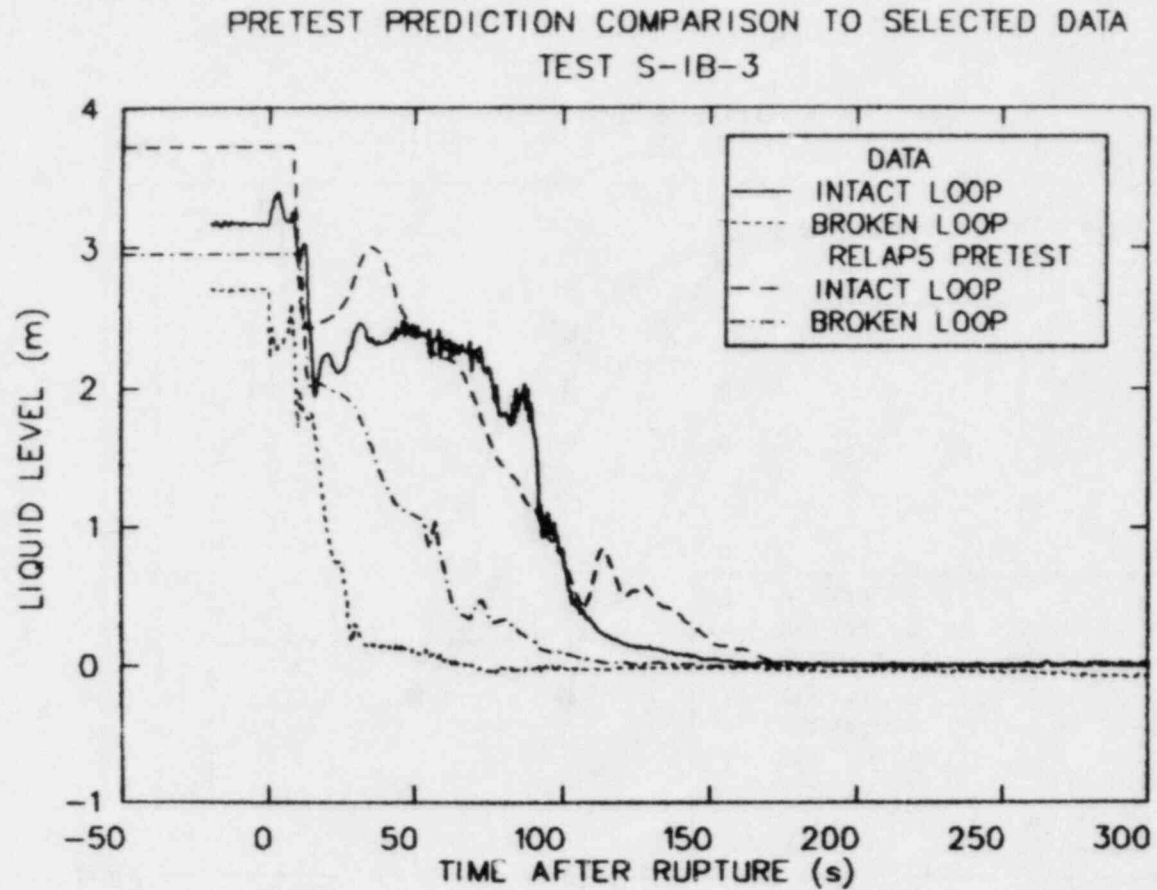


Figure 38. Comparison of measured and calculated pump suction collapsed liquid levels (downside).

was essentially shut early in the experiment, the secondary pressure remained high relative to the calculated secondary response (which modeled an open steam valve as specified). The effect of the shut steam valve was to significantly reduce the broken loop thermal sink (and condensation potential) early in the transient. Consequently, the broken loop pump suction blew out earlier than predicted. Figures 39 and 40 show the steam generator secondary and upper plenum pressures which were measured and predicted, respectively. The times at which the steam generator secondaries were observed and calculated to become a heat source correspond to the respective time at which the pump suction liquid seals cleared.

The discrepancy between the observed and calculated pump suction behavior was compounded by an inaccurate model representation of the differential pressure across the steam generator. The depression of the vessel collapsed level during pump suction liquid seal formation was, therefore, influenced by a poor calculation of the driving differential pressures. Figures 41 and 42 show the vessel and downcomer collapsed liquid levels from data and the pretest calculation, respectively. The calculation does not show the large manometric imbalance between the downcomer and vessel levels shown in the data. The effect of this discrepancy in the vessel hydraulic response on the core thermal response is shown in Figure 43 which compares the observed and calculated heater rod cladding temperatures where the peak temperature occurred.^a Both curves correspond to the same axial core location. The first core dryout, observed at approximately 50 s, was not predicted in the pretest calculation, since the intact loop pump suction level depression was not predicted.

Following the observed clearing of the intact loop pump suction, the predicted core boil-off agrees fairly well with the observed trend. The

a. The difference between the calculated and measured initial cladding temperatures (50 K) is a result of comparing a calculated surface temperature with an imbedded thermocouple measurement. The calculated radial profile yields a more representative comparison of initial conditions at the same radial location.

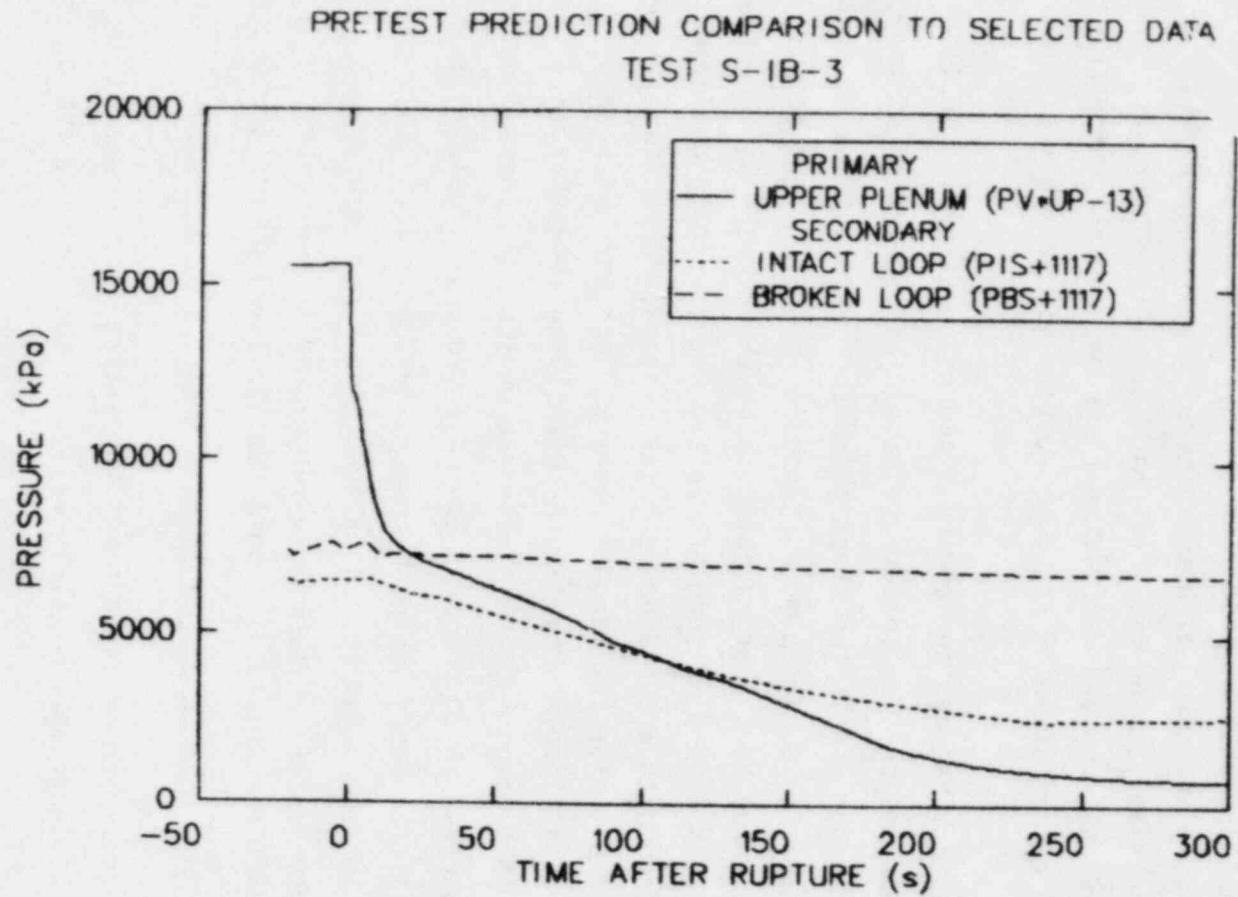


Figure 39. Comparison of measured primary and secondary pressures.

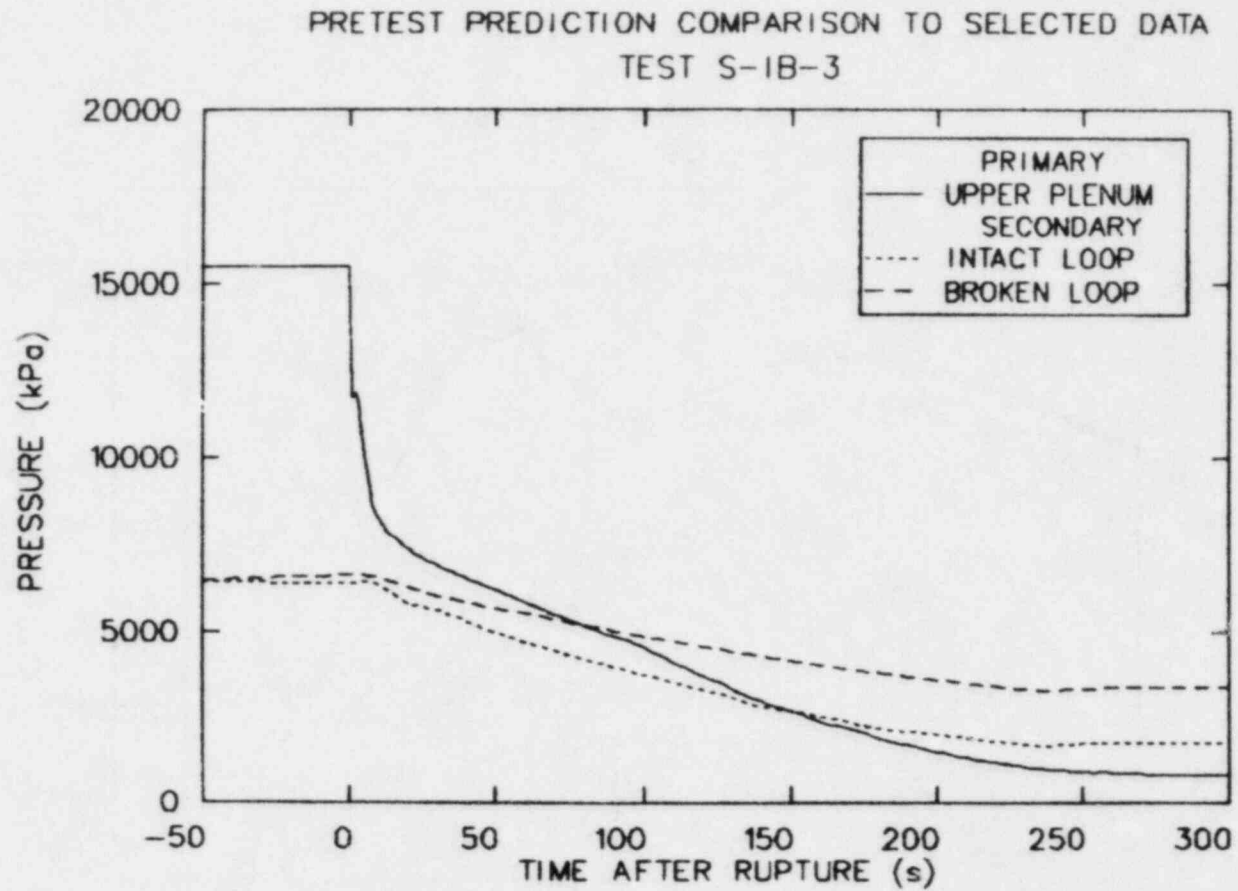


Figure 40. Comparison of calculated primary and secondary pressures.

PRETEST PREDICTION COMPARISON TO SELECTED DATA
TEST S-1B-3

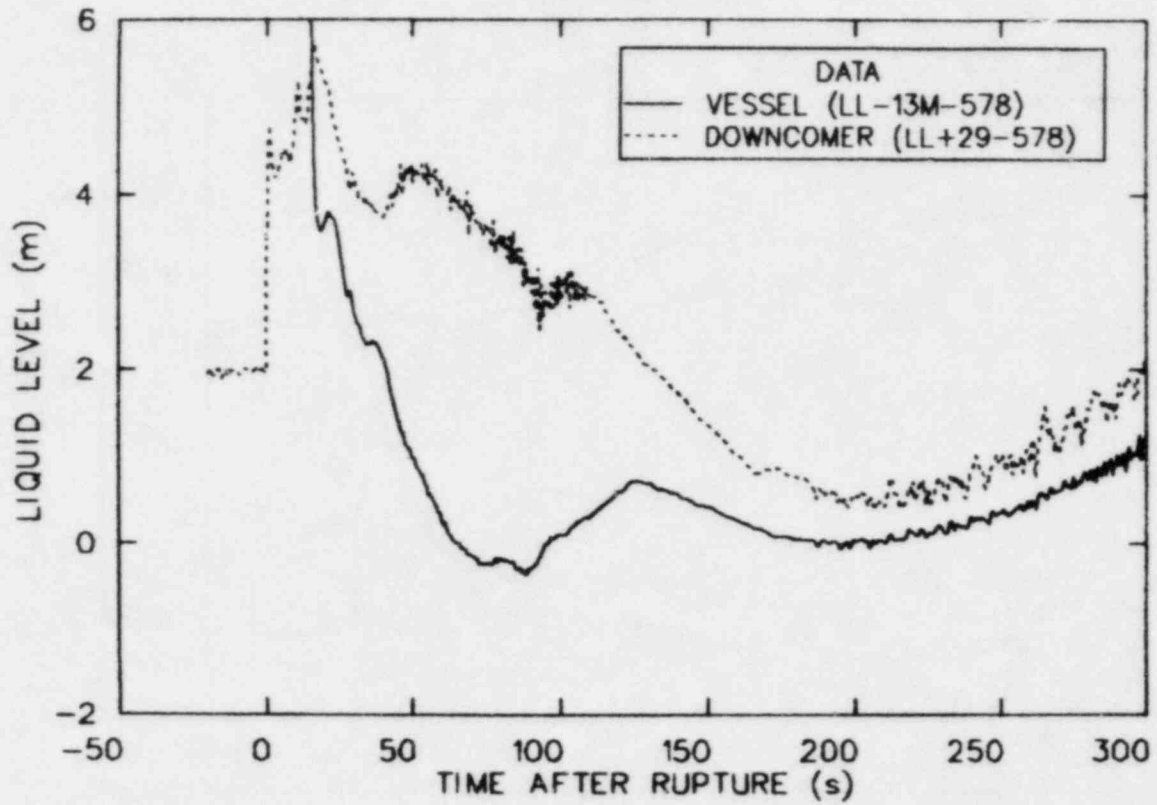


Figure 41. Comparison of measured vessel and downcomer collapsed levels.

PRETEST PREDICTION COMPARISON TO SELECTED DATA
TEST S-1B-3

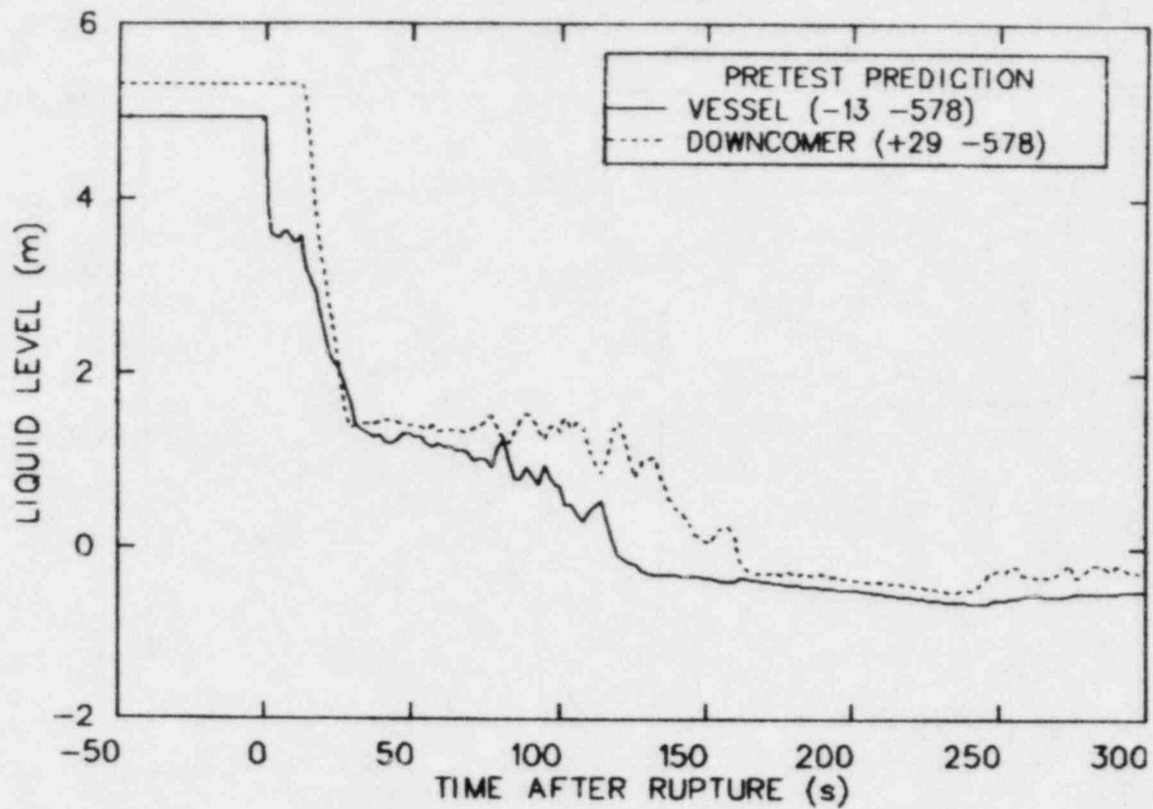


Figure 42. Comparison of calculated vessel and downcomer collapsed levels.

PRETEST PREDICTION COMPARISON TO SELECTED DATA
TEST S-1B-3

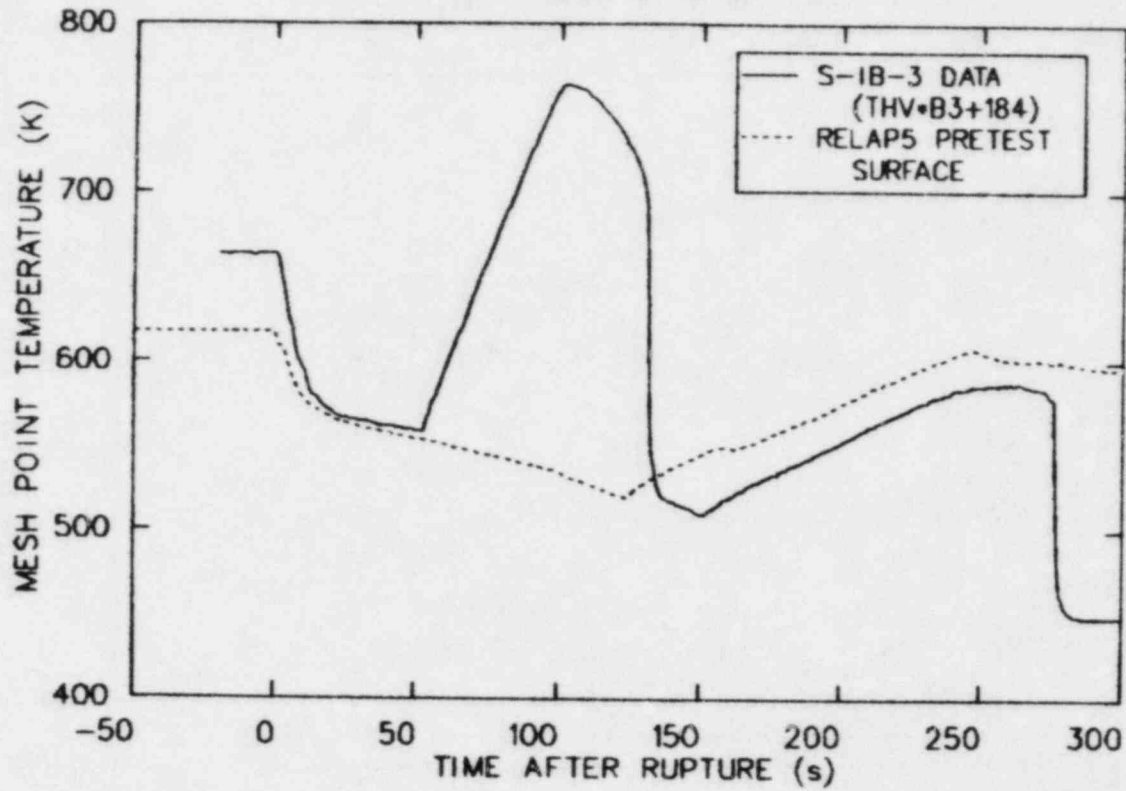


Figure 43. Comparison of measured to calculated core heater rod peak cladding temperature.

resulting core heater rod thermal response was predicted between 150 and 250 s in the transient (Figure 43). Precursory cooling was predicted to prevent further heatup of the rod surface after 250 s, however, a quench was not predicted to occur before 300 s. The effects of precursory cooling are evident in the data after 250 s as the slope of the heater rod temperature signature becomes negative. The entire core was observed to quench at approximately 280 s, however. The pretest calculation did not predict the core quench because the initiation of vessel refill was underpredicted.

Intact loop accumulator injection was observed to begin at approximately 160 s and vessel refill began at approximately 190 s. Figure 41 shows the monotonically increasing vessel liquid level. Although the calculated accumulator injection rate agrees quite well with data^a (Figure 44), the calculated rate of vessel refill, shown in Figure 42, does not agree with data. Vessel refill was not predicted, because little of the injected accumulator was delivered to the downcomer (note the relatively constant downcomer level in Figure 42).

The pretest calculation predicted the accumulator fluid would bypass the downcomer (through the inlet annulus) to the broken loop cold leg and exit the break. Evidence of the calculated ECC downcomer bypass is shown in Figures 45 and 46. As the accumulator injects fluid into the cold leg, density in the cold leg control volumes (26201 and 26301 in Figure 45) increases. None of the injected coolant is retained in the downcomer as indicated by the low, constant inlet annulus density. Due to an error in the structural mass data in the RELAP5 input deck, wall heat transfer vaporized the liquid added to the inlet annulus control volume. The high density, low velocity mass flow from the intact loop cold leg was transferred directly to the broken loop cold leg as a high velocity, low

a. The offset in initiation of accumulator injection is a result of the accumulator experimental setpoint being approximately 30 psi lower than specified.

PRETEST PREDICTION COMPARISON TO SELECTED DATA
TEST S-IB-3

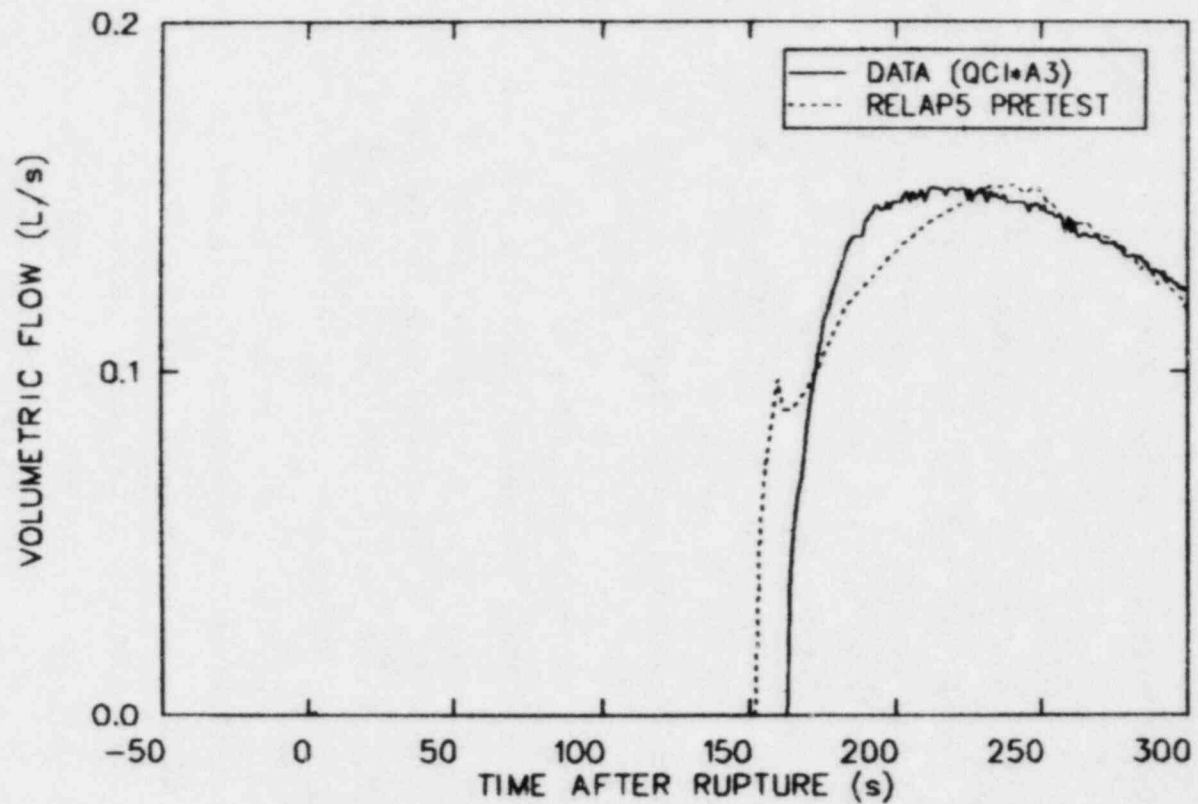


Figure 44. Comparison of measured to calculated Intact loop accumulator flow rate.

PRETEST PREDICTION COMPARISON TO SELECTED DATA
TEST S-1B-3

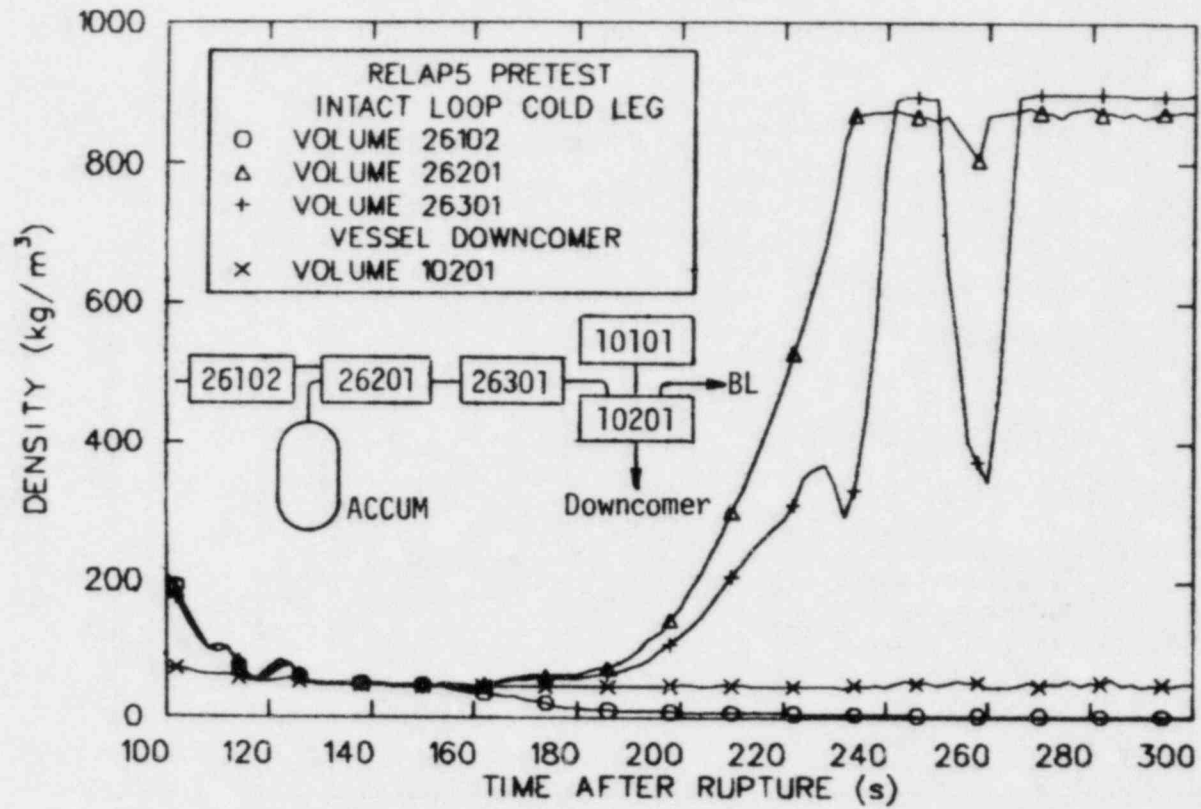


Figure 45. RELAP5 calculated cold leg densities.

PRETEST PREDICTION COMPARISON TO SELECTED DATA
TEST S-1B-3

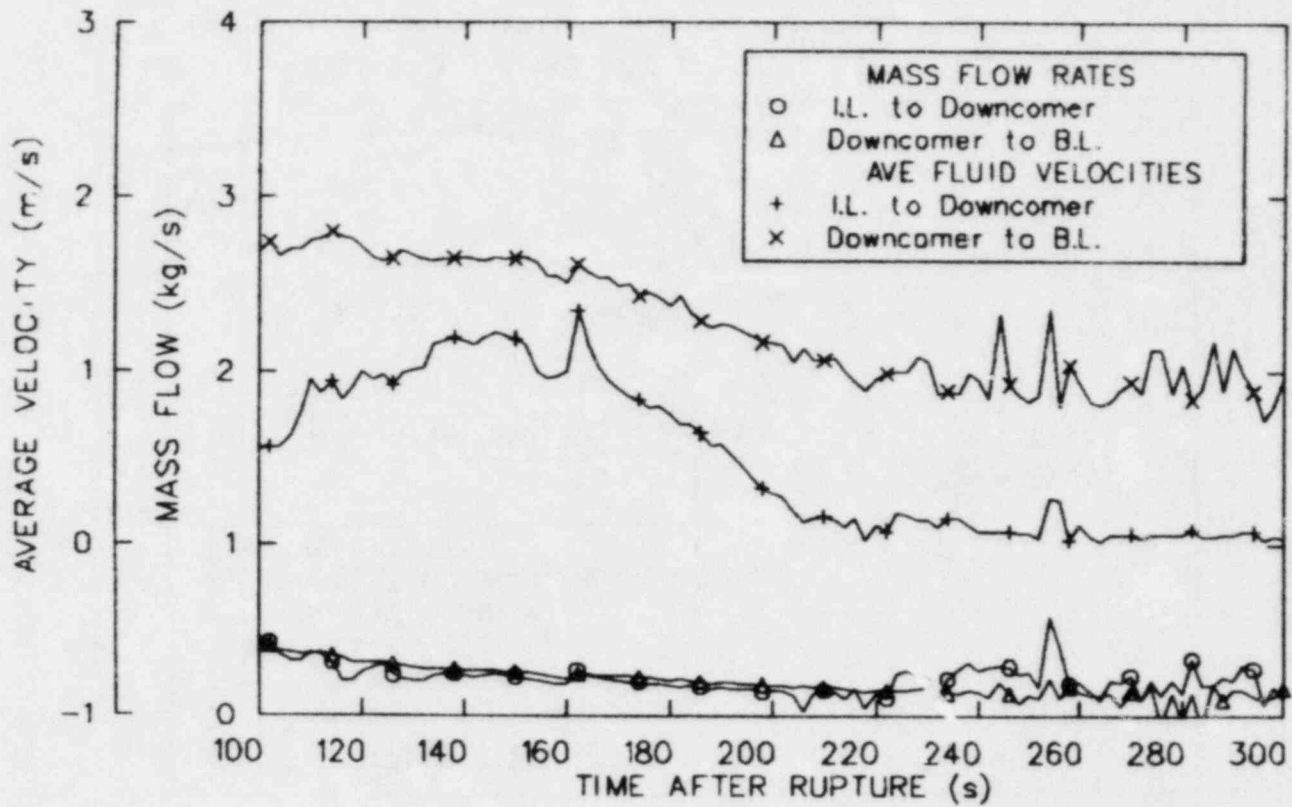


Figure 46. Calculated mass flows and velocities through inlet annulus.

density fluid which exited the break. The increased fluid velocity for a continuous mass flow through the inlet annulus is shown in Figure 46.

A posttest analysis of Test S-IB-3 will be performed with RELAP5/MOD1.5. The Semiscale system RELAP5 model will reflect the modeling corrections and system initial conditions shown to have significantly influenced the predicted hydraulic response of the system. The analysis will investigate the code's capability of calculating the observed system response through both blowdown and reflood.

5. CONCLUSIONS

The primary objective of this test was to provide reference data for comparison of Semiscale test results to LOBI B-R1M test results. Also, another important objective was to provide reference data for evaluation and assessment of reactor safety code capabilities to predict integral blowdown, refill/reflood experiments for intermediate break sizes. Still another important objective was to expand the break spectrum data base to cover the 10 to 200% range in order to determine if other phenomena are important to core cooling and to evaluate the Mod-2A system response to breaks in this range.

Results from Test S-IB-3 have provided information about system pressure response, fluid mass distribution, core dryout phenomena and ECC effects for an intermediate (21.7%), communicative, cold leg break, loss-of-coolant experiment with cold leg ECC injection.

1. The test provided data which may be used for comparison to the LOBI B-R1M Test.
2. The test met its objective of providing thermal-hydraulic data to be used in assessing computer code performance.
3. The test also provided baseline data which may be used for comparison to tests in the 10% to 200% break range.

A preliminary analysis of Test S-IB-3 data has shown that the early portion of the transient was dominated by the general phenomena of gravity drain and pump suction liquid seal formation. The refill/reflood portion of the transient was characterized by a slow boiloff of coolant in the core, causing a very gradual temperature rise, until LPIS and accumulator coolant reached the core and quenched most of the core by about 280 seconds.

The RELAP5/MOD1 pretest calculation was shown to have predicted the overall blowdown system response for this intermediate break experiment. The observed effect of pump suction liquid seal formation on the core

thermal-hydraulic response was not predicted, however. The discrepancy between the observed and predicted vessel level depression during liquid seal formation is attributed to a difference in the specified and experimental operation of the broken loop steam generator, and inaccuracies in modeling the steady state conditions of the Mod-2A system. Although the vessel hydraulic response during liquid seal formation was not accurately predicted, subsequent core coolant boiloff and heater rod temperature excursions were calculated in good agreement with data.

Two specific code modeling areas were identified as yielding unrealistic behavior in comparison to test data. First, RELAP5/MOD1 was shown to not preserve an abrupt liquid/vapor interface in a vertical stack of control volumes as liquid was drained out through the lowest volume. Secondly, an error in the structural mass information in the input deck prevented cold leg ECC from penetrating the downcomer and refilling the vessel.

6. REFERENCES

1. T. J. Boucher, Experiment Operating Specification (EOS) for Semiscale Mod-2A Experiment S-IB-3, EG&G Idaho, Inc., Idaho Falls, Idaho, EGG-SEMI-5787, February 1982.
2. T. K. Larson, J. L. Anderson, and D. L. Shimeck, Scaling Criteria and An Assessment of Semiscale Mod-3 Scaling for Small Break Loss-of-Coolant Transients, EG&G Idaho, Inc., Idaho Falls, Idaho, EGG-SEMI-5121, March 1980.
3. J. E. Blakely, R. G. Hanson, and D. L. Shimeck, Quick Look Report for Semiscale Mod-2A Test S-UT-1, EG&G Idaho, Inc., Idaho Falls, Idaho, EGG-SEMI-5331, January, 1981.
4. K. E. Sackett, and L. Bruce Clegg, Experiment Data Report for Semiscale Mod-2A Small Break Test Series (Tests S-UT-1 and S-UT-2), EG&G Idaho, Inc., Idaho Falls, Idaho, NUREG/CR-2176, EGG-2108, July, 1981.
5. M. T. Leonard, Semiscale Mod-2A Test S-IB-3 Pretest Prediction Report, EG&G Idaho, Inc., Idaho Falls, Idaho, PN-36-82, February, 1982.

APPENDIX

The measurements and initial condition values are listed in the following order. Within each subgroup, e.g., "Downcomer", measurements are listed alphabetically by parameter symbols and by elevation for a given parameter.

1. Reactor Vessel

1.1 Core

1.2 Downcomer

1.3 Upper and Lower Plenum

1.4 Upper Head and Core Bypass

2. Intact Loop

2.1 Hot Leg (at Reactor Vessel Outlet)

2.2 Pressurizer

2.3 Steam Generator Inlet and Primary Side

2.4 Steam Generator Secondary

2.5 Steam Generator Outlet (Primary)

2.6 Pump Suction and Pump Parameters

2.7 Pump Discharge

2.8 Cold Leg (at Downcomer Inlet)

2.9 Loop ΔP 's

3. Broken Loop

3.1 Hot Leg

3.2 Steam Generator Inlet and Primary Side

3.3 Steam Generator Secondary

3.4 Steam Generator Outlet (Primary)

3.5 Pump Suction and Pump Parameters

3.6 Pump Discharge

3.7 Cold Leg

3.8 Loop ΔP 's

4. ECCS

4.1 Accumulator

4.2 HPIS/LPIS

5. Break Flow and Pressure Suppression

5.1 Break Flow

5.2 Pressure Suppression Tank

6. Miscellaneous

The parameter symbols and units are listed below.

<u>Parameter</u>	<u>Symbol</u>	<u>Units</u>
Differential pressure	D, DP	kPa
Voltage	E	volts
Force	F	Newtons
Current	I	amps
Power	kW	kW
Level	L	cm
Pressure	P	MPa
Volumetric flow	Q	ℓ/s
Density	R	kg/m ³
Fluid temperature	TF	K
Metal temperature	TM	K
Heater rod temperature	TH	K
Angular speed	W	radians/s
Position (valve)	X	volts

1. REACTOR VESSEL

1.1 Core

<u>System</u>	<u>Measurement ID</u>	<u>Initial Condition</u>
I	EV*HIPWBUS	279.05 Volts
I	EV*LOPWBUS	279.26 Volts
I	IV*HIPWBUS	1939.10 amps
I	IV*LOPWBUS	3258.93 amps
I	KW*HIBUS	541.10 kW
I	KW*LOBUS	910.09 kW
I	KW*TOTAL	1451.19 kW
II	LV-105-195	-19.29 kPa
II	LV-195-278	-7.67 kPa
II	LV-278-360	-7.54 kPa
II	LV-360-442	-4.90 kPa
II	LV-442-501	-1.56 kPa
I	RV*AB-6	739.68 kg/m ³
II	RV*23+13	732.95 kg/m ³
II	RV*23+113	728.12 kg/m ³
II	RV*AB+173	707.92 kg/m ³
II	RV*23+183	707.89 kg/m ³
II	RV*23+253	666.25 kg/m ³
II	RV*23+342	674.23 kg/m ³
I	TFV*A4+79	569.12 K
I	TFV*A4+162	573.65 K
I	TFV*A4+242	595.09 K
I	TFV*A4+283	600.27 K
I	TFV*A4+323	603.34 K
I	TFV*A4+361	595.55 K
I	TFV*B3+45	F ^a
I	TFV*B3+122	572.61 K
I	TFV*B3+162	581.12 K
I	TFV*B3+242	598.17 K

1. REACTOR VESSEL (continued)

1.1 Core

<u>System</u>	<u>Measurement ID</u>	<u>Initial Condition</u>
I	TFV*B3+323	605.03 K
I	TFV*D1+122	574.15 K
I	TFV*D1+162	579.05 K
I	TFV*D1+323	603.00 K
II	THV*A1+115	F ^a
I	THV*A2+112	636.59 K
I	THV*A2+182	656.69 K
I	THV*A2+353	604.33 K
II	THV*A3+137	642.10 K
II	THV*A3+208	644.39 K
II	THV*A3+228	657.51 K
II	THV*A3+291	637.73 K
II	THV*A4+115	640.70 K
II	THV*A4+185	666.29 K
II	THV*A4+355	618.78 K
II	THV*A5+185	661.72 K
I	THV*B1+11	578.89 K
I	THV*B1+183	650.97 K
I	THV*B1+253	655.08 K
I	THV*B2+107	628.23 K
I	THV*B2+180	662.45 K
I	THV*B2+227	660.23 K
I	THV*B2+353	636.72 K
I	THV*B3+114	642.71 K
I	THV*B3+184	663.17 K
I	THV*B3+229	662.43 K
I	THV*B3+354	627.87 K
I	THV*B4-12	564.92 K
II	THV*B4+140	653.65 K

1. REACTOR VESSEL (continued)

1.1 Core

<u>System</u>	<u>Measurement ID</u>	<u>Initial Condition</u>
II	THV*B4+170	660.58 K
II	THV*B4+256	666.22 K
I	THV*B5+133	654.11 K
I	THV*B5+180	659.18 K
I	THV*B5+252	654.20 K
I	THV*C1+140	646.96 K
I	THV*C1+211	667.89 K
I	THV*C1+232	669.17 K
I	THV*C1+292	650.16 K
II	THV*C2+15	579.31 K
II	THV*C2+137	649.04 K
II	THV*C2+168	650.18 K
II	THV*C2+254	653.75 K
II	THV*C3+140	650.67 K
II	THV*C3+231	664.59 K
II	THV*C3+292	660.62 K
II	THV*C4+20	582.36 K
II	THV*C4+142	652.33 K
II	THV*C4+187	658.32 K
II	THV*C4+257	661.66 K
I	THV*C5+133	645.73 K
I	THV*C5+207	657.11 K
I	THV*C5+228	659.40 K
I	THV*C5+290	643.48 K
I	THV*D1+131	641.90 K
I	THV*D1+178	655.68 K
I	THC*D1+251	657.33 K
I	THV*D2+16	580.53 K
II	THV*D2+138	651.46 K

1. REACTOR VESSEL (continued)

1.1 Core

<u>System</u>	<u>Measurement ID</u>	<u>Initial Condition</u>
II	THV*D2+185	660.14 K
II	THV*D2+254	667.33 K
II	THV*D3+109	632.62 K
II	THV*D3+227	661.56 K
II	THV*D3+354	621.37 K
II	THV*D4+106	F ^a
II	THV*D4+179	660.80 K
II	THV*D4+228	668.83 K
II	THV*D4+352	F ^a
II	THV*D5+13	582.56 K
II	THV*D5+139	649.07 K
II	THV*D5+184	660.42 K
II	THV*E1+172	659.31 K
II	THV*E2+109	631.78 K
II	THV*E2+181	654.01 K
II	THV*E2+354	615.20 K
II	THV*E3+141	654.04 K
II	THV*E3+211	651.00 K
II	THV*E3+231	662.32 K
II	THV*E3+292	634.45 K
II	THV*E4+112	631.88 K
II	THV*E4+183	654.55 K
II	THV*E4+199	F ^a
II	THV*E4+354	605.02 K

1. REACTOR VESSEL (continued)

1.2 Downcomer

<u>System</u>	<u>Measurement ID</u>	<u>Initial Condition</u>
I	LVD+29-170	15.75 kPa
I	LVD-170-435	17.27 kPa
I	LVD-435-578	4.76 kPa
I	LVD+29-578	35.47 kPa
I	PV*DC+29	15.58 MPa ^b
II	RV*DC-72	745.87 kg/m ³
II	RV*DC-260	749.31 kg/m ³
I	TFV*DC-84	562.90 K
I	TFV*DC-270	563.69 K
I	TMV*DC-83	564.72 K
I	TMV*DC-222	F ^a
I	TMV*DC-364	F ^a

1.2.1 Outlet Flow

I	FV*DC-441	3.88 N
I	PV*DC-435L	9.75 MPa ^{b,c}
I	QV*DC-423	10.92 ℓ/s
I	RV*DC-456	745.38 kg/m ³
II	TFV*DC-436	561.62 K

1.3 Upper and Lower Plenum

I	FV*UP-9	2.53 N
I	LV-13M-105	-10.67 kPa
I	LV-13M-578	-54.98 kPa
I	PV*UP-13	15.58 MPa ^b
I	QV*UP+1	11.33 ℓ/s
I	RV*UP-11	F ^a

1. REACTOR VESSEL (continued)

1.3 Upper and Lower Plenum

<u>System</u>	<u>Measurement ID</u>	<u>Initial Condition</u>
II	TFV*UP-13	594.98 K
I	TFV*UP-63	596.88 K
I	TFV*UP+79	573.77 K
I	TMV*FPD+79	573.52 K
I	LV-501-578	-15.53 kPa
I	PV*LP-578L	9.64 MPa ^{b,c}
II	TFV*LP-552	562.91 K

1.4 Upper Head and Core Bypass

II	DVD+29+421	73.30 kPa
I	FV*GT+330	0.07 N
I	LV+421+160	6.11 kPa
I	LV+160+135	7.31 kPa
I	LV+135-13M	4.13 kPa
I	LV+421-13M	18.75 kPa
I	LV+421-578	-38.23 kPa
I	PV*UH+421	15.54 MPa ^b
I	QV*GT+321	0.06 s/s
I	QV*BYPASS	F ^a
I	RV*UH+173	762.25 kg/m ³
I	RV*UH+339	776.83 kg/m ³
II	TFV*BYPASS	561.98 K
I	TFV+UHQ180	555.50 K
I	TFV+UHQ282	559.81 K
I	TFV*UH+343	546.51 K
I	TFV*UH+402	554.09 K
I	TMV+FPF221	550.83 K
I	TMV+TSQ221	556.81 K

2. INTACT LOOP

2.1 Hot Leg

<u>System</u>	<u>Measurement ID</u>	<u>Initial Condition</u>
I	FI*1	1.37 N
I	PI*1	15.55 MPa ^b
I	QI*1	8.77 m^3/s
I	RI*1B	672.56 kg/m^3
I	RI*1T	676.38 kg/m^3
I	TFI*1	596.14 K

2.2 Pressurizer

I	DP*PRZ*13	-67.35 kPa
I	LPRZ158+25	7.79 kPa
I	P*PRZ+158	15.53 MPa ^b
I	Q*PRZ-30	-.01 m^3/s
II	TF*PRZ-73	535.90 K
II	TF*PRZ+132	619.05 K
II	TF*PRZ*13	541.15 K

2.3 Steam Generator Inlet and Primary Side

I	FI*5	1.64 N
I	QI*6	7.48 m^3/s
II	RI*5M	708.95 kg/m^3
II	TFI*5	595.25 K
I	LIP970-55E	24.64 kPa
I	TFIP+LC211	563.05 K
I	TFIP+LH30	593.68 K
I	TFIP+LH452	581.09 K
I	TFIP+LH922	572.50 K

2. INTACT LOOP (continued)

2.4 Steam Generator Secondary Feedwater

<u>System</u>	<u>Measurement ID</u>	<u>Initial Condition</u>
I	DPSC*IGFDW	75.40 kPa
I	TFSC+IGFDW	493.61 K
I	TFSC+IGFWL	492.46 K

2.4.1 Riser and Steam Dome

I	LIS1117+50	50.79 kPa
I	PIS+1117	6.48 MPa
I	TFIS+1117	554.16 K
I	TFIS+LC211	553.68 K
I	TFIS+LH30	550.00 K
I	TFIS+LH452	554.17 K
I	TFIS+LH922	553.81 K

2.4.2 Steam Flow

I	DPSC*IGSTM	53.64 kPa
I	PSC*IGSTM	6.56 MPa
I	TFSC*IGSTM	553.50 K

2.5 Steam Generator Outlet (Primary)

I	FI*9	1.42 N
II	RI*9M	748.09 kg/m ³
II	TFI*9	563.20 K

2. INTACT LOOP (continued)

2.6 Pump Suction and Pump Parameters

<u>System</u>	<u>Measurement ID</u>	<u>Initial Condition</u>
I	FI*15	1.27 N
I	PI*14L	9.62 MPa ^{b,c}
I	QI*15	8.00 m^3/s
II	TFI*15	562.80 K
I	TFI*17	562.63 K
I	DPI*21*18	219.20 kPa
II	EI*PUMP	210.65 volts
II	II*PUMP	40.59 amps
I	WI*PUMP	177.37 rad/s

2.7 Pump Discharge

I	QI*21	8.04 m^3/s
I	RI*21B	755.68 kg/m^3
I	RI*21T	755.98 kg/m^3
II	TFI*21	560.63 K

2.8 Cold Leg

I	FI*22	1.32 N
II	PI*22L	3.52 MPa ^{b,c}
I	QI*22	8.01 m^3/s
I	RI*22B	F ^a
I	RI*22T	755.43 kg/m^3
II	TFI*22	559.38 K

2. INTACT LOOP (continued)

2.9 Loop ΔP 's

<u>System</u>	<u>Measurement ID</u>	<u>Initial Condition</u>
I	D-V13A*I1	7.79 kPa
I	DPI*1*3	5.05 kPa
I	DPI*3*5	1.27 kPa
I	DPI*5*9	117.18 kPa
I	DPI*9*14	15.12 kPa
I	DPI*14*18	-2.51 kPa
I	DPI*21*22	1.06 kPa
I	D*I22+VD29	6.40 kPa

3. BROKEN LOOP

3.1 Hot Leg

I	FB*50	.47 N
II	PB*50	15.44 MPa ^b
I	QB*50	3.02 g/s
I	RB*50M	691.03 kg/m^3
I	RB*50T	689.28 kg/m^3
I	TFB*50	589.64 K

3.2 Steam Generator Inlet and Primary Side

I	FB*57	.41 N
I	QB*57	2.94 g/s
II	RB*57M	669.45 kg/m^3
I	TFB*57	596.87 K
I	TFBP+LH211	589.92 K
I	TFBP+LH452	585.53 K

3. BROKEN LOOP (continued)

3.2 Steam Generator Inlet and Primary Side

<u>System</u>	<u>Measurement ID</u>	<u>Initial Condition</u>
I	TFBP+LH668	582.64 K
I	TFBP+LH922	579.12 K

3.3 Steam Generator Secondary

3.3.1 Feedwater

I	DPSC*BGFDW	23.42 kPa
I	TFSC*BGFDW	494.33 K
I	TFSC*BGFWL	484.69 K

3.3.2 Riser and Steam Dome

I	LBS1117+50	49.39 kPa
I	PBS+1117	7.53 MPa
I	TFBS+1117	564.89 K
I	TFBS+LH211	564.06 K
I	TFBS+LH452	564.51 K
I	TFBS+LH668	564.21 K
I	TFBS+LH922	564.63 K

3.3.3 Steam Flow

II	DPSC*BGSTM	68.80 kPa
II	PSC*BGSTM	F ^a
I	TFSC*BGSTM	564.40 K

3. BROKEN LOOP (continued)

3.4 Steam Generator Outlet (Primary)

<u>System</u>	<u>Measurement ID</u>	<u>Initial Condition</u>
I	FB*62	.39 N
II	RB*62M	730.13 kg/m ³
I	TFB*62	571.61 K

3.5 Pump Suction and Pump Parameters

I	TFB*64	570.49 K
II	PB*65L	F ^a
I	QB*73	3.29 ℓ /s
II	RB*73	F ^a
I	TFB*73	552.56 K
I	DPB*74*73	254.74 kPa
II	KWB*PUMP	2.11 kW
I	WB*PUMP	872.63 rad/s

3.6 Pump Discharge

I	FB*74	0.44 N
I	PB*74L	9.55 MPa ^{b,c}
I	QB*74	2.75 ℓ /s
II	RB*74M	738.21 kg/m ³
II	RB*74T	739.31 kg/m ³
I	TFB*74	567.19 K

3.7 Cold Leg

II	DPB*79.25D	-3.16 kPa ^f
II	DPB*79.50D	F ^a
II	DPB*79.75D	F ^a

3. BROUEN LOOP (continued)

3.7 Cold Leg

<u>System</u>	<u>Measurement ID</u>	<u>Initial Condition</u>
I	FB*79	F ^a
II	PB*79L	9.62 MPa ^{b,c}
I	QB*79	2.74 m^3/s
I	RB*79M	740.28 kg/m^3
I	RB*79T	741.12 kg/m^3
I	TFB*79	566.41 K

3.8 Loop ΔP 's

I	D-V13A*B50	6.85 kPa
I	DPB*50*55	5.28 kPa
I	DPB*55*57	.63 kPa
I	DPB*57*62	112.96 kPa
I	DPB*62*65	15.83 kPa
I	DPB*65*73	1.10 kPa
I	DPB*74*76U	8.16 kPa
I	DPB*76U*79	4.16 kPa
I	D*B79+VD29	0.15 kPa

4. ECCS

4.1 Accumulator

I	LCI*A3+277	4.03 kPa
I	PCI*A3+277	2.60 MPa ^e
I	QCI*A3	0.0 m^3/s ^d
I	TFCI*A3+76	298.43 K
I	TFCI*I22	351.40 K

4. ECCS (continued)

4.2 HPIS/LPIS

<u>System</u>	<u>Measurement ID</u>	<u>Initial Condition</u>
I	QCI*ILLPIS	0.0 g/s

5. BREAK FLOW AND PRESSURE SUPPRESSION

5.1 Break Flow^d

II	DPB*76.25D	18.70 kPa
II	DPB*76.50D	-8.10 kPa
I	DB*76F*76D	2.56 kPa
I	FB*76	F ^a
I	PB*76L	3.88 MPa ^{b,c}
I	PB*76D(1)	15.61 MPa ^b
II	PB*76D(2)	15.63 MPa ^b
II	RB*76M	741.86 kg/m ³
II	RB*76T	743.27 kg/m ³
I	TFB*76	F ^a
I	DB*76U*76D	305.99 kPa ^b
II	PB*76U	15.57 MPa ^b
I	TFB*76U	564.86 K

5.2 Pressure Suppression

I	LPS+105+48	-1.26 kPa
I	PPS*1T+384	0.25 MPa ^{b,e}
I	TFPS*1T+43	290.38 K
I	TFPS*1T330	406.38 K

6. MISCELLANEOUS

<u>System</u>	<u>Measurement ID</u>	<u>Initial Condition</u>
I	LPS*LOWRNG	-0.30 kPa
I	PB*RDP	F ^a
I	XSC*IGFDW	F ^a
I	XSC*IGSTM	2.04 volts
II	XSC*BGFDW	1.38 volts
II	XSC*BGSTM	1.83 volts
II	THV*AVG	653.98 K

An optical probe was mounted at the upstream side of the break, looking directly across the flow at the (upstream) face of the 21.7% break nozzle. See Figure 6 for configuration. A video tape was produced showing fluid conditions at that position during the entire experiment.

NOTES

-
- a. F - failed during warmup or during test.
 - b. These measurements supplied with 50 Hz amplifier filters.
 - c. These are low range transducers. They are saturated at initial conditions, thus this reading is not the true value of the parameter.
 - d. There is no flow in this leg at initial conditions.
 - e. These tanks are isolated from the primary coolant system at initial conditions, but pressurized by their own pressurizing source.
 - f. The pitot tubes point toward the downcomer, and so do not provide readings of the initial condition flow, which is toward the downcomer.
 - g. The above listed 317 entries consist of 314 measurements and three calculated values (power on the high and low power buses and total core power). The 314 measurements coincide with those on the final copy of the log sheet for this test. The other 16 channels on the log sheet consist of eight for calibration, ground noise monitoring and sequencer checking, and eight spare channels.
-